

Back Analysis of Mount Polley Tailing Dam Failure

Md Abdullah Al Arafat

A thesis submitted to the faculty of graduate studies

In partial fulfillment of the requirements for the degree of

Master of Science

Graduate Program in Earth and Space Science

York University

Toronto, Ontario

January 2017

© Md Abdullah Al Arafat, 2017

ABSTRACT

Mount Polley Tailings Storage Facility (MP-TSF) failed on its perimeter embankment on August 4, 2014. The failure released millions of m³ of toxic tailings, supernatant water and construction materials to downstream. After the failure incident, the Government of British Columbia established an Independent Review Panel (IRP) to investigate the incident. The final report was published on January 30, 2015. IRP concluded that a weak Glaciolacustrine (GLU) layer, which was not detected at the time of site investigation, was the cause of the failure. The designers did not consider this weak layer during the design phase. Consequently, the computed design Factor of Safety was higher than it should have been (Morgenstern *et al.* 2015). The motivation of this research was to verify the findings of IRP by conducting a numerical analysis using industry-standard geotechnical finite element analysis software. The finite element models indeed confirmed that the foundation of the perimeter embankment would have failed along the weak GLU layer because of excessive shear deformation in the layer. Additionally, the finite element models also highlighted the importance of choosing correct relative stiffness values for various foundation layers for a realistic development of failure mechanisms for stability analyses done using the Strength Reduction technique. This observation is novel and is of considerable practical significance because designers pay little attention to obtaining stiffness parameters for foundation soils and focus more on obtaining realistic shear-strength parameters. A numerical parametric study conducted to investigate potential ways of preventing failure of the perimeter embankment revealed downstream slope flattening to be the most effective solution.

Keywords: Mount Polley tailings dam failure, slope stability, foundation failure; finite element modelling, Strength Reduction technique, shear strength, relative stiffness.

ACKNOWLEDGMENT

First of All, I would like to thank the creator of the universe for what He has bestowed upon me.

I am deeply indebted to my supervisor Dr. Jitendrapal Sharma and supervisory committee member Dr. Rashid Bashir. Without their personal and scientific guidance and feedback, the outcome of the research would never see the light. Special thanks are also extended to Dr. Regina Lee of Earth and Space Science and Engineering (ESSE) and Dr. Dan Palermo and Dr. Usman T. Khan of Civil Engineering department. I would also like to thank Ms. Gillian Moore of Civil Engineering office, Ms. Marcia Gaynor of ESSE office, fellow MASc student Mr. Prateek Jindal and Dr. Jennifer Lewin for their different roles throughout the study period.

I would like to express gratitude to my parents, my wife Sanjida Moury who stayed with me in critical moments of our shared journey and my son Owais Al Omar, the gifted.

Finally, I like to thank York University for giving me the opportunity to be a part of it.

TABLE OF CONTENTS

Abstract.....	ii
Acknowledgment.....	iii
List of Tables	vii
List of Figures.....	viii
List of Symbols	xi
List of ABBREVIATIONS	xii
1 Introduction.....	1
1.1 Overview of Mount Polley Tailings Storage Facility (MP-TSF).....	2
1.1.1 The Failure Event.....	5
1.2 Objective and Scope of the Research.....	9
1.3 Thesis Structure.....	10
2 Literature Review	12
2.1 Tailings.....	12
2.2 Engineering Properties of Tailings.....	14
2.2.1 Hydraulic Conductivity in Tailings	15
2.2.2 Compressibility	16
2.2.3 Consolidation	16
2.2.4 Shear Strength.....	17

2.3	Tailings Dams	20
2.4	Tailings dam in Mount Polley Tailings Storage Facility (MP-TSF).....	23
2.5	Failure Mechanism in Tailings Dams	24
2.5.1	Geotechnical Instability	25
2.5.2	Hydraulic Instability	27
2.5.3	Human Interventions.....	28
2.6	Stability Analysis Methods	29
2.6.1	Limit Equilibrium Method (LEM).....	30
2.6.2	Finite Element Method (FEM).....	31
3	Numerical Analysis on Failure Mechanism.....	33
3.1	Data Sources.....	34
3.2	Numerical Tools for the Simulations	34
3.2.1	SIGMA/W.....	34
3.2.2	SLOPE/W	35
3.2.3	SEEP/W	35
3.3	Review of the Published Analyses	36
3.3.1	Analysis 1: Preliminary Design Report by Knight Piésold Consulting (2005)	36
3.3.2	Analysis 2: 9 th Stage Dam Design by AMEC (2012)	39
3.3.3	Analysis 3: Independ Review Report by Morgenstern <i>et al.</i> (2015)	42
3.3.4	Analysis 4: Finite Element Analysis (FEA).....	45

3.4	Deformation Analysis	62
3.5	Summary of Results	65
4	Parametric Study for Performance Improvement	70
4.1	Numerical Parametric Study	70
4.2	Study 1: Downstream Slope Flattening.....	70
4.3	Study 2: Addition of Berms to Downstream Slope.....	72
4.4	Study 3: Widening of Core	73
4.5	Study 4: Addition of Extra layer of Rockfill.....	75
4.6	Study 5: Thickened Tailings	76
4.7	Sensitivity Study	77
4.8	Summary of Results	78
5	Conclusion	79
5.1	Summary of Results	79
5.2	Recommendations That Could Have Prevented the Failure	80
5.3	Future Research Possibilities	81
	References	82
	Appendix.....	87

LIST OF TABLES

<i>Table 1: Typical values of Coefficient of Consolidation, C_v (after Sarsby 2013).....</i>	<i>17</i>
<i>Table 2: Typical values for drained shear strength (after Sarsby 2013).....</i>	<i>17</i>
<i>Table 3: Typical total stress parameter for Copper tailings (after Vick 1990).....</i>	<i>20</i>
<i>Table 4: List of some major tailings dam failure.....</i>	<i>25</i>
<i>Table 5: Comparison among LEM</i>	<i>30</i>
<i>Table 6: Material properties used in Preliminary design (2005).....</i>	<i>38</i>
<i>Table 7: Factors of Safety in Preliminary design (2005)</i>	<i>39</i>
<i>Table 8: Material properties used by AMEC (2012) in 9th stage design.....</i>	<i>41</i>
<i>Table 9: Factors of Safety 9th Stage Design by AMEC (2012).....</i>	<i>42</i>
<i>Table 10: Material properties used by Morgenstern et al. (2015)</i>	<i>44</i>
<i>Table 11: Factors of Safety obtained by Morgenstern et al. (2015).....</i>	<i>45</i>
<i>Table 12: Factors of Safety of each stage obtained by using LEM (Morgenstern-Price).....</i>	<i>47</i>
<i>Table 13: Stiffness Parameters of the materials</i>	<i>51</i>
<i>Table 14: Factors of Safety FEA of each stage for all cases.....</i>	<i>62</i>
<i>Table 15: Factor of safety for different tailings properties</i>	<i>77</i>

LIST OF FIGURES

<i>Figure 1: Location of Mount Polley on Canadian Map (Modified from Atlas Canada).....</i>	<i>2</i>
<i>Figure 2: 3D overview of MP-TSF (Imperial Metals 2015).....</i>	<i>4</i>
<i>Figure 3: Layout of MP-TSF (as per Morgenstern et al. 2015).....</i>	<i>6</i>
<i>Figure 4: Chronological Google Earth images of Mount Polley.....</i>	<i>7</i>
<i>Figure 5: Post failure images of the MP-TSF Dam (source: Morgenstern et al. 2015)</i>	<i>8</i>
<i>Figure 6: Procedures in tailings productions (after Vick 1990)</i>	<i>13</i>
<i>Figure 7: Tailings disposal methods. (a) Spigotting (b) Single point discharge (after Vick 1990)</i>	<i>14</i>
<i>Figure 8: Curvature of the envelop in shear-normal stress (redrawn after Vick 1990).....</i>	<i>18</i>
<i>Figure 9: Variation in Φ' with effective normal stress (redrawn after Vick 1990).....</i>	<i>18</i>
<i>Figure 10: Conceptual drawing for Retention Tailings dam (modified from US EPA 1994).....</i>	<i>20</i>
<i>Figure 11: Conceptual drawing for Upstream Tailings dam (modified from Vick 1990).....</i>	<i>21</i>
<i>Figure 12: Conceptual drawing for Downstream Tailings dam (modified from Vick 1990).....</i>	<i>22</i>
<i>Figure 13: Conceptual drawing for Centreline Tailings dam (modified from Vick 1990).....</i>	<i>23</i>
<i>Figure 14: Sample slicing procedure in LEM</i>	<i>31</i>
<i>Figure 15: Preliminary design section reproduced from Knight Piesold Consultant (2005).....</i>	<i>37</i>
<i>Figure 16: Pore water pressure (in kPa) contour for the Preliminary design.....</i>	<i>37</i>
<i>Figure 17: Geometry for the 9th stage dam design by AMEC (2012).....</i>	<i>40</i>
<i>Figure 18: Pore water pressure (in kPa) contour for the 9th stage dam design.....</i>	<i>40</i>
<i>Figure 19: Cross sectional geometry used in analysis by Morgenstern et al. (2015).....</i>	<i>43</i>
<i>Figure 20: Pore water Pressure (in kPa) contour for the analysis of Morgenstern et al. (2015).....</i>	<i>43</i>
<i>Figure 21: Development of Construction stages at MP-TSF (Completed)</i>	<i>50</i>

<i>Figure 22: Maximum Shear Strain (ϵ_{max}) at 8th stage (ESA: Case 1)</i>	53
<i>Figure 23: Maximum Shear Strain (ϵ_{max}) at 9th stage (ESA: Case 1)</i>	53
<i>Figure 24: Maximum Shear Strength and Strain plot for GLU in 8th stage (ESA: Case 1)</i>	54
<i>Figure 25: Maximum Shear Strength and Strain plot for GLU in 9th stage (ESA: Case 1)</i>	54
<i>Figure 26: Maximum Shear Strain (ϵ_{max}) at 8th stage (ESA: Case 2)</i>	55
<i>Figure 27: Maximum Shear Strain (ϵ_{max}) at 9th stage (ESA: Case 2)</i>	55
<i>Figure 28: Maximum Shear Strength and Strain plot for GLU in 8th stage (ESA: Case 2)</i>	56
<i>Figure 29: Maximum Shear Strength and Strain plot for GLU in 9th stage (ESA: Case 2)</i>	56
<i>Figure 30: Maximum Shear Strain (ϵ_{max}) at 8th stage (TSA: Case 3)</i>	58
<i>Figure 31: Maximum Shear Strain (ϵ_{max}) at 9th stage (TSA: Case 3)</i>	58
<i>Figure 32: Maximum Shear Strength and Strain plot for GLU in 8th stage (TSA: Case 3)</i>	59
<i>Figure 33: Maximum Shear Strength and Strain plot for GLU in 9th stage (TSA: Case 3)</i>	59
<i>Figure 34 Maximum Shear Strain (ϵ_{max}) at 8th stage (TSA: Case 4)</i>	60
<i>Figure 35 Maximum Shear Strain (ϵ_{max}) at 9th stage (TSA: Case 4)</i>	60
<i>Figure 36: Maximum Shear Strength and Strain plot for GLU in 8th stage (TSA: Case 4)</i>	61
<i>Figure 37: Maximum Shear Strength and Strain plot for GLU in 9th stage (TSA: Case 4)</i>	61
<i>Figure 38: Global vertical deformation in meter after 9th stage (Case 4)</i>	63
<i>Figure 39: Global horizontal deformation in meter after 9th stage (Case 4)</i>	63
<i>Figure 40: Comparison of global vertical deformation along S.O.L</i>	64
<i>Figure 41: Comparison of global horizontal deformation along S.O.L</i>	64
<i>Figure 42: Perimeter dam with downstream slope of 2H:1V</i>	71
<i>Figure 43: Maximum shear strain (ϵ_{max}) along GLU layer for 8th & 9th stage (With flattened d/s slope)</i>	71

Figure 44: New berm has been added to the downstream slope of perimeter dam..... 72

Figure 45: Maximum shear strain (ϵ_{max}) along GLU layer for 8th and 9th stage (with a new d/s berm)..... 73

Figure 46: Perimeter dam with widened core of 10 m..... 74

Figure 47: Maximum shear strain (ϵ_{max}) along GLU layer for 8th and 9th stage (With widened core)..... 74

Figure 48: New rockfill patch added to the downstream of the perimeter dam..... 75

Figure 49: Maximum shear strain (ϵ_{max}) along GLU layer for 8th and 9th stage (new rockfill patch in downstream)..... 76

Figure 50: Sensitivity of the perimeter dam analysis (UW refers to Unit Weight)..... 78

LIST OF SYMBOLS

Greek Symbol	Name	Unit
γ	Unit weight	kN/m^3
Φ'	Angle of internal friction	Degree
τ	Shear stress	kN/m^2
σ	Normal stress	kN/m^2
σ'_v	Effective vertical stress	kN/m^2
ϵ_{\max}	Maximum shear strain	-

LIST OF ABBREVIATIONS

Roman Symbol / Abbreviation	Name	Unit
C	Apparent cohesion	kN/m ²
d ₁₀	10% particles passing by weight in sieve analysis	mm
E	Young's modulus	kN/m ²
FOS	Factor of Safety	-
k	Hydraulic conductivity	m/s
S	Shear strength of soil	kN/m ²
S _u	Undrained peak shear strength of soil	kN/m ²
SOL	Setting Out Line	-
SRF	Strength Reduction factor	-

1 INTRODUCTION

Since the advent of modern technology, the world has seen a rapid growth in mineral extraction from mines all over the world. Only a small percentage of valuable minerals and materials, however, can be extracted from the large volume of excavated rocks and soils. The large amount of remaining by-products, termed as the ‘tailings’, are disposed into the impoundment facilities, which generally consist of two components: tailings lagoons and tailings dams (Sarsby 2013; Vick 1990). The demand for various precious metals and minerals has been increasing exponentially; however, high quality metal ores have become sparse due to heavy exploitation. The mines with these sub-par quality ores produce huge amount of tailings, which are required to be safely stored within the impoundments.

Tailings dams are built to retain tailings within their embankments (Penman 2001; Vick 1990). Although the basic principles of earth dam engineering are shared by tailings dams and water retention dams, the differences in terms of some added considerations in tailings dams regarding material sourcing, piping, filter, geochemistry, structural support and multi-staging in construction may have contributed to the higher failure percentage of the tailings dams (McLeod and Murray 2003; Mittal and Morgenstern 1975). The failure analyses of the tailings dams are very common in literature. Each failure mode review gives valuable engineering insights, which help to improve future engineering practices.

The present study focuses on the numerical review of Mount Polley Tailings Storage Facility (MP-TSF) failure, which happened on August 4, 2014.

1.1 Overview of Mount Polley Tailings Storage Facility (MP-TSF)

MP-TSF is an open pit copper-gold (metal ore) mining facility with an underground component located in the Cariboo region of the Southern Central zone of British Columbia, Canada (Figure 1). The total mining area is 18,794 ha which is owned by Imperial Metals and operated by its subsidiary: Mount Polley Mining Corporation (MPMC). The mining mills started operation in 1997. Since then, it has been running continuously, except for a 3-years hiatus in production between 2002 and 2005, with a maximum tailings production capacity of 20,000 tonnes per day (Imperial Metals 2015; Morgenstern *et al.* 2015).

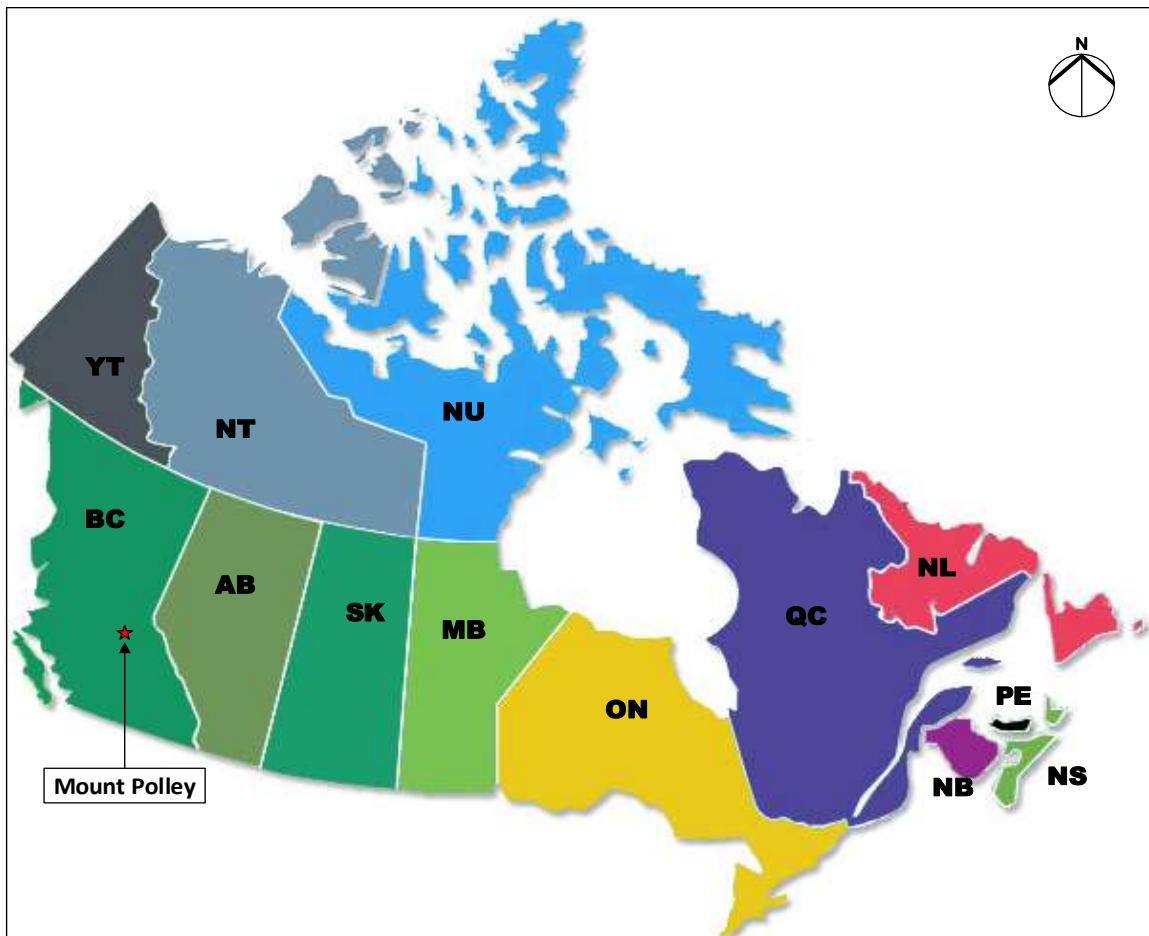


Figure 1: Location of Mount Polley on Canadian Map (Modified from Atlas Canada)

The subsurface soil layers of the mine site consist of Surficial Glacial Till, Glaciolucustrine sediments, and Lower Tills over a weak bedrock layer (Knight Piésold Consulting 2005; Morgenstern *et al.* 2015). The thicknesses and sedimentary compositions of these soil layers vary over the mill site. The area is located on the low seismic zone in the Canadian Seismic Hazard Map (version 2010; Source: EarthquakesCanada.nrcan.gc.ca). Based on historical data, the maximum seismic magnitude of earthquake for the area has been set as 6.5. (Basham *et al.* 1982; Cassidy *et al.* 2010).

Mean annual temperatures and precipitation are obtained from the nearest weather stations at Likely and Barkerville (Data source: www.climate.weather.gc.ca). The mean annual temperature is 4° C with the extreme maximum of 33.9° C and the extreme minimum of -37° C. The average frost free days range from 199 to 244 (Knight Piésold Consultant 1997). The mean annual precipitation in MP-TSF area is 740 mm. The annual evaporation is estimated as 423 mm (Knight Piésold Consulting 2005). As per Thornthwaite Climate Classification (Thornthwaite 1948), the climate of the MP-TSF area is humid.

A 3D overview of the MP-TSF is shown in Figure 2. The main mining mill area, consisting of a number of pits and stockpiles, is sandwiched between two lakes: Polley Lake and Boot Jack Lake. The produced tailings materials are transported in ‘slurry’ form by means of pipelines to a tailings facility located approximately 1.5 km to the south of the main mining area (end-to-end distance). This tailings facility was originally designed to contain approximately 85 million tons of tailings materials (Knight Piésold Consulting 2005).

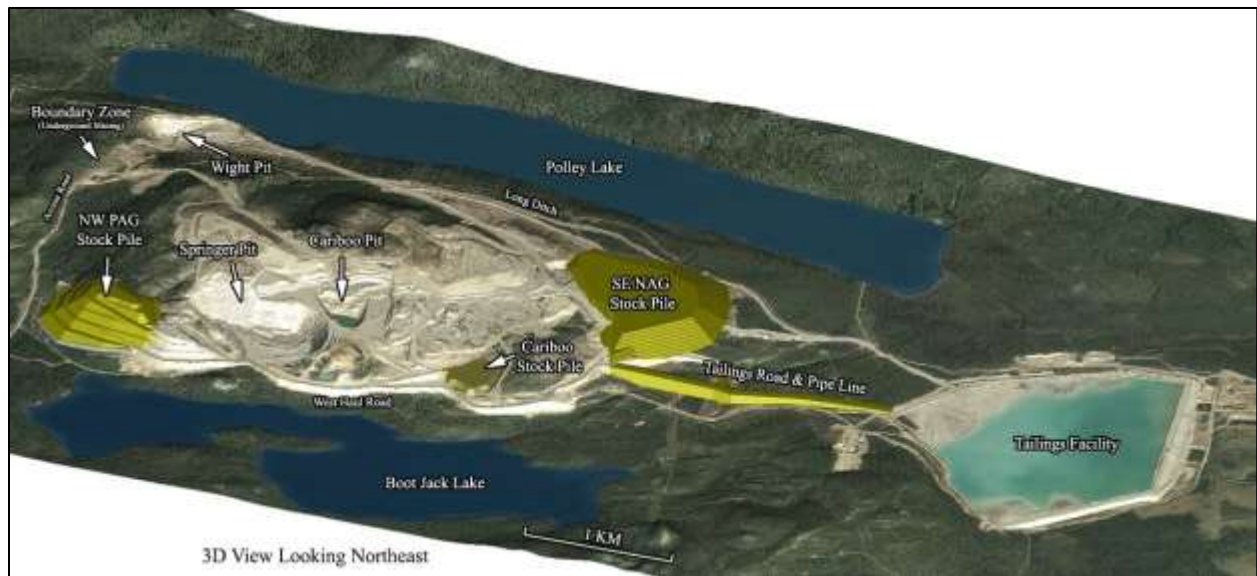


Figure 2: 3D overview of MP-TSF (Imperial Metals 2015)

The tailings facility is built with 3 embankments – main, perimeter and south – with a naturally elevated ground covering the other side (Figure 3). The original design perceived nine stages of an embankment construction up to an elevation of 965 m. The final average heights of the main, perimeter and south embankments are about 55 m, 34 m and 25 m, respectively. The top elevations of each stage of the dam were kept uniform. This allowed the true height of the dam to be different in different locations to match the undulation of the natural ground of the site. The Modified Centerline Method was adopted for the construction of all the stages (details on the tailings dam construction methods are provided in Chapter 2: Literature review). The dam body, however, had varying cross sections all over the embankments (Knight Piesold Consultant 2005; Morgenstern *et al.* 2015).

The components of the drainage systems consisted of foundation drains, chimney drains, longitudinal drains, outlet drains, and upstream toe drains (Knight Piesold Consultant 1997). The seepage collection ponds were excavated in the immediate downstream of all the dams. These

seepage collection ponds collected water from the embankment drain systems and from local runoff. The ponds were noted to be working properly until the failure event.

1.1.1 The Failure Event

The perimeter embankment of the MP-TSF failed after the completion of 9th stage construction, between the survey stations 4+200 and 4+300 on August 4, 2014 (Figure 3). At the time of failure, the 10th stage design documents, proposing an additional 6.5 m increase in embankment height, were sent to the regulator for approval. The physical damage of the breach included sudden erosion of the dam body and toxic tailings material, which flowed towards Polley Lake, Hazeltine Creek, and Quesnel Lake. Two Google Earth images (Figure 4) clearly demonstrate the pollution caused by the failure in the nearby lakes. It was estimated that the failure released about 10.5 million cubic meter of supernatant water, 7.3 million m³ of tailing solid, 6.5 million m³ of interstitial water and 0.6 million m³ of construction materials towards downstream (Imperial Metals 2015).

The monitoring data at the mine site did not note any excess precipitation prior to the failure. No abnormal activity in the dam body in terms of horizontal translation, dipping of crest or piezometric anomaly was found in the log book or witness's details (Morgenstern *et al.* 2015). The post failure aerial images, taken just after failure from upstream and downstream directions, show the extent of horizontal movement of the tailings materials.

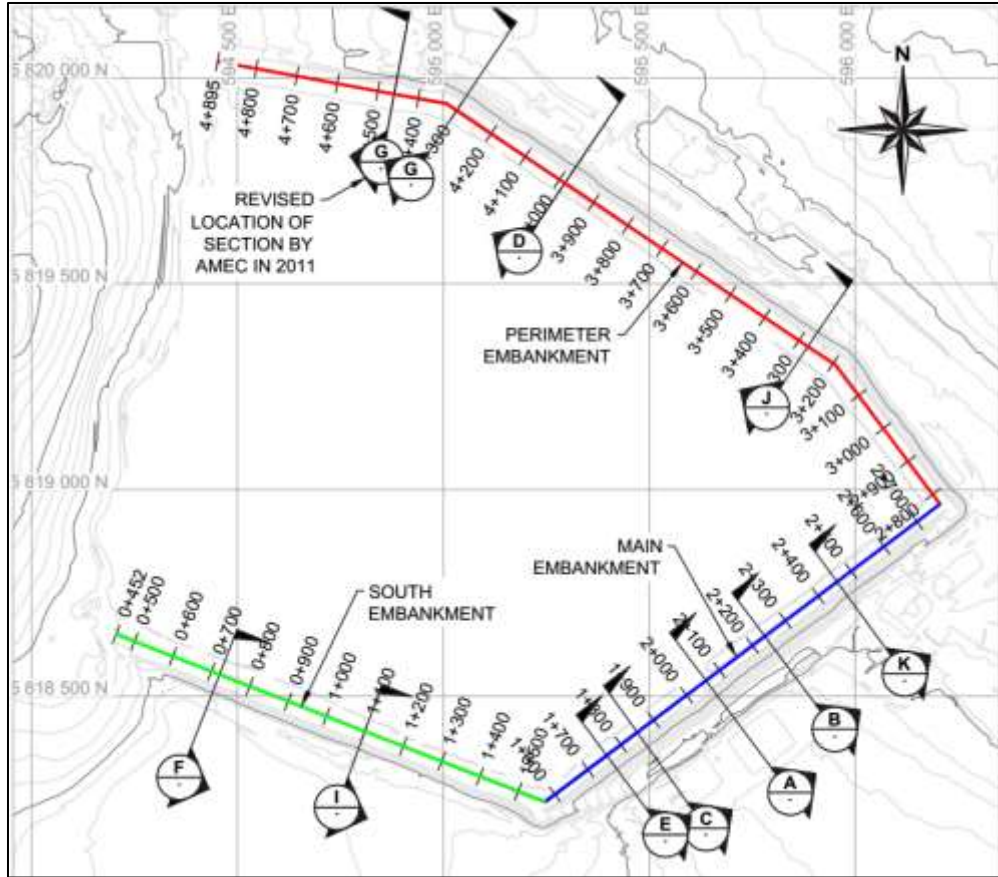
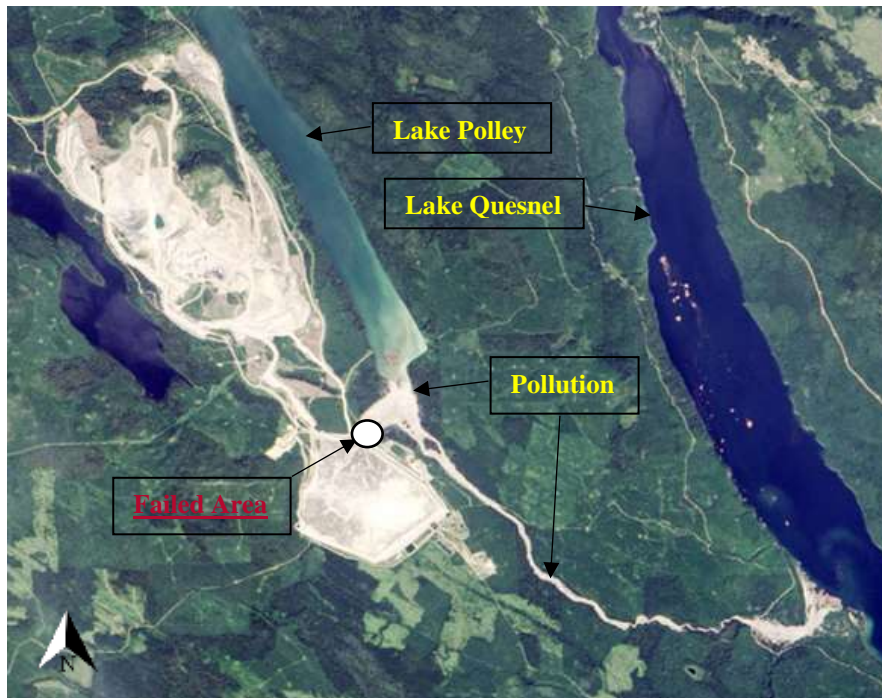


Figure 3: Layout of MP-TSF (as per Morgenstern *et al.* 2015)

After the failure incident, the British Columbia government established an Independent Review Panel (IRP) to investigate the matter (Morgenstern *et al.* 2015). The IRP reviewed available design documents, reports and other relevant documents as well as conducted a separate subsurface investigation to obtain soil properties. The final report was published on January 30, 2015. Using the Limit Equilibrium Method of stability analyses, they concluded that a weak Glaciolacustrine (GLU) layer was the cause of the failure. The designers did not consider this weak layer during the design phase as they failed to recognize the complexity of sub-glacial and pre-glacial geological environment in the failed area. As a result, the obtained Factor of Safety (FOS) was higher than it should have been. The omission of this GLU layer in design subsequently caused the dam to fail (Morgenstern *et al.* 2015).



(a) Before failure on July 29, 2014



(b) After failure on August 06, 2014

Figure 4: Google Earth images of MP-TSF before and after failure



(a) Looking towards downstream



(b) Looking towards downstream

Figure 5: Post-failure images of the MP-TSF (source: Morgenstern et al. 2015)

1.2 Objective and Scope of the Research

The general objective of this study is to achieve a better understanding of the factors that can lead to the failure of tailings dams. The specific research objectives are as follows:

- To investigate the dam breach incident of MP-TSF with the viewpoint of verifying the findings by Morgenstern *et al.* (2015).
- To conduct a parametric back study of Mount Polley tailings dam to test different ways in which the failure could have been prevented.

The present study investigates the geo-structural stability of the failed dam; however, the hydraulic stability analysis encompasses a few assumptions. The effects of unsaturated geohydrology, such as capillary rise, have not been considered in the analyses. To simplify the analyses, the deposition rate of the tailings into the impoundments and real time climatic boundary conditions were not also considered. The stability is presented in terms of the Factor of Safety (FOS), which is generally defined as the ratio of available shear strength in the soil to the mobilized shear stress or the ratio of forces and/or moments resisting failure to forces and/or moments causing failure. Stability is assessed using both the traditional limit-equilibrium-based method (LEM) as well as using finite-element-based Strength Reduction Method (SRM). Technical details of these two methods are presented in Chapter 2.

The accuracy of the study heavily relies on various published design, soil investigation and review reports (e.g. AMEC Consultant 2013a,b; Morgenstern *et al.* 2015) because no lab investigation has been performed to obtain the engineering parameters of the soil. The missing data are assumed from the literature by using appropriate engineering judgements. Pre and post failure observations are also considered when setting boundary conditions for simulations.

Morgenstern *et al.* (2015) noted from the existing monitoring logs that no earthquake or excessive precipitation events had preceded the failure events. Morgenstern *et al.* (2015) also noted that all the piezometers, inclinometers and seepage collection ponds were working properly. Their post-failure site investigation revealed no signs of internal erosions and tension cracks. So, the effects of these parameters were incorporated accordingly, and where possible were omitted, in the current simulations.

A commercially available geotechnical FEM software suite, Geo-Studio 2012, was used in this research. Two components of Geo-Studio 2012: SEEP/W and SIGMA/W were used for finite element simulations. Strength Reduction Method (SRM) was used for stability analysis using the finite element method. SLOPE/W was used to compare the results from the Limit Equilibrium Method (LEM), where necessary. The FOS values were assessed in accordance with the recommended FOS values of 1.3 in the operational stages and 1.5 after the closure provided by the Canadian Dam Association (2012). The SRM results were improved by optimizing meshes as well as spatial and temporal boundary conditions.

1.3 Thesis Structure

The thesis comprises 5 (five) chapters as follows:

Chapter 1 (this chapter) presents an introduction to the thesis. It provides the background of the failed tailings dam at Mount Polley Tailing Storage Facility (MP-TSF), along with the failure event and consequences of the failure. This introductory chapter also provides the objectives and the scope of the present study.

Chapter 2 constitutes relevant literature on tailings, construction methods and failure mechanisms tailings dams followed by failure prevention techniques. A brief discussion on analysis methods is provided in this chapter. Three past case studies of failed tailings dams complement this chapter.

Chapter 3 provides a brief overview of numerical methods in geotechnical engineering perspectives. Verification of the existing designs by numerical analysis is also present in this chapter. The chapter ends with a summary of the results.

Chapter 4 provides results of the parametric study on the dam in which the failure could have been prevented. The most suitable modification that could have prevented the failure is also suggested.

Conclusions of research outcomes and recommendations are summarized in **Chapter 5**. This chapter also has suggestions for further research.

A list of references completes this thesis.

2 LITERATURE REVIEW

This chapter provides an in-depth literature review on tailings, tailings dams and their construction methods. The potential failure modes in tailings dams along with the stability improvement techniques are also discussed in this chapter. The chapter concludes with the brief discussions on stability analysis methods: Limit Equilibrium Method (LEM) and Finite Element Method (FEM).

2.1 Tailings

Tailings are the waste products of the mining industry. They consist of the ground-up rocks that remain after the minerals have been removed from the ore (Vick 1990). Ore quality has deteriorated through the years as the best sources have become exhausted, causing a corresponding increase in the amount of tailings left after the extraction of each ton of metal (Sarsby 2013). Generally, any waste materials produced by the mining activities are considered as tailings; however, the definition of tailings could have been narrowed down to the wastes which are only generated by the ore processing. Because, the wastes, which are produced by other activities such as near-surface cut and fill or waste rocks, might require lesser attention during disposal due to their relatively ‘tame’ chemical composition.

The process of tailings generation and disposal has a number of steps, which are shown in Figure 6. The selection of tailing disposal method is generally driven by topography, climatic, operational, economic, geotechnical or geochemical considerations (Kujawa 2011). Tailings are disposed mainly in two ways: (i) Underground disposal and (ii) On-surface disposal in the form of mine dump, waste piles and impoundments (Priscu 1999; Vick 1990). Underground disposal

technique in terms of backfilling assists the miners by giving working floor, wall support and maximize ore recovery. Underground disposal is not independent of mining planning or operation because of the possible groundwater contamination, however. (Thomson *et al.* 1986; Vick 1990).

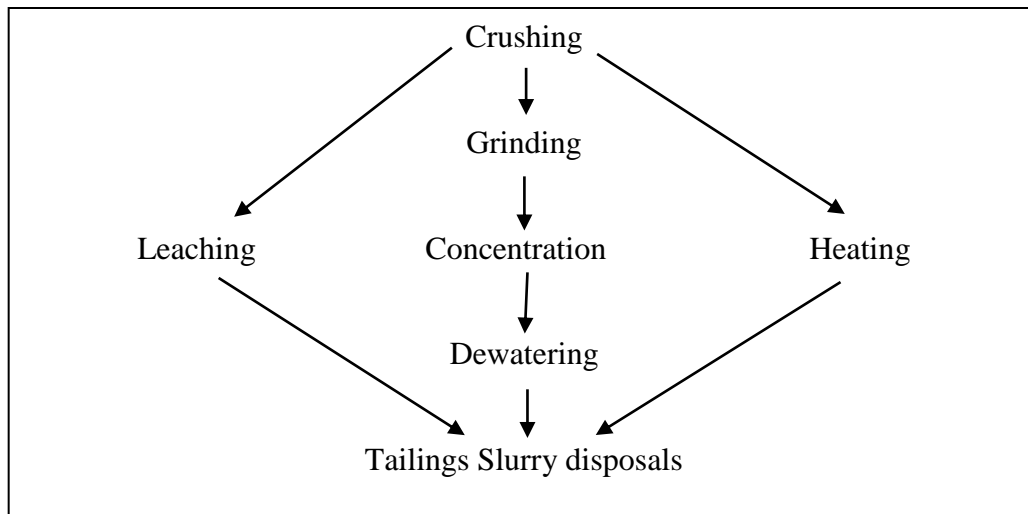


Figure 6: Procedures in tailings productions (after Vick 1990)

In surface disposal method, produced tailings are transported in slurry forms by conduits or channels to the impoundments (Vick 1990). The impoundments are surrounded by tailings dams and embankments. Tailings can be discharged into the impoundments either in sub-aqueous (below water) or sub-aerial (above the water line, on the ground or on the beach) mode. Single point discharge and spigots (multipoint) discharges are used to dispose the tailings into the impoundments. Figure 7 provides a graphical presentation of both of the disposal methods. In spigotting, trial and error procedure might be required to determine the ideal spacing between the discharge points. In single point discharge method, the discharge point may need to move with time to form a uniform beach along the embankments (US EPA 1994; Vick 1990).

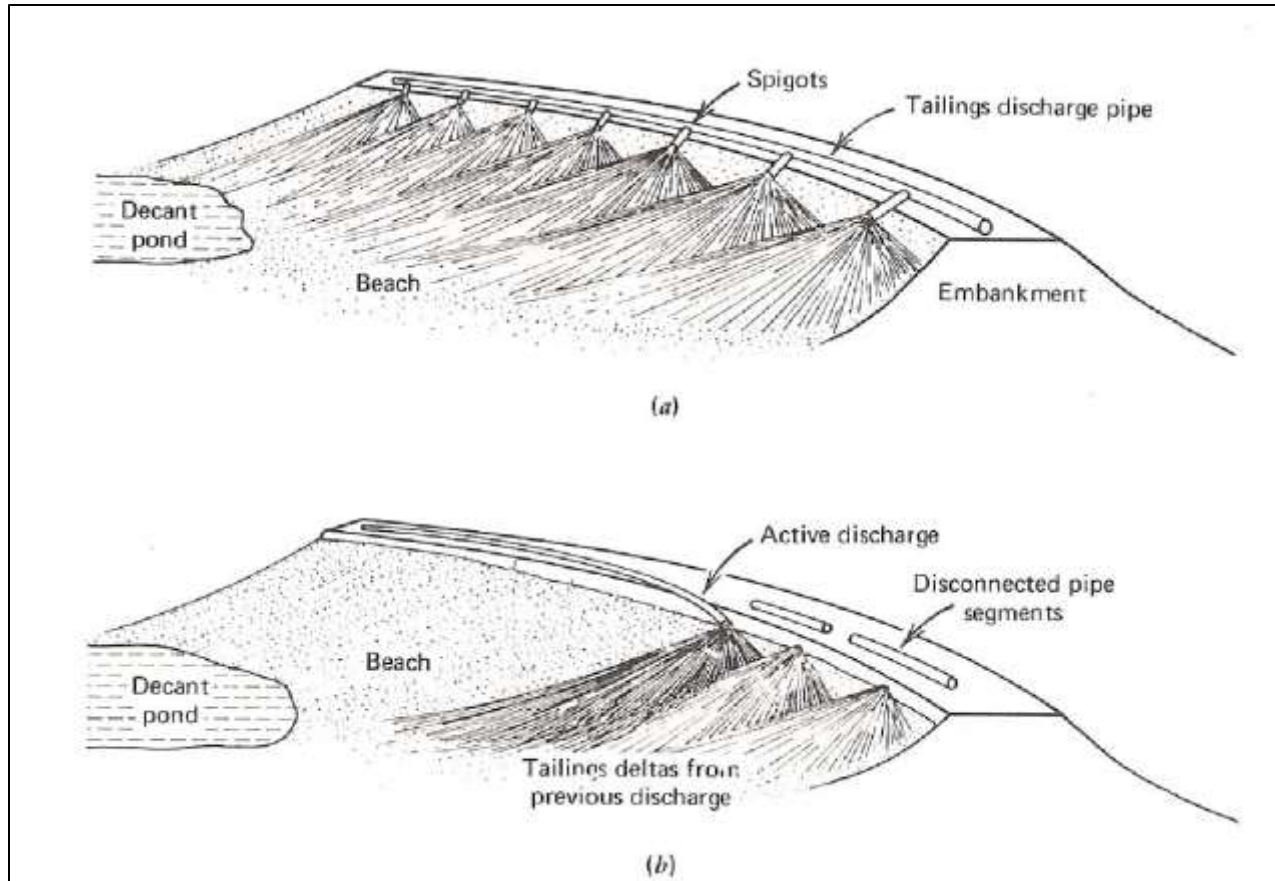


Figure 7: Tailings disposal methods. (a) Spigotting (b) Single point discharge (after Vick 1990)

2.2 Engineering Properties of Tailings

Tailings are usually angular, bulky, grained sand and silt size particles; except for the tailings from the oil sands which are sub-round or round (Sarsby 2013). This angularity is a common feature due to the crushing of ore materials (Bjelkevik and Knutsson 2005). However, weathering and transportation processes of the tailings reduce the angularity in the particles (Rodriguez *et al.* 2014). The chemical and particle composition of the tailings materials effect all the mechanical properties of the tailings (Vick 1990). The grain size and the clay content control void ratio which is typically ranges from 0.6 to 0.9 for tailings sands; and, from 0.7 to 1.3 for slimes with low to moderate plasticity. Density of the tailings shows scattered values based on

the source metal; generally between 45 and 113 lb/ft³. Few slimes, however, have lower density values than this range (Vick 1990).

2.2.1 Hydraulic Conductivity in Tailings

Hydraulic Conductivity in tailings can range widely due to the variability of the grain size distribution, deposition method, plasticity (Vick 1990), chemical composition of the tailings materials and stress history (Alsharedah 2015). Average tailings hydraulic conductivity decreases with increasing fine contents as porosity decreases. The classic Hazen's formula, shown below, can be used to calculate the average tailings hydraulic conductivity (Mittal and Morgenstern 1975).

$$k = Cd_{10}^2 \quad (\text{Eq. 2.1})$$

Where, k = average hydraulic conductivity (cm/s); d_{10} is the grain size in millimeter for which 10% particles pass by weight and C is the correlating constant.

Alsharedah (2015) and Zardari (2011) reported from Bjelkevik and Knutsson (2005) that any empirical formula for predicting the hydraulic conductivity for tailings could be erroneous; the calculated values mostly provide overestimation. Hydraulic conductivity in tailings shows great variation with depth. For the sand deposits, a decrease of 5 orders of magnitude is typical at greater depths (Sarsby 2013). Due to the layered manner of the tailings deposition, significant variation in hydraulic conductivity between horizontal and vertical directions is observed. Typically k_h/k_v values range 2-10 for reasonably beached sand deposits; and 100 or more for clean sands and slimes (Sarsby 2013; Vick 1990). In the literature, the typical values of hydraulic

Conductivities in tailings sands and slimes were found between 1×10^{-3} and 1×10^{-8} cm/s (Blight 2010; Mittal and Morgenstern 1975; Qiu and Segó 2001; Sarsby 2013; Vick 1990).

2.2.2 Compressibility

Both tailings sand and slimes are more compressible than most natural soils due to their depositional stage, angularity and grading characteristics (Vick 1990). The effects of stress history on compressibility is similar to that on natural clays (Lambe and Whitman 1969). One dimensional compression (consolidation) test is commonly used to evaluate the compressibility of the tailings (Qiu and Segó 2001; Vick 1990). Tailings do not often show ‘recompression’ and ‘virgin compression portion’ of the loading curve, however. The compression index, C_c ranges between 0.05 to 0.10 for sands and 0.20 to 0.30 for the slimes (Vick 1990).

2.2.3 Consolidation

Consolidation is the time dependant settlement of soil resulting from the expulsion of water from the soil pores. The consolidation consists of primary consolidation and secondary consolidation or creep. Primary consolidation is the volume change of the fine-grained soil caused by expulsion of water from the voids and the transfer of loads from the water to soil particles. Secondary compression is a result of particle orientation adjustment in the soil fabric after the primary consolidation has ended (e.g.; Das 2010). However, a different hypothesis exists which states that the primary and secondary consolidation start simultaneously after the application of the load (e.g.; Degago *et al.* 2011). The technical debate between different hypotheses is out of the scope of this study.

Primary consolidation of tailings sands occurs so rapidly that it is difficult to measure in the laboratory (Vick 1990). A few consolidation data are available which suggest that the coefficient of consolidation, C_v varies from about $5E-01$ to 10^2 cm/s for beach and sand deposits; and 10^{-2} to 10^{-4} cm/s from slimes (Sarsby 2013). Table 1 provides the values of C_v from different sources.

Table 1: Typical values of Coefficient of Consolidation, C_v (after Sarsby 2013)

Source	Sands ($m^2/year$)	Slime ($m^2/year$)
Vick (1990)	-	0.3–30
Genevois and Tecca (1993)	-	60
Volpe (1979)	1200	-
Mittal and Morgenstern (1975)	-	3–300
Nelson <i>et al.</i> (1977)	320 000	-
Chandler and Tosatti (1995)	-	95
Routh (1984)	39–142	11–43
Qiu (2001)	32–104	0.3–14

2.2.4 Shear Strength

Drained shear strength occurs when the pore water pressure dissipates (e.g.; Das 2010). Tailings have high drained shear strength (effective stress) due to its high degree of particular angularity. It is not uncommon to have an effective angle of internal friction, Φ' higher than that of natural soils at same density and stress level (Vick 1990). For tailings, cohesion excerpts are generally considered as zero (Vick 1990). Typical values for Φ' are shown in Table 2.

Table 2: Typical values for drained shear strength (after Sarsby 2013)

Material	Φ'	Effective stress range (KPa)	Source
Copper sands	34	0-816	Mittal and Morgenstern, 1975
Copper sands	33-37	0-672	Volpe, 1975
Copper slimes	33-37	0-672	Volpe, 1975
Gold slimes	20-40.5	960	Blight and Steffen, 1979

Stress level plays an influential role for Φ' . Even at low effective stress levels, the point to point contacts of the angular grains are very high which produce particle crushing (Alsharedah 2015; Vick 1990). Hence, that results in curvature of the strength envelope. Figure 8 shows that Φ' shows curvature of the envelope for loose sands, resulting the range from 41° to 29° . Figure 9 shows the variation of Φ' with the increase of effective stress. At higher stresses, the particle crushing and dilatancy emerge which reduces the Φ' (Vick 1990).

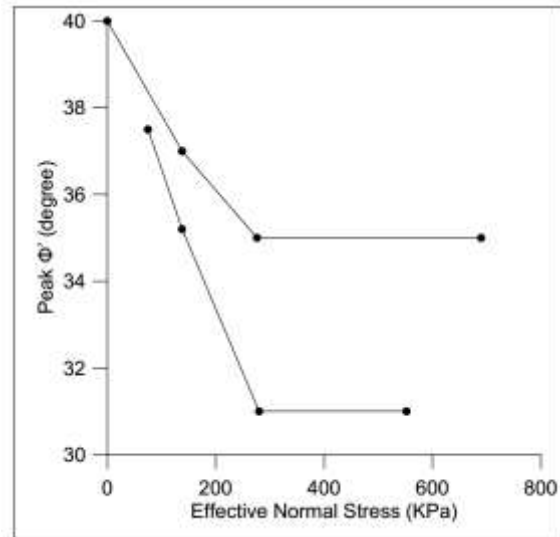
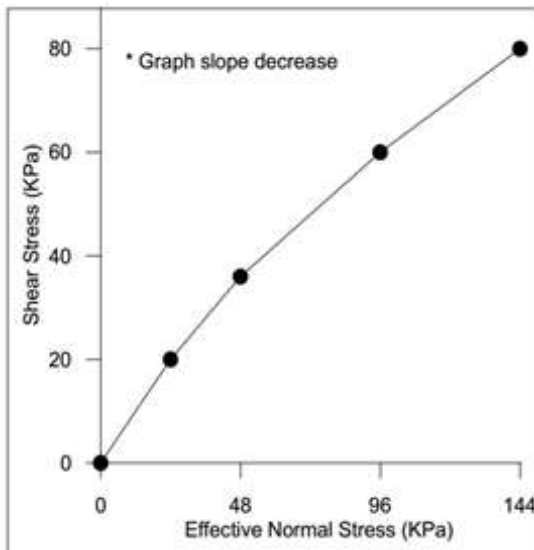


Figure 8: Curvature of the envelop in shear-normal stress (redrawn after Vick 1990)

Figure 9: Variation in Φ' with effective normal stress (redrawn after Vick 1990)

Undrained condition occurs when the pore water pressure cannot drain rapidly from the soil (e.g. Das 2010). When the rate of dissipation is slower than the development of the pore water pressure by the loading, the volume change will not occur. For fine-grained soil like clay, the pore water pressure increase makes the soil to exhibit flow-like behaviour. This mechanism is called Static Liquefaction (e.g., Konrad and Watts 1995). This is not applicable for coarse-grained soil as hydraulic conductivity is very high within coarse grained soils. However, during

dynamic shaking of soil, the excess pore water develops so quickly that even the coarse grained soil can show liquefaction. This mechanism is called dynamic liquefaction. (e.g.; Fourie *et al.* 2001; Ishihara *et al.* 2015; Konrad and Watts 1995; Stark and Mesri 1992). Sarsby (2013) stated that tailings with 50%-60% relative density do not liquefy under 0.1-g acceleration. It is also noted by Sarsby (2013) that the liquefaction only occurs in saturated zone, i.e. below the phreatic surface. It is not uncommon, however, to have tailings with relative density 30%-50%. Such tailings are prone to dynamic liquefaction during earthquakes.

Undrained shear strength is dependent on effective vertical stress on the soil. Stark and Mesri (1992) described the relation between the undrained shear strength and the vertical effective stress by the following simple equation.

$$S_u = m * \sigma'_p \quad (\text{Eq. 2.2})$$

Where, S_u is the undrained shear strength of a soil, σ'_p is the vertical effective stress and m is the multiplication factor. Stark and Mesri (1992) stated that the value of the factor, m is 0.22; however, many researchers proposed different values for the factor of m , ranging from 0.15 to 0.30 (Sarsby 2013). The undrained shear strength is commonly determined by consolidated undrained test in the laboratory (e.g.; Das 2010). For the most tailings deposits, the total angle of friction, Φ ranges from 14° to 24° which is roughly less than half of the effective angle of friction, Φ' (Vick 1990). A list of total angle of friction and total cohesion excerpts are shown in Table 3.

Table 3: Typical total stress parameter for Copper tailings (after Vick 1990)

Material	Initial void ratio, e_0	Total angle of friction, Φ (degree)	Total cohesion excerpt, C_T (KPa)	Source
Copper tailings	0.6	13-18	0-96	Volpe, 1979
Copper beach	0.7	19-20	34-43	Wahler, 1974
Copper slimes	0.6	14	62	Wahler, 1974
Copper slimes	0.9-1.3	14-24	0-19	Wahler, 1974

2.3 Tailings Dams

Tailings materials are retained on the earth surface with the help of tailings dams or embankments; however, the design and construction of a tailings dam is highly site specific. On-site topography, type of the mines, foundation condition, disposal method are among the factors that influence the design of a tailings dams (Berghe *et al.* 2011; Sarsby 2013; US EPA 1994; Vick 1990). Generally, two different types of tailings impoundment structures exist: (i) Retention type and (ii) Raised Embankment type.

Retention type of tailings dam (Figure 10) is similar to the water retention dam in terms of soil properties, surface and ground water controls and stability considerations. This type of dam is built to its full height before the tailings disposal. Rapid drawdown condition is not experienced by this type of dam, which makes it feasible for any type of impoundment with large run-off. (US EPA 1994)

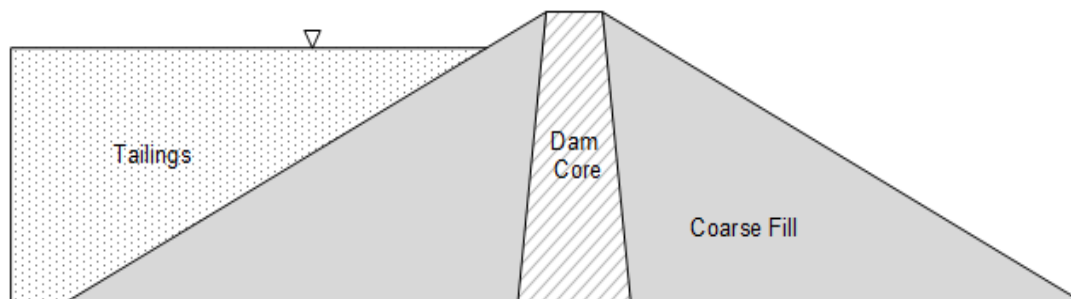


Figure 10: Conceptual drawing for Retention Tailings dam (modified from US EPA 1994)

All the raised embankment types of dams start with a starter dike, followed by subsequent raisings (Vick 1990). In the **upstream method**, subsequent raisings are constructed in upstream direction (Figure 11). Tailings disposed in the impoundment form a beach. This method takes the advantages of self-consolidated beach materials. Subsequent dykes are placed on these consolidated beach materials. This procedure saves material costing. Hence this is the most popular construction method in the mining industry. Upstream method is not favorable in many cases, since its long term stability condition is uncertain. The location of phreatic line is critical element of embankment stability. The faster raisings can develop excess pore water pressure in the foundation which creates static liquefaction (Martin 1999; Vick 1990). This method is not also recommended for the areas with high seismicity due to the dynamic liquefaction potential failure (e.g.; Villavicencio *et al.* 2014). This is why this method is not preferable from the design point of view although it gained huge popularity among the miners due to its economy.

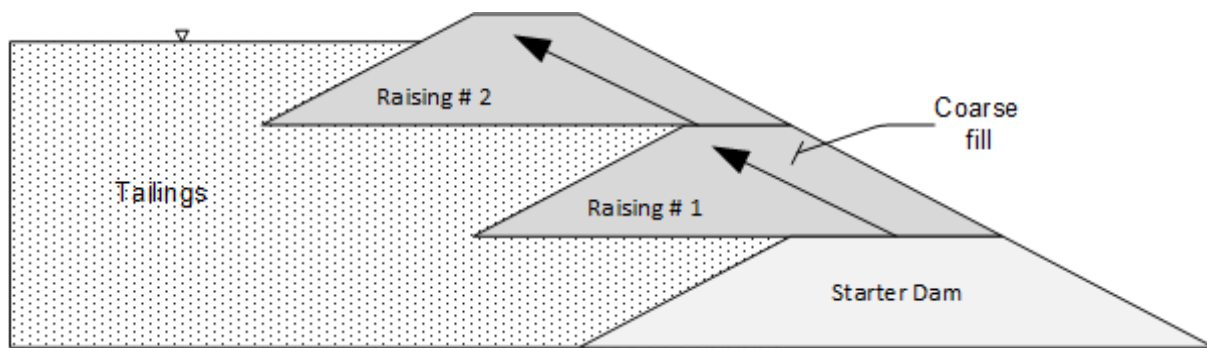


Figure 11: Conceptual drawing for Upstream Tailings dam (modified from Vick 1990)

The **downstream method** is illustrated in Figure 12. Tailings are disposed at the back of the starter dike and subsequent raisings are constructed in downstream direction. Impervious cores and drainages system provide better control of phreatic line in downstream method. There is limited restriction of raising rates, because subsequent dikes not dependent on the tailings materials. Thus, this method provides the most stable embankment condition. However, this

method requires careful advance planning. Because, the toe of the dam progresses outward with each raisings, sufficient space must be left during the starter dike. Another major disadvantage of this method is the requirement of comparatively large fill volume, which makes the dam costly. (Sarsby 2013; Vick 1990)

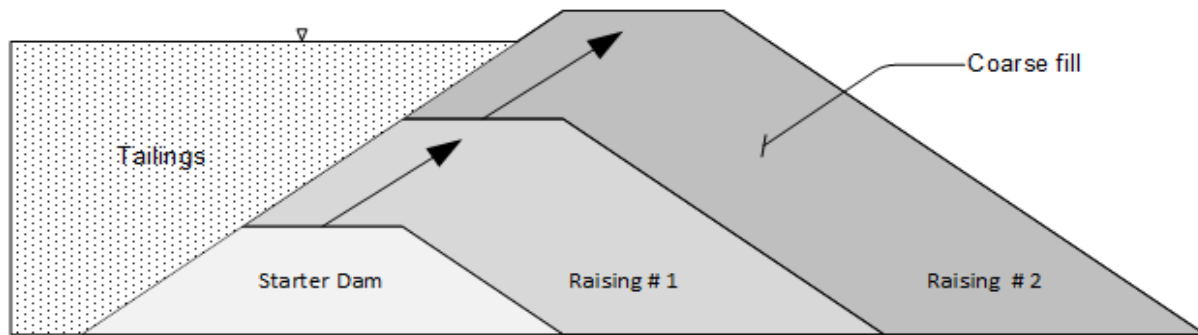


Figure 12: Conceptual drawing for Downstream Tailings dam (modified from Vick 1990)

In the **centerline method** (*Figure 13*) the dam is raised in both upstream and downstream sides simultaneously, keeping the centerline same for all the raisings. As the internal drainage zones can be provided in this method, control of phreatic line is not sensitive to tailing beach development. Nevertheless, the dams constructed using centerline method cannot retain large of water as downstream method does. Centreline method provides a well balance between upstream and downstream construction method as less fill required than downstream method for the construction and raising rate is less restrictive than the upstream method. Centerline method also gives good seismic resistance. Even if the upstream portion sitting on the tailings liquefies, the central and downstream sides may remain stable. This is, however, valid if the material is properly compacted and good internal drainage is provided (Vick 1990).

Water management in tailings dams is an important issue. A well-managed supernatant pond is one of the most important procedures in managing a tailings storage facility. Inadequate control

in supernatant pond may result in overtopping, increased pore water pressure, reduction in freeboard, high seepage rate and embankment settlement (Engels and Dixon-Hardy 2012). Decant tower and reclaim ponds are used to control the elevation of the supernatant pond. The phreatic surface is controlled in design phase by zoning of materials based on permeability in tailings dams and different zoning facilities (Vick 1990).

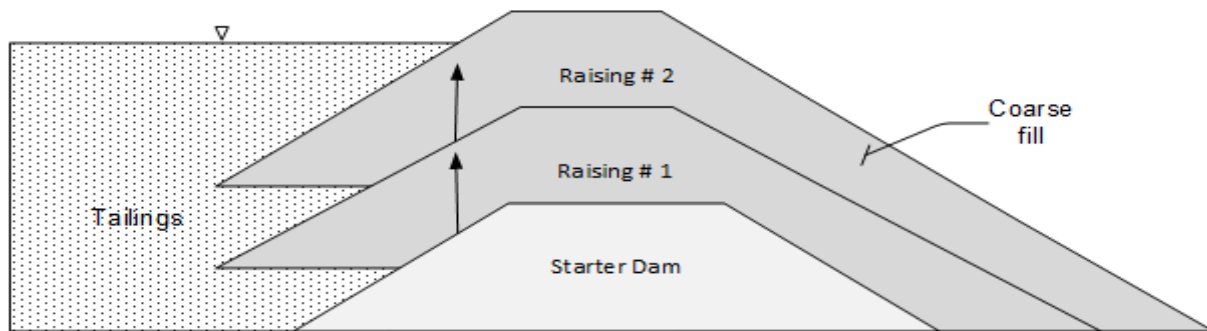


Figure 13: Conceptual drawing for Centreline Tailings dam (modified from Vick 1990)

2.4 Tailings dam in Mount Polley Tailings Storage Facility (MP-TSF)

At MP-TSF, all three tailings dams: Main, Perimeter and South were constructed in modified centreline method (AMEC Consultant 2013b). In modified centreline method, the dam is gradually constructed along the centreline with a small tilt towards either to upstream or downstream direction (Haile and Brouwer 1994). For MP-TSF, the core of the dam, which was made of compacted till, had slight upstream inclination. The construction of the starter dam began in 2005. After the 9 stages of construction, the maximum dam elevation reached 965 m. True height varied from 35 m to 50 m along the embankments (AMEC Consultant 2013b; Morgenstern *et al.* 2015). Significant freeboard was maintained throughout the dam lifetime; a freeboard of 2.3 m was recorded just before the failure. An upstream toe drain conveyed the

water flows to the downstream seepage collection ponds, which had been reported to be working fine till the failure (Morgenstern *et al.* 2015).

2.5 Failure Mechanism in Tailings Dams

“A failure or fault is the cessation of the ability of a component” (Santos *et al.* 2012). The failure rate in tailings dams is significantly high: 1.2% whereas the failure rate in traditional water retention dams is just 0.1% (Azam and Li 2010). Since the start of the past century, there have been more than 225 tailings dam failures reported in the literature (Azam and Li 2010; Rico *et al.* 2008; WISE Uranium Project 2016). It is also perceived that the number of failures are under-reported due to fears of bad publicity and legal ramifications (Davies 2002), particularly in China and Russia (Kossoff *et al.* 2014). The increased rate of failure may be attributed to the rapid constructions of the tailings dams along with the poor monitoring system. In general, three types of failure mechanisms in tailing dams are found in literature. These are:

- Geotechnical instability
- Hydraulic instability
- Failure due to human interventions

Some of the major failure events in tailings dams are listed below:

Table 4: List of some major tailings dam failure

Name of the failure	Year	Possible Cause of Failure
Mochikoshi # 1, Japan	1978	Dynamic liquefaction due to Earthquake
Stava dam, Italy	1985	Slope instability, excess seepage
Merriespruit, South Africa	1994	Precipitation induced overtopping, liquefaction
Omai, Guyana	1995	Filter inadequacy, internal erosion
Aznalcollar , Spain	1998	Weak foundation layer beneath embankment
Baia Mare, Romania	2000	Overtopping due to rain & snow melt
Samarco, Brazil	2015	Vandalism

The types of failures in tailings dams are described below in order.

2.5.1 Geotechnical Instability

Geotechnical stability includes the dam's resistance to failure against slope instability (Vick 1990), pre-shearing bedding planes instability (Alonso and Gens 2006; Kossoff *et al.* 2014), liquefaction in tailings (for upstream dams; Martin and McRoberts 1999) and foundation (Cambridge 2014), excessive deformation in foundation layers (Pastor *et al.* 2002), etc. Other important factors that have effects on geo-structural stability of the tailings dams are weathered crack on the downstream slope (Gao *et al.* 2015; Vick 1990) and tension crack in curved embankment (Ormann *et al.* 2013), high deposition rate of tailing which may cause excessive horizontal translation or thrust towards the downstream (Priscu 1999) and chemical degradation/erosion in the upstream side of the embankment (Blight and Amponsah-da Costa 1999).

Slope failure in tailings dams can occur in either upstream or downstream direction. When the movement of a soil mass due to gravity and applied stress surpasses the strength of the soil, the slope becomes unstable. Factors that increase the stresses (e.g. additional load) and factors that decrease soil strength (e.g. pore water pressure development, strain softening) contribute to the slope instability (Das 2010). The available approaches to stabilize a vulnerable slope include a well-designed 'milder' slope (e.g.; Fell *et al.* 2014), a rockfill patch (riprap) added to the downstream slope (Ormann *et al.* 2013), vegetation on the downstream slope (Vick 1990), upstream stability improvement by adding chemical/ soil additives in tailings materials to increase their strengths (Alsharedah 2015) or thickened tailings (Azam *et al.* 2009), and reinforcing the soil with geotextile (List 1999; Yi-Shu *et al.* 2015). However, Federal Emergency Management Agency (2008) recommends not using geotextile in structurally critical sections of the dam.

Davies and Martin (2002) reported that static liquefaction is the most common cause of tailings dam failure. In static liquefaction, pore water pressure can develop due to fast construction process (generally more than 5-10 m added height per year; Sarsby 2013), high phreatic level, low hydraulic conductivities in tailings and foundation layers or excessive precipitation (Fourie *et al.* 2001; Vick 1990; Zardari 2011). Thus, it decreases the effective strength of soil (Martin 1999; Vick 1990). Relative density, confining pressure, strain softening behaviour and initial shear stress of the soil are the major factors controlling the static liquefaction (Davies and Martin 2002). Active tailings dams are more vulnerable to liquefaction than the inactive dams (Rico *et al.* 2008). The reason behind this is the cementation in tailings and soils which increases approximately 20% in 30 years. This cementation increases the liquefaction resistance (Kossoff

et al. 2014). Merriespruit tailings dam in South Africa is an example of failure due to static liquefaction (Strydom and Williams 1999).

Pore water pressure can also develop due to ground-shaking mainly in high seismic countries like Chile and Japan (Ishihara *et al.* 2015; Villavicencio *et al.* 2014). This mechanism is an example of dynamic liquefaction (Vick 1990). Psarropoulos and Tsompanakis (2008) reported from (Vick 1990) that downstream construction method is more resistant against earthquakes. Dams constructed using this method also showed smaller deformation compared to other construction methods. In upstream method, dams resting on thickened tailings has greater liquefaction potential at higher peak ground acceleration in earthquake (Poulos and Bunce 2008).

2.5.2 Hydraulic Instability

The soil always shows a love-hate relationship with water. Too much or too little water in the soil affects the strength of the soil. This is why, hydraulic aspects of the soils, such as the location of the phreatic surface in soil, are closely related to the geotechnical aspects. The phreatic surface location partially controls the factor of safety of the dam. Low permeability of foundation layers, excessive precipitation, flooding, inefficient drainage and seepage collection system elevate the phreatic surface in the dam body (Vick 1990). Thus it decreases the soil's effective strength within the dam material. Zandarín *et al.* (2009) stated that the capillary rise of water also further reduces the stability of the dam. Void ratio and moisture content of tailings determine the degree of capillarity in the tailing materials (Carelsen 2013). The inefficiency of filter material increases the phreatic level by clogging the particles to the downstream direction (Reddi *et al.* 2000).

Introduction of geotextile as a filter material can improve the filter capacity of the tailing dams (List 1999). Choice of deposition method of tailings (Vick 1990), under-drains provided at the bottom of tailings (McLeod and Murray 2003) or the decant pipes to take out water from the ponding zone on the tailing surface (Breitenbach 2009) can also help to reduce phreatic level. Inefficiency of filter material create internal erosion, termed as ‘piping’ in the embankment. The piping, along with the cracking, reduces the stability of the dam (Foster *et al.* 2000; Hu *et al.* 2015; Vick 1990).

Excessive precipitation or external sources of water into impoundment due to flood-like events in absence of an effective spillway drainage system can initiate an overtopping incident (Javadi and Mahdi 2014; Sun *et al.* 2012). Stava tailing dam in Italy (Chandler *et al.* 1995) and Merriespruit tailing dam in South Africa failed due to excess rainfall (Van Niekerk and Viljoen 2005). In both cases, rainfall in excess also caused static liquefaction by increasing pore water pressure in the foundation (Fourie *et al.* 2001; Lucchi and Tosatti 2009; Strydom and Williams 1999). Change in atmospheric boundary conditions due to climate change also should be considered while designing a new tailing dam or reviewing an existing one (Kwon 2015).

2.5.3 Human Interventions

Other than human errors during engineering design and construction, tailing dams also failed few times due to human interventions. Vandalism in Samarco tailing dam in Brazil caused pollution in Doce River for over 300 km downstream. The failure dam unleashed at least 40 million cubic meters of tailings on the valley. At least 30 people were killed and 800 people lost their homes in the incident (McCrae 2015). Negligence in Karamken Dam in Russia caused 1 death and the loss of 11 houses (Robinson 2008).

A good managerial practice in terms of better monitoring, maintenance, corporate culture and establishing a dam safety review board would reduce the risk of human interventions (Morgenstern *et al.* 2015).

2.6 Stability Analysis Methods

The stability analysis of a slope or a particular geologic and physical feature is performed to assess the safety factors. Factors of safety (FOS) can be defined as the ratio of available shear strength (S) of the slope to its equilibrium stress (τ) (Duncan 1996).

$$FOS = \frac{S}{\tau} \quad (\text{Eq. 2.3})$$

The slope stability can be performed for the following usages (Das 2010; Duncan 1996):

- To assess the safety of a slope structure
- To locate the critical failure surface
- To assess the movement of the slope
- To understand the sensitivity of a slope to its geologic parameters and climatic conditions
- To assess the remedial measures and aid in the design

To perform a slope stability analysis, the geometry of the slope, external and internal loading, soil engineering properties and the variation of ground water table must be well defined. For a slope to be stable, the resisting forces in the slope must be significantly greater than the forces causing the failure (Duncan 1996). Various codes, regulations and guidelines around world have different recommended values for a slope to be stable. According to Canadian Dam Association (2012), the factors of safety of any dam must conform to the following values:

During Operating Stage	1.3
After Closure	1.5
Rapid Drawdown	1.2

2.6.1 Limit Equilibrium Method (LEM)

Several Limit Equilibrium Methods (LEM) have been developed for the slope stability analysis. Fellenius (1936) introduced the first method, alternatively known as the Ordinary or the Swedish method, for a circular slip surface. All LEM methods are solved using either of the two approaches: (a) selecting the entire mass of soil and solve for a single free body and (b) dividing the soil into a number of slices where each slice has to satisfy all the force equilibrium (Duncan 1996). Regardless of the approach taken for the analysis, all methods require certain assumptions; and none of them considers stress-strain behavior of the soil. For slice-based methods, the basic difference among the methods is how the interslice normal (E) and shear (S) forces are determined. In addition, the shape and size of the slip surface can also differ between the analysis methods. Table 5 compares different LEM methods based on the shape of the slip circle and the force-moment equilibrium.

Table 5: Comparison among LEM

Methods	Circular	Non-circular	$\sum M = 0$	$\sum F = 0$
Ordinary	Yes	-	Yes	-
Bishop simplified	Yes	Yes	Yes	Yes
Janbu simplified	-	Yes	-	Yes
Janbu GPS	Yes	Yes	Yes	Yes
Lowe-Karafiath	-	Yes	Yes	Yes
Corps of Engineers	-	Yes	Yes	Yes
Sarma	Yes	Yes	Yes	Yes
Spencer	Yes	Yes	Yes	Yes
Morgenstern-Price	Yes	Yes	Yes	Yes

Figure 14 shows a simple slope and its slip circle. A detailed figure of a single slice is shown in the right hand side of the figure. In this figure, W represents weight of the slice, E_1 and E_2 are normal forces acting on the sides of the slice, and N' is the normal force and S is the shear force acting on the base of the slice. By using these forces, resisting and driving moments are calculated and their ratio gives the factor of safety value. (Das 2010)

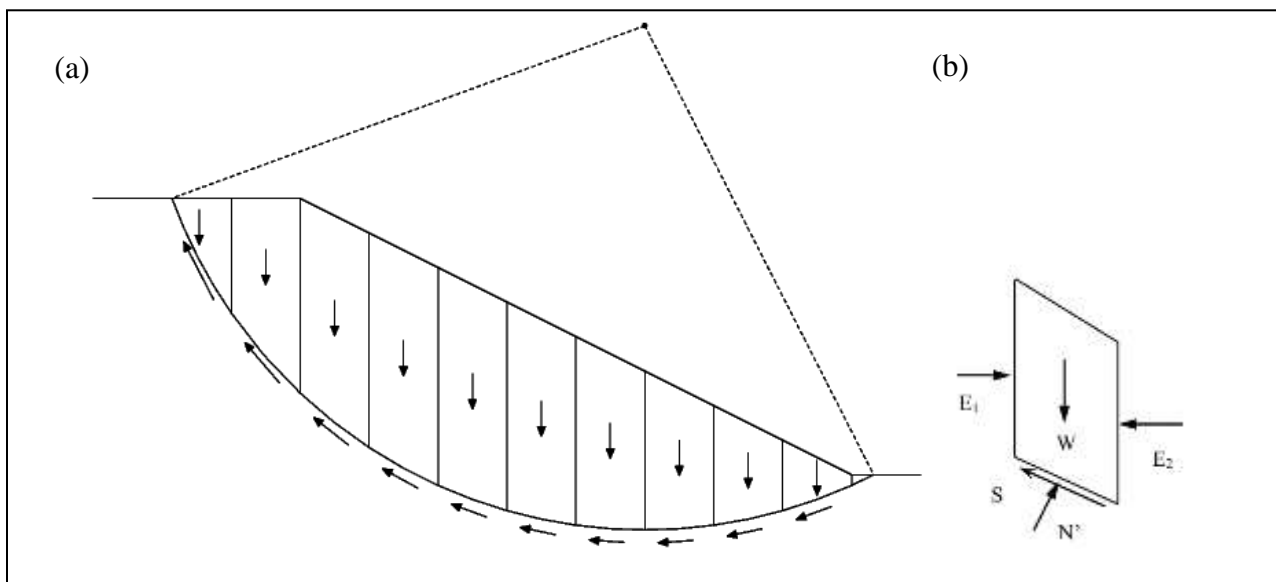


Figure 14: Sample slicing procedure in LEM

2.6.2 Finite Element Method (FEM)

Finite Element Method (FEM) is relatively a new method for slope stability analysis. It was first used in geotechnical analysis in 1966 (Kondalamahanthy 2013). Unlike limit equilibrium method, the finite element method considers linear and non-linear stress-strain behavior of the soil (e.g.; Griffiths 2001). This is why the results obtained by FEM are considered more realistic than that of LEM. Shear Strength Reduction (SSR) technique within FEM involves in reduction

of the soil strength parameters (Mohr-Coulomb) using a factor in the following equation (e.g.; Cheng and Lau 2008).

$$\frac{\tau'}{SRF} = \frac{C'}{SRF} + \frac{\tan\Phi'}{SRF} \quad (\text{Eq. 2.4})$$

Where, τ' , C' , Φ' are Shear Strength, Cohesion intercept and Angle of internal friction respectively in effective stress parameter. And, SRF is the Shear Strength Reduction factor.

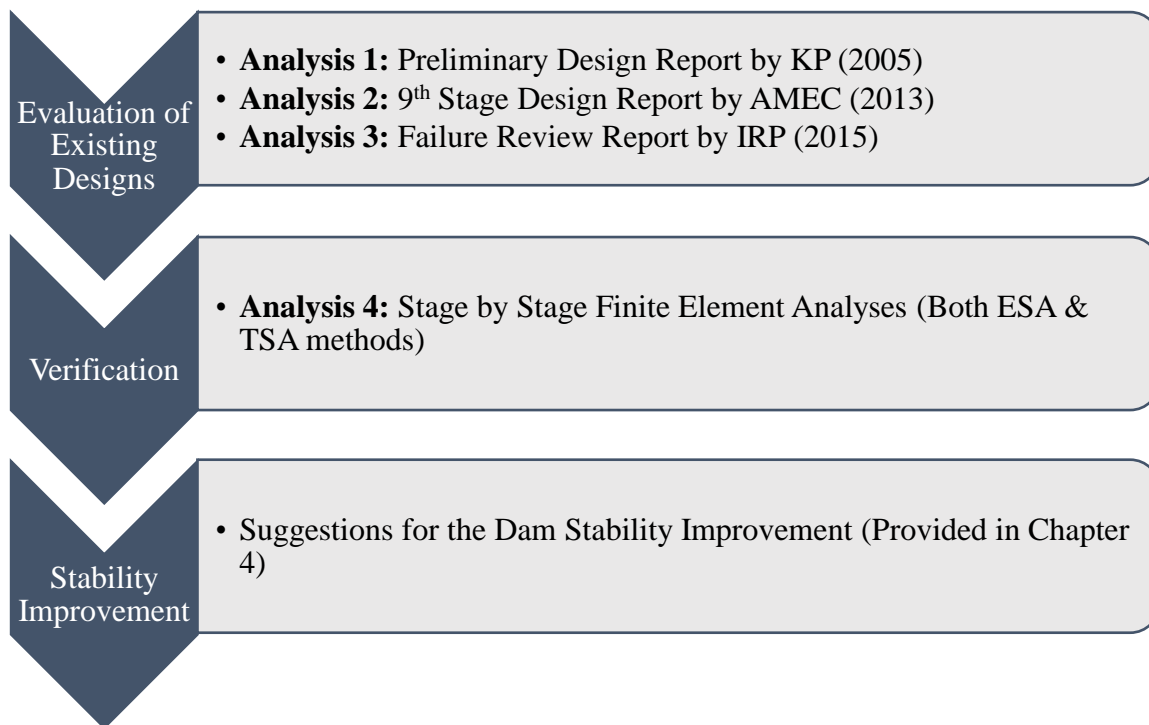
The reduction of the strength parameters by trial SRF values continues until the slope materials reach on the verge of failure i.e. the safety factor becomes 1. At this moment, SRF become the factor of safety of the slope (Griffiths 2001). In finite element based software like SIGMA/W, the failure is presented by the non-convergence in the system (Krahn 2004a). For the slopes that already have factors of safety less than 1, the strength parameters are increased by a factor until the analysis converges to a solution (Griffiths 2001).

FEM is advantageous over LEM in many aspects; such as FEM does not consider the soil domain as a rigid body and the stress-strain field is established within it. Another major advantage is that there is no need to assume imaginary slices, or the entry or exit surfaces for the slip circle. The failure occurs automatically through the zones in which soil strength is unable to resist the applied shear forces (Griffiths 2001). FEM take more time for analysis due to the processes of discretization of domains and optimization of elements. That is why, for simple stability problems LEM analysis is sufficient.

3 NUMERICAL ANALYSIS ON FAILURE MECHANISM

This chapter presents the results of the numerical analysis of the failed perimeter embankment at MP-TSF. The first three analyses using Limit Equilibrium Method (LEM) replicated the engineering designs and post-failure reviews which already have been published. The fourth analysis was done in multi-stages by using Finite Element Method (FEM) to verify the findings by Morgenstern *et al.* (2015). The details of data, boundary conditions and results are provided in each analysis separately. A summary of results of all analyses completes the chapter. All the factors of safety (FOS) obtained by these analyses were compared against the recommended FOS (1.3 for operational stage and 1.5 in post-closure) by Canadian Dam Association (2012).

The work flowchart for the analyses is shown below:



3.1 Data Sources

For the current study, no lab testing for the materials was performed to obtain the soil parameters. All the engineering data were taken from the published design, soil investigation, annual review, and post failure review reports. The following sources provide most of the material properties of soils. The missing data were assumed from the existing literature (e.g. Fell *et al.* 2014; Sarsby 2013; Vick 1990).

- Preliminary design report by Knight Piésold Consulting (2005)
- 9th Stage design report by AMEC (2013)
- Annual review reports of MP-TSF (2005-2014)
- Failure review report by Morgenstern *et al.* (2015)
- Soil investigation report by ConeTec Investigations Ltd (2014)

3.2 Numerical Tools for the Simulations

In this study, GeoStudio 2012 was used for the purpose of two dimensional stability and seepage analysis. Out of eight components of GeoStudio 2012, only the following three were used: SIGMA/W, SLOPE/W and SEEP/W. The pore water conditions obtained from the SEEP/W analyses were imported into the analyses of SIGMA/W and SLOPE/W. Appropriate boundary conditions in all the analyses were assumed to simulate the existing site conditions.

3.2.1 SIGMA/W

SIGMA/W is finite element based software, which is used to determine the stress-strain conditions in earth structures. It can simulate multi-stage constructions, pore-water pressure conditions, soil-structure interaction and consolidation analyses. Mesh generation is an automatic

process in SIGMA/W; however, optimization of meshes in terms of size and shape is possible. Included Soil constitutive models are Linear Elastic model, Anisotropic Elastic model, Elastic-Plastic model, Cam-Clay model etc. Boundary conditions can be provided by restraining or allowing horizontal or vertical translation and rotation (Krahn 2004a).

3.2.2 SLOPE/W

SLOPE/W is a powerful tool to analyze the stability of the slope. It works on LEM framework. Many LEM analysis methods are included in SLOPE/W such as: Morgenstern-Price method, Spencer's method, Bishop's simplified method, Janbu's generalized method and Ordinary slices method etc. Finite Element stress-strain based stability analysis can be done within it by using SIGMA/W or QUAKE/W stresses. Soil Models included in SLOPE/W are Mohr-Coulomb method, Undrained strength method, Anisotropic strength model, Bilinear models etc. SLOPE/W can also analyze different types of reinforcement such as anchors, geo-fabrics, soil nails, piles, sheet piles etc. (Krahn 2004b).

3.2.3 SEEP/W

SEEP/W analyzes the flow of water through both saturated and unsaturated soils for geotechnical purposes. Both Steady-state and Transient seepage analyses can be performed by using various boundary conditions in terms of pressure and total heads and fluxes. Mesh generation and staged construction processes are similar to that of SIGMA/W. Material properties can be entered in both Total and Effective Stress parameters. It can also simulate anisotropy in hydraulic conductivities. (Krahn 2004c).

3.3 Review of the Published Analyses

The first three analyses replicated already published design reports of MP-TSF. All of them were done only for the final construction stage (stage 9) by using Morgenstern-Price type of LEM analysis within SLOPE/W environment. Pore water conditions were obtained by setting arbitrary ‘high’ and ‘low’ phreatic surfaces in different analyses. The results of the stability are presented in terms of the FOS. The following sections provide detailed description and the results of each analysis.

3.3.1 Analysis 1: Preliminary Design Report by Knight Piésold Consulting (2005)

The first design report for the TSF was produced before the mining operation had started in 1997; however, it was revised in 2005. Stability analyses were performed for both static and dynamic conditions. Only the static part, however, was reproduced for this study as any seismic activity prior to the failure wasn’t recorded. A toe drain was added to all three dams: main, perimeter and south. The dams to be built in nine (9) stages had an ultimate elevation of 965 m. A schematic diagram of the dam is shown in Figure 15.

The material properties of the embankment materials are shown in Table 6. Most of the soil properties are described by using Mohr-Coulomb model. Tailings materials are additionally presented in terms of ‘Overburden function’ to assess the liquefaction effects. Hydraulic conductivities are also presented in the material properties tables; however, it was missing for Rockfill. A higher saturated hydraulic conductivity of 1E-05 m/s was assumed for the Rockfill in all the following analyses. However, hydraulic conductivities were only used in filter design; not in coupled stability analyses. Thin chimney drain, transition layer and clay liner were merged into Rockfill and Till layers respectively for the simplicity of the simulation.

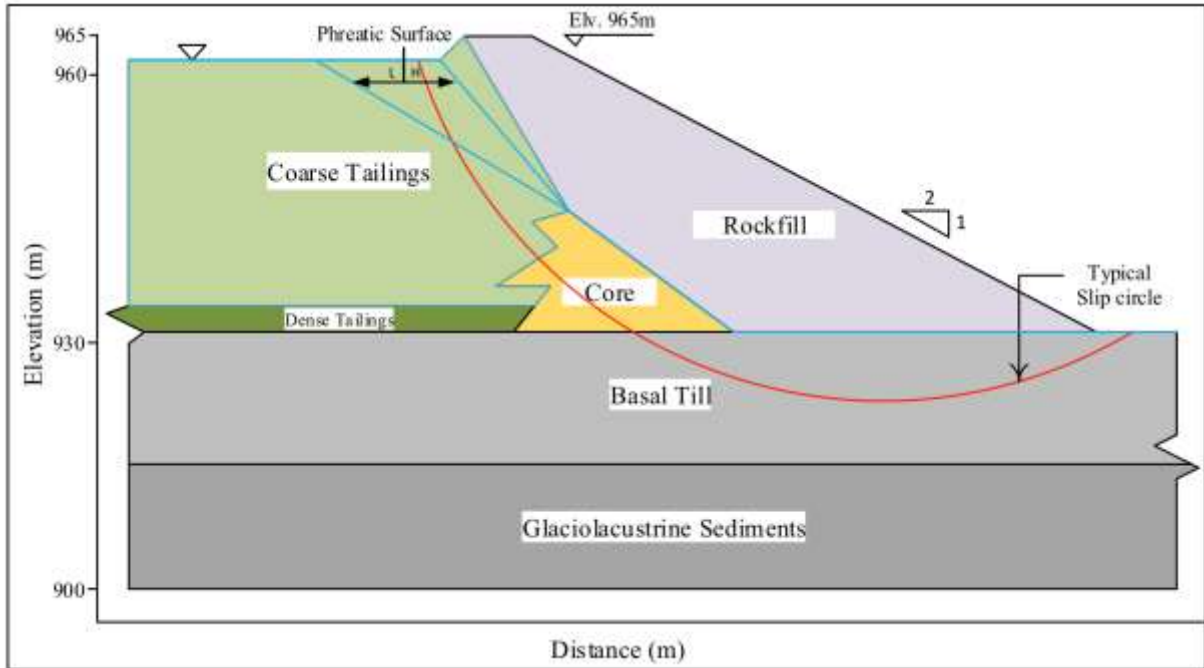


Figure 15: Preliminary design section reproduced from Knight Piesold Consultant (2005)

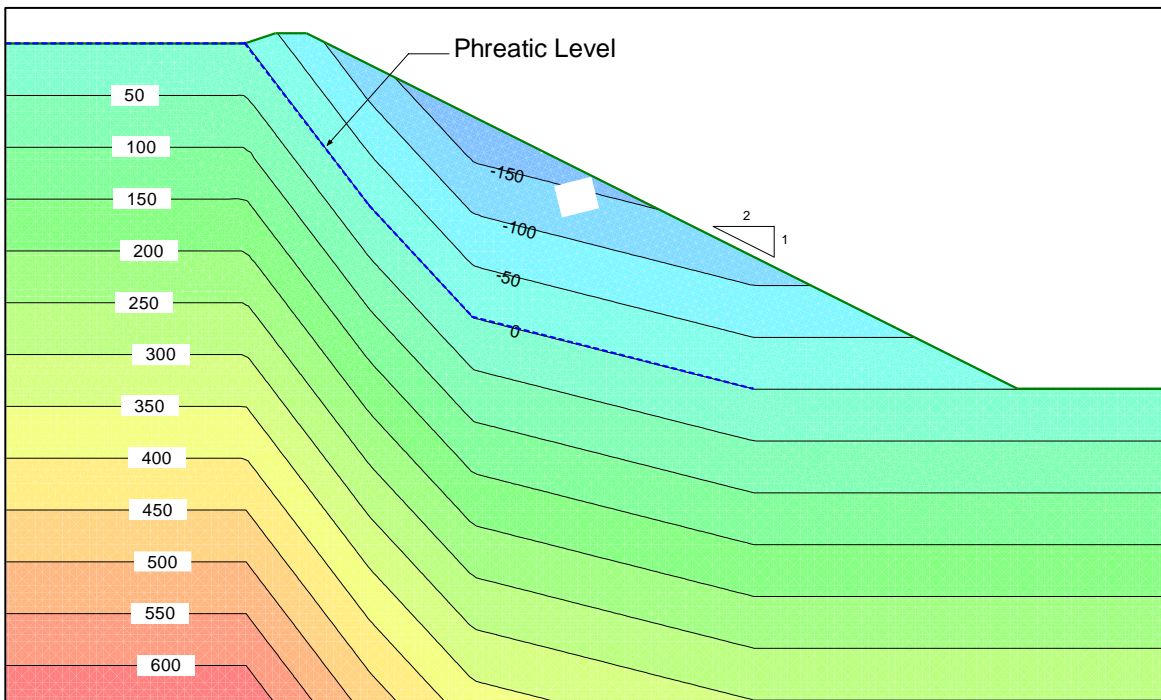


Figure 16: Pore water pressure (in kPa) contour for the Preliminary design

Pore water conditions were obtained differently by setting two different arbitrary phreatic surfaces: ‘High’ and ‘Low’. The pore water pressure contour for high phreatic surface, being the

critical of the two, has been shown in Figure 16. The analysis was done for both Pre-liquefied and post-liquefied tailings as well as for drained condition using Mohr-Coulomb model. The results are presented in terms of FOS are shown in Table 7. The undrained response in the foundation was not considered in the Preliminary design. The results indicate that FOS, being higher than the recommended FOS, did not change significantly between High and Low phreatic surfaces.

Table 6: Material properties used in Preliminary design (2005)

Soil Layers	Soil Model	Material properties	
		Mechanical	Hydraulic Conductivity (m/s)
Bedrock	-	-	-
Lower Till	Mohr-Coulomb	$\gamma = 21 \text{ kN/m}^3$, $\Phi = 33^\circ$, $C = 0$	1.0 E-08
Upper Till			
Glaciolacustrine (GLU)	Mohr-Coulomb	$\gamma = 20 \text{ kN/m}^3$, $\Phi = 33^\circ$, $C = 0$	1.0 E-06
Tailings	Mohr-Coulomb	$\gamma = 18 \text{ kN/m}^3$, $\Phi = 30^\circ$, $C = 0$	Coarse: 7.0E-06 Dense: 1.0 E-08
	S = F(Overburden)	[Pre-liquefied] $\gamma = 18 \text{ kN/m}^3$, $\tau/\sigma = 0.3$	
		[Post-liquefied] $\gamma = 18 \text{ kN/m}^3$, $\tau/\sigma = 0.1$	
Core	Mohr-Coulomb	$\gamma = 22 \text{ kN/m}^3$, $\Phi = 35^\circ$, $C = 0$	1.0E-09
Rockfill	Mohr-Coulomb	$\gamma = 22 \text{ kN/m}^3$, $\Phi = 40^\circ$, $C = 0$	1E-05
Filter / Chimney drain	-	-	-
Transition	-	-	-
Clay- liner	-	-	-

Table 7: Factors of Safety in Preliminary design (2005)

Tailings Type	Phreatic Surface condition	Factor of Safety
Pre-liquefied ($\tau/\sigma_v' = 0.3$)	High	1.54
Pre-liquefied ($\tau/\sigma_v' = 0.3$)	Low	1.60
Post-liquefied ($\tau/\sigma_v' = 0.1$)	High	1.54
Post-liquefied ($\tau/\sigma_v' = 0.1$)	Low	1.60
Mohr-Coulomb ($\Phi = 30^\circ, C = 0$)	High	1.54
Mohr-Coulomb ($\Phi = 30^\circ, C = 0$)	Low	1.60

3.3.2 Analysis 2: 9th Stage Dam Design by AMEC (2012)

Over time, the design of the tailings dams changed significantly; however, the reason for the changes are unclear. The final height of the dam was modeled as 970 m which was greater than proposed 965 m in the original design. The downstream slope, however, changed from 2H:1V to 1.3H:1V. The cross sectional geometry also became irregular. The design foundation layers varied considerably from the previous analysis. A sandwiched till layer between two Glaciolustrine layers was used, possibly to simulate the irregularity of soil layers beneath the ground. The schematic diagram of the failed dam section is provided in Figure 17. The material parameters of the embankment soils were kept similar, with minor modifications, to that of Knight Piésold Consulting (2005). The angle of internal friction for GLU layer was reduced from 33° to 28° . The Rockfill was provided using an arbitrary shear-normal function described in Leps (1970) instead of Mohr-Coulomb function. Like the previous analysis, thin chimney drain and transition layers were merged into Rockfill. The clay liner wasn't used in the simulation.

Table 8 provides the summary of the material properties for the simulation.

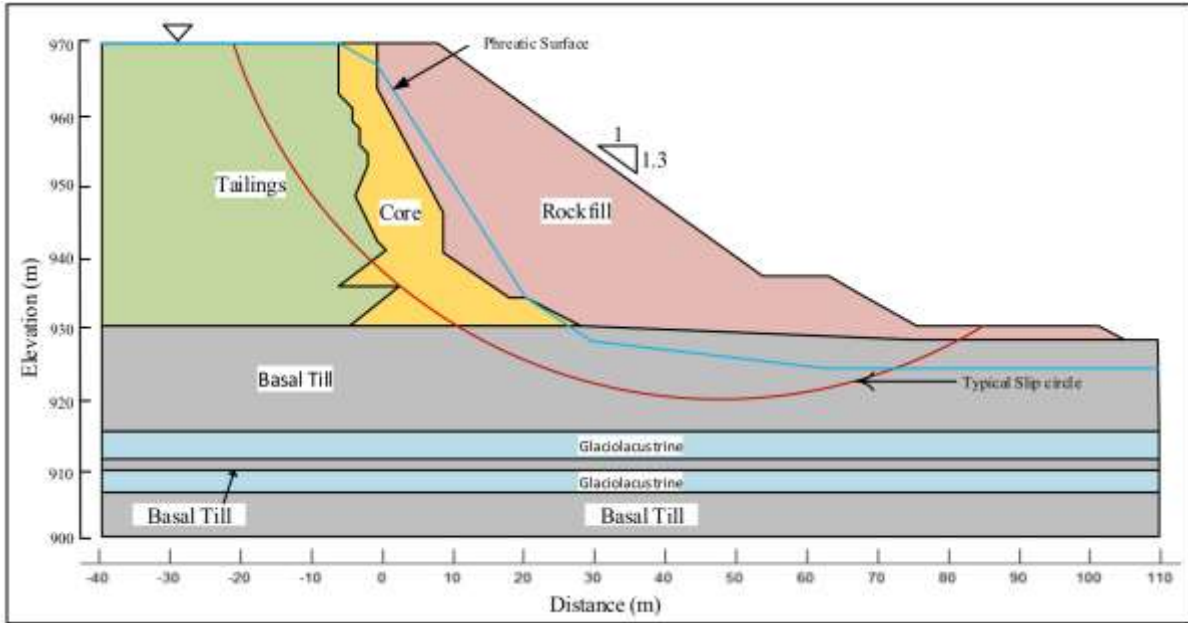


Figure 17: Geometry for the 9th stage dam design by AMEC (2012)

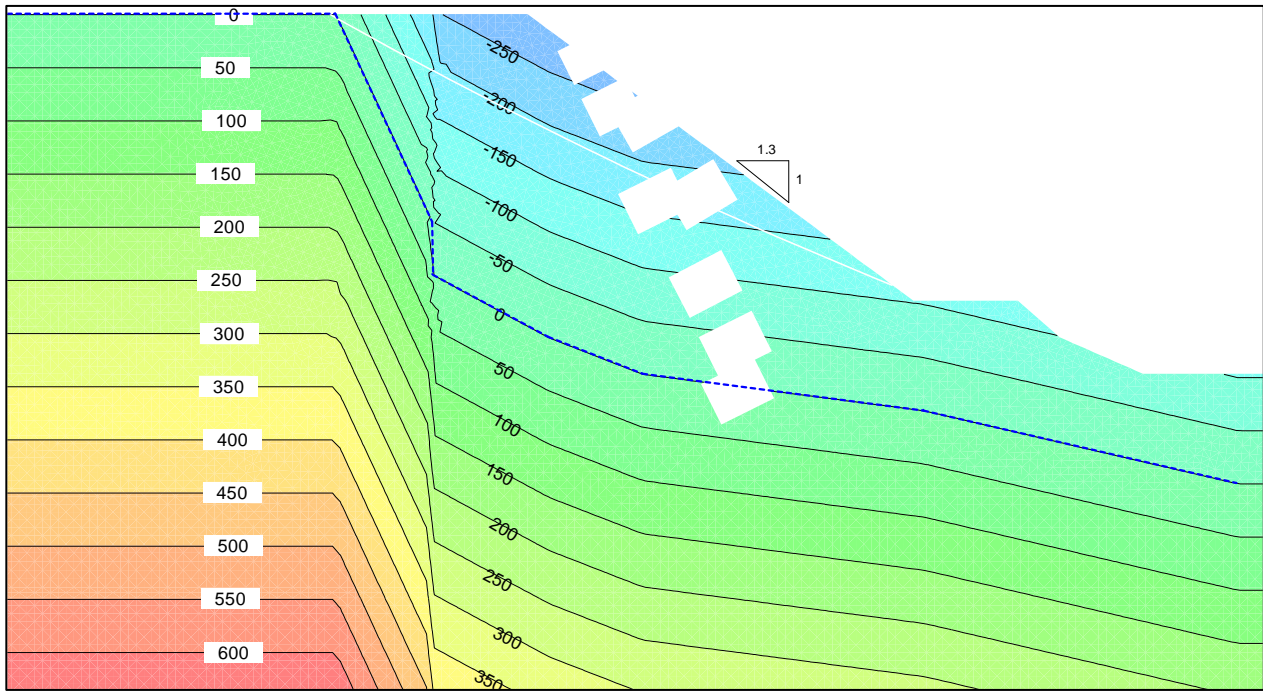


Figure 18: Pore water pressure (in kPa) contour for the 9th stage dam design

Table 8: Material properties used by AMEC (2012) in 9th stage design

Soil Layers	Soil Model	Material properties	
		Mechanical	Hydraulic Conductivity (m/s)
Bedrock	-	-	-
Upper Till	Mohr-Coulomb	$\gamma = 21 \text{ kN/m}^3$, $\Phi = 33^\circ$, $C = 0$	1.0 E-08
Lower Till			
Glaciolacustrine (GLU)	Mohr-Coulomb	$\gamma = 20 \text{ kN/m}^3$, $\Phi = 28^\circ$, $C = 0$	1.0 E-06
Tailing	Mohr-Coulomb	$\gamma = 18 \text{ kN/m}^3$, $\Phi = 30^\circ$, $C = 0$	Coarse: 7.0E-06 Dense: 1.0 E-08
	S = F(Overburden)	$\gamma = 18 \text{ kN/m}^3$, $\tau/\sigma = 0.1$	
Core (Compacted Till)	Mohr-Coulomb	$\gamma = 20.5 \text{ kN/m}^3$, $\Phi = 35^\circ$, $C = 0$	1.0E-09
Rockfill	Shear-Normal	$\gamma = 22 \text{ kN/m}^3$, [function defined by (Leps 1970)]	1.0E-05
Filter / Chimney drain	-	-	-
Transition	-	-	-
Clay- liner	-	-	-

The analysis was performed in SLOPE/W by using Morgenstern-Price type of LEM. Like the previous analysis, hydraulic conductivities were used only for the filter design. Phreatic surface was selected 'high' arbitrarily to provide the critical scenario. The entry and exit slip surfaces were determined carefully; because if the entry and exit slip surface entered into rockfill, it would create shallow slip circle and provided lower FOS apparently. Like the Preliminary design (2005), liquefaction effects were only considered for tailings materials, not for foundation materials. The calculated FOS are shown in Table 9. These FOS are not much different to each other in different conditions. Nevertheless, they are significantly higher than the recommended FOS. The Pore water pressure contour is also shown in Figure 18.

Table 9: Factors of Safety 9th Stage Design by AMEC (2012)

Tailings Type	Phreatic Surface condition	Factor of Safety
Pre-liquefied ($\tau/\sigma_v' = 0.3$)	High	1.68
Post-liquefied ($\tau/\sigma_v' = 0.1$)	High	1.72
Drained ($\Phi = 30^\circ, C = 0$)	High	1.72

3.3.3 Analysis 3: Independ Review Report by Morgenstern *et al.* (2015)

Morgenstern *et al.* (2015) conducted a post failure analysis of the failed dam. The geometry of the failed dam section roughly replicated the geometry of the 9th stage design. The foundation conditions, however, differed significantly from the previous analyses. The design soil layers were determined based on two post-failure soil investigation reports conducted by Morgenstern *et al.* (2015) and ConeTec Investigations Ltd (2014). The choice of appropriate material models was also different. A newly introduced Upper Glaciolacustrine (GLU) layer was assigned in Overburden (SHANSEP) model to replicate the undrained condition. The geometry of the failed section is shown in Figure 19. The stability was analyzed incorporating Morgenstern-Price type of LEM in SLOPE/W. The material properties are shown in Table 10 which differed in mechanical properties from the previous analysis to some extents. Undrained shear strength ratio of 0.22 and 0.27 were used for GLU layers to understand the undrained response in overall dam stability. In a different simulation, this GLU layer was assigned using Mohr-Column model (similar to AMEC 2012, $C=0, \Phi = 30^\circ$) to test drained response of the dam. Lower till layer was found very stiff in the latest soil investigation; and so it was assigned as a weak bedrock. Due to unavailability of a defined shear-normal function in the report, the function used in Leps (1970) was used for the rockfill material.

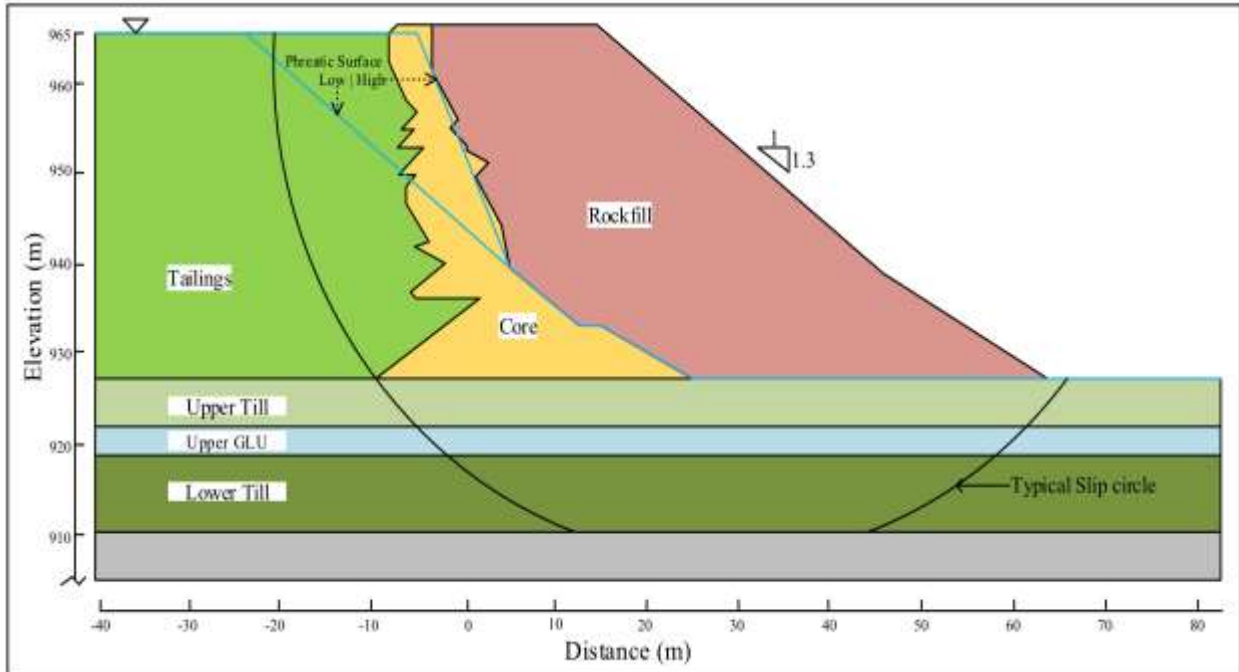


Figure 19: Cross sectional geometry used in analysis by Morgenstern et al. (2015)

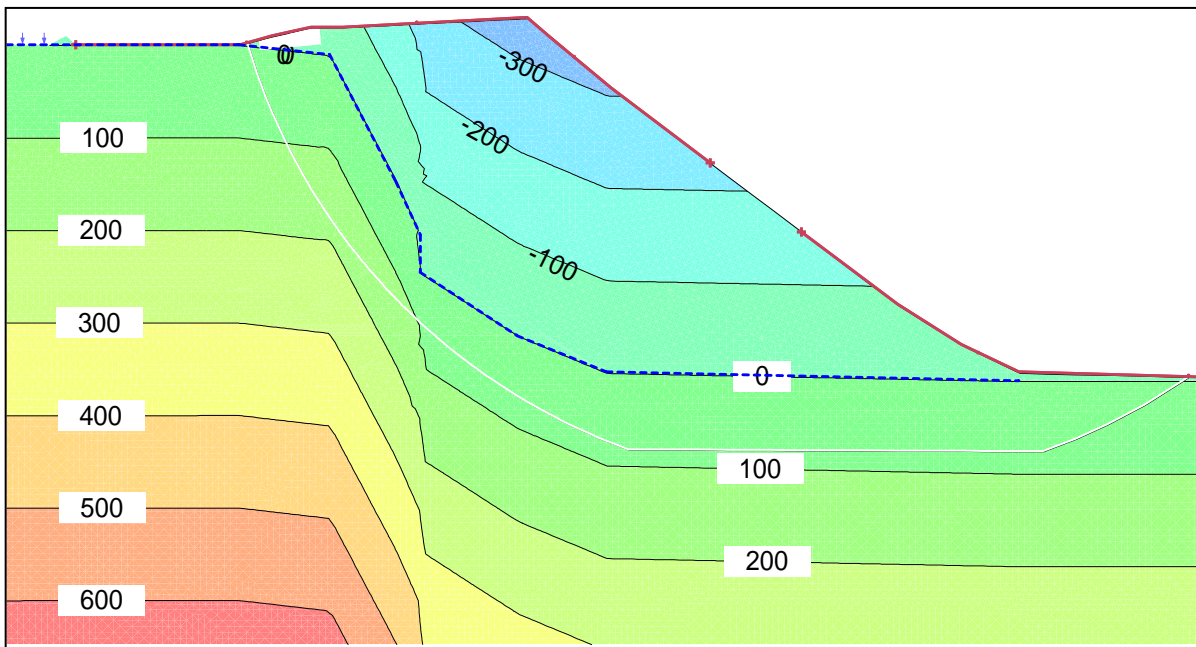


Figure 20: Pore water Pressure (in kPa) contour for the analysis of Morgenstern et al. (2015)

Table 10: Material properties used by Morgenstern *et al.* (2015)

Soil Layers	Soil Model	Material properties	
		Mechanical	Hydraulic Conductivity (m/s)
Bedrock	Bedrock	Impenetrable	-
Lower Till	Bedrock	Impenetrable	-
Upper Till	Mohr-Coulomb	$\gamma = 21 \text{ kN/m}^3$, $\Phi = 35^\circ$, $C = 0$	1.0 E-08
Glaciolucastine (GLU)	S = F(Overburden)	$\gamma = 21 \text{ kN/m}^3$, $\tau/\sigma' = 0.27$	1.0 E-06
		$\gamma = 21 \text{ kN/m}^3$, $\tau/\sigma' = 0.21$	-
Tailing	Mohr-Coulomb	$\gamma = 18 \text{ kN/m}^3$, $\Phi = 30^\circ$, $C = 0$	7.0E-06
Core	Mohr-Coulomb	$\gamma = 20.5 \text{ kN/m}^3$, $\Phi = 35^\circ$, $C = 0$	1.0E-09
Rockfill	Shear-Normal	$\gamma = 22 \text{ kN/m}^3$ [Assumed as Leps 1970]	1.0 E-05
Filter / Chimney drain	Merged with Rockfill	-	-
Transition	Merged with Rockfill	-	-
Clay- liner	-	-	-

Like the previous analyses, this set of analyses was performed without considering the field hydraulic boundary conditions. The locations of the phreatic surfaces were arbitrarily selected as ‘high’ and ‘low’. Thus, the effects of hydraulic conductivities of different layers of soil did not come into effects. The pore water pressure contour for higher phreatic surface is shown in Figure 20. Table 11 shows that the FOS of both undrained responses (Undrained shear strength ratio of 0.22 and 0.27) for GLU were close to 1. The drained response of the layer, however, shows much higher value of factor of safety. The sudden nature of the failure and these analyses results convinced Morgenstern *et al.* (2015) that the failure happened in an undrained manner in the ‘weak’ GLU layer.

Table 11: Factors of Safety obtained by Morgenstern et al. (2015)

GLU Layer	Phreatic Surface condition	Factor of Safety
Undrained Shear Strength ($\tau/\sigma_v' = 0.27$)	High	1.05
Undrained Shear Strength ($\tau/\sigma_v' = 0.27$)	Low	1.12
Undrained Shear Strength ($\tau/\sigma_v' = 0.22$)	High	0.94
Undrained Shear Strength ($\tau/\sigma_v' = 0.22$)	Low	1.02
Mohr-Coulomb ($C=0, \Phi = 30^\circ$)	High	1.76
Mohr-Coulomb ($C=0, \Phi = 30^\circ$)	Low	1.94

3.3.4 Analysis 4: Finite Element Analysis (FEA)

Finite Element Analysis on the stability of the failed dam was performed using SIGMA/W. FEA is advantageous over LEM, because it does not consider the slip mass as a rigid body and a strain field is established within it (Alsharedah 2015). Pore water conditions from each stage of SEEP/W analysis were imported into the respective SIGMA/W analysis. SLOPE/W was used where it was necessary to compare the stability. The FEA on the stability in GeoStudio 2012 can be performed in two different ways as follows. However, the second method, which has broader acceptance, was used to determine the stability of the dam:

- By importing Stress data from SIGMA/W into SLOPE/W
- By using Strength Reduction Method in SIGMA/W

GeoStudio works well in auto meshing. A global auto-meshing for the element size of 1 m was selected for the analysis. Nevertheless, the meshing was made finer in the interface of the material regions. The shapes of the meshes were quads and triangles. Secondary nodes were selected to get more accurate results in stress-strain conditions.

Material properties and cross sectional geometry of the failed dam section were kept similar to the design report provided by Morgenstern et al. (2015). The newly detected ‘weak’ GLU layer, however, was assigned according to various material properties in terms of stiffness to see the variation in simulation results. Both drained response in Effective Stress Analysis (ESA) and undrained response in Total Stress Analysis (TSA) of the analyses have been presented in the following sections.

3.3.4.1 Boundary Conditions in Multistage Construction

Unlike other published designs, the current FEA considers a stage-by-stage development in the construction. Since 2005, the dam has been built in nine stages. The shape and the size of the dam section changed over this time. A qualitative diagram of stage-by-stage dam development is shown in Figure 21. To accommodate this temporal and spatial variation, appropriate boundary conditions were assigned in each stage of the simulation.

Hydraulic boundary conditions were simulated by using SEEP/W. In the upstream side, the ponded water in the tailings zone for each stage of the construction was simulated by setting ‘Total Head’ boundary up to the tailings beach, equal to the top elevation of the ponded surfaces of each stage. The information on the tailings beach width was not found in the design and annual reports. Thus, it had been assumed approximately 8 m to 10 m away from the top-left side of the core material. This assumption was supported by Google map historical images dated between 2005 and 2014. In the downstream side of the dam, the atmospheric pressure head (zero pressure head) was applied along the ground surface to simulate the ground water table at the ground surface.

For the stability analysis in SIGMA/W, the vertical sides of the soil domain were kept fixed in horizontal direction. The bottom boundary was kept as fixed in both vertical and horizontal directions. Neither any displacement nor rotational boundary was present in the system. Each set of analysis started from an ‘insitu’ condition. ‘Load/Deformation’ method was selected for the development of each embankment stage. This method provides the changes in Stress-strain in the domain when new load is applied or withdrawn. Each stage acted as ‘parent’ for the next stage. Deformation and cumulative values from the previous analysis were excluded in each stage. ‘Stress Redistribution’ method, however, was selected to find the FOS of each stage. The details of these methods can be found in GeoStudio SIGMA/W manual (Chapter 7).

FOS of each stage using LEM are presented in Table 12. Drained responses of FOS are relatively higher than the undrained responses. When the undrained shear strength of 0.22 was used, FOS are significantly lower than the recommended FOS by Canadian Dam Association (2012). The series of lower values in the undrained analysis suggests that the failure mechanism might be different than the review made by Morgenstern *et al.* (2015). The detailed discussion of these results is provided in the summary of results section at the end of this chapter.

Table 12: Factors of Safety of each stage obtained by using LEM (Morgenstern-Price)

Stage	GLU in Mohr-Coulomb Model (C=0, $\Phi = 30^\circ$)	GLU in Undrained Shear Strength of 0.22
One	1.20	1.23
Two	1.19	1.23
Three	1.74	1.19
Four	1.60	1.16
Five	1.64	1.00
Six	1.63	1.15
Seven	1.59	1.05
Eight	1.32	0.97
Nine	1.35	0.97

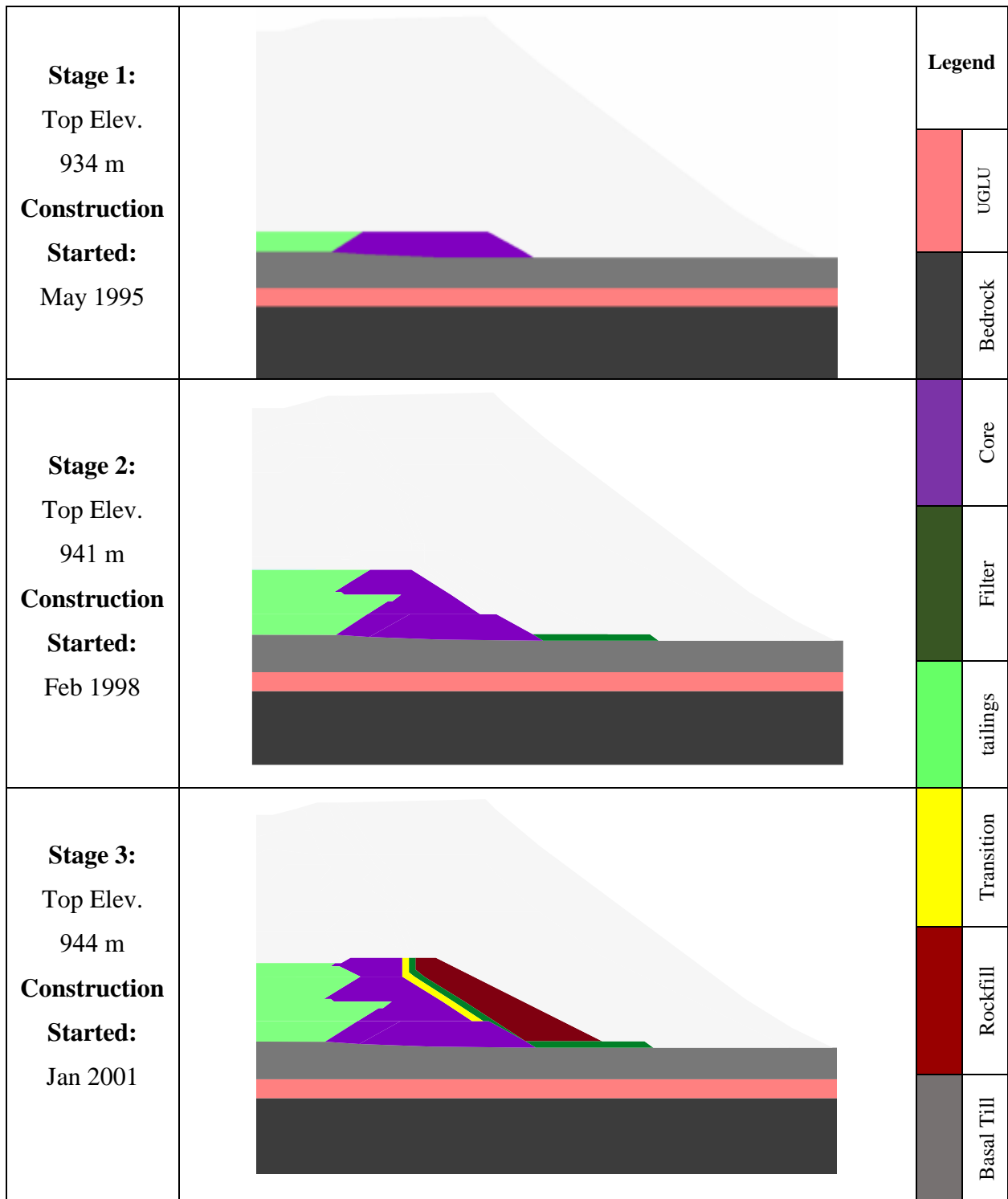


Figure 21: Development of Construction stages at MP-TSF (continued to next page)

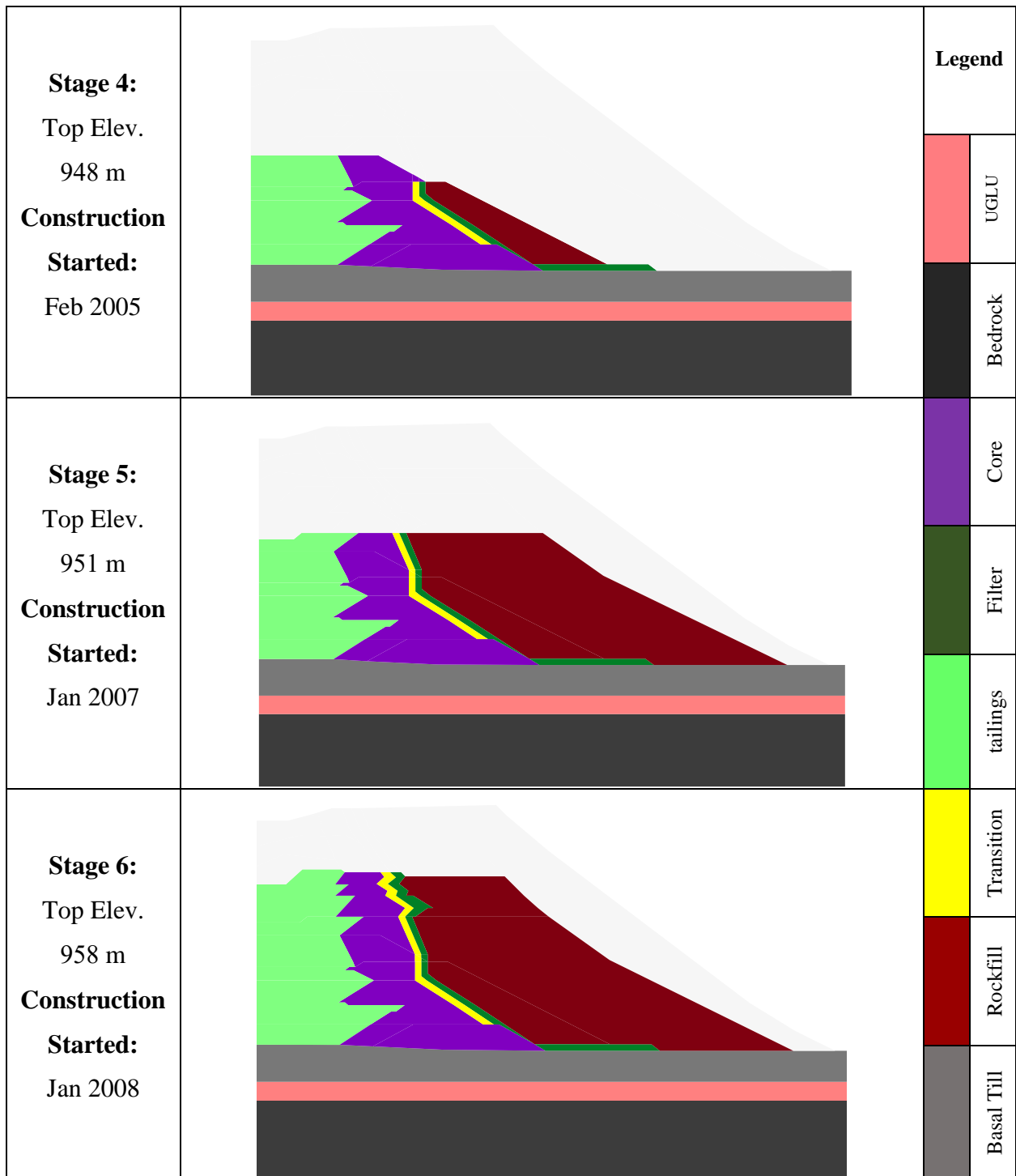


Figure 21: Development of Construction stages at MP-TSF (continued to next page)

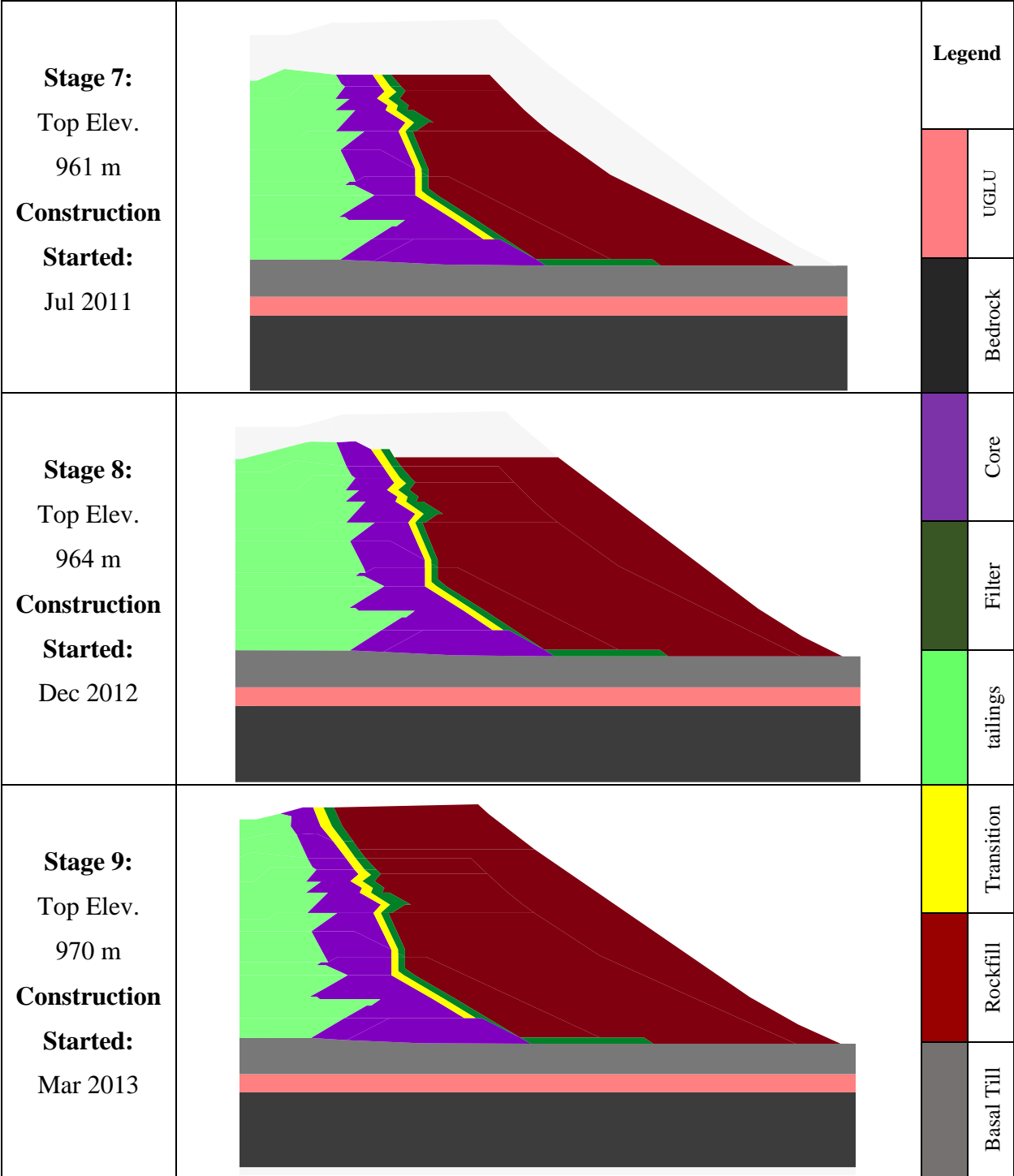


Figure 21: Development of Construction stages at MP-TSF (Completed)

3.3.4.2 Strength Reduction Method (SRM)

Strength Reduction Method (SRM) is a Finite Element technique, which determines a Stress Reduction factor. This Stress Reduction Factor (SRF) brings the structure on the verge of the failure by reducing the material strength properties. If the factor of safety is already less than 1, then a different strength factor is used to increase the strength of the material until the analysis converges to a solution (e.g., Duncan 1996).

Along with the stress parameters of the soil, stiffness is very important in finite element analysis of stability. Table 13 refers 4 cases where the stiffness parameters of all the soil materials are listed. Case 1 & 3 represent higher relative stiffness of GLU and Case 2 & 4 represent lower relative stiffness. The relative stiffness is defined as the ratio of the stiffness of the concerned soil layer to the average stiffness of the adjacent layers. The values of the stiffness were taken from the soil test data and from various published literature. All the stiffness data are presented in Effective Stress parameter except for GLU layer in Case 3 and 4. All four cases were simulated using SIGMA/W and computed factors of safety are provided in Table 14.

Table 13: Stiffness Parameters of the materials

Material	Effective Stiffness Parameters (kPa)			
	Case 1	Case 2	Case 3	Case 4
Tailings	15,000	15,000	15,000	15,000
Core	20,000	20,000	20,000	20,000
Rockfill	75,000	75,000	75,000	75,000
Upper Till	50,000	50,000	50,000	50,000
GLU	20,000	5,000	24,000¹	8,000¹
Lower Till	85,000	85,000	85,000	85,000

¹ The Stiffness parameter is taken in Total Stress parameter. Undrained strength is set as 107 KPa which matches test results by ConeTec Investigations Ltd (2014)

3.3.4.3 Effective Stress Analysis (ESA)

Effective Stress analysis provides a drained response of the soil domain. In ESA, the soil parameters are presented in terms of effective parameters. For the current part of analysis, all the layers, including the concerned GLU layer, were provided in effective stress parameter. The strength properties of the materials are given in Table 10 and the stiffness parameters were taken from Table 13.

Figure 22, 23, 26 and 27 show the maximum shear strain (ϵ_{\max}) contours of 8th and 9th stages of the construction in ESA for Case 1 and 2. These contour plots provide the extents and patterns of the maximum shear strains (ϵ_{\max}) when a new layer of embankment is constructed. Figure 24 and Figure 25 provide super-imposed graphs of shear strength and maximum shear strains of the GLU layer. These graphs provide clearer view of the maximum shear strain (ϵ_{\max}) and stress in the GLU layer.

It has been shown for Case 1 (higher relative stiffness) in Figure 24 that maximum shear stress was mobilized in the section is close to 300 KPa. For this stress, the amount of shear strain was as low as 0.8%. A new layer of construction in the 9th stage (Figure 25) increased the shear stress in the system; however, it did not increase the shear strain of GLU layer. For Case 2 (lower relative stiffness), the values of shear strain were not high (2% max) and the changes in shear strain from 8th to 9th stage were marginal (Figure 26 and Figure 27).

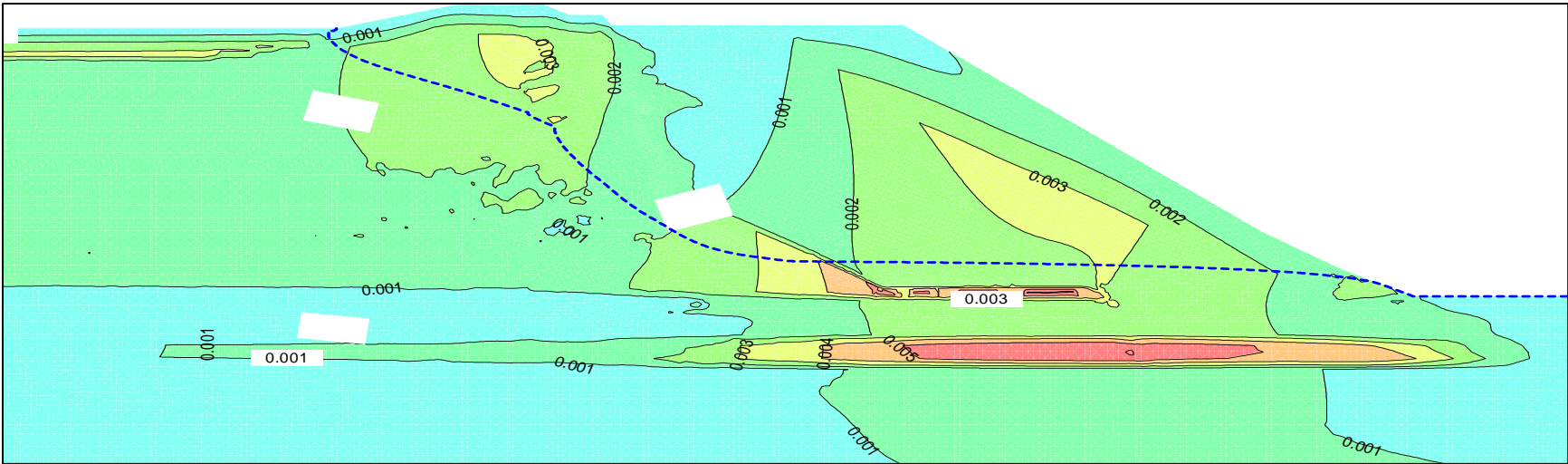


Figure 22: Maximum Shear Strain (ϵ_{max}) at 8th stage (ESA: Case 1)

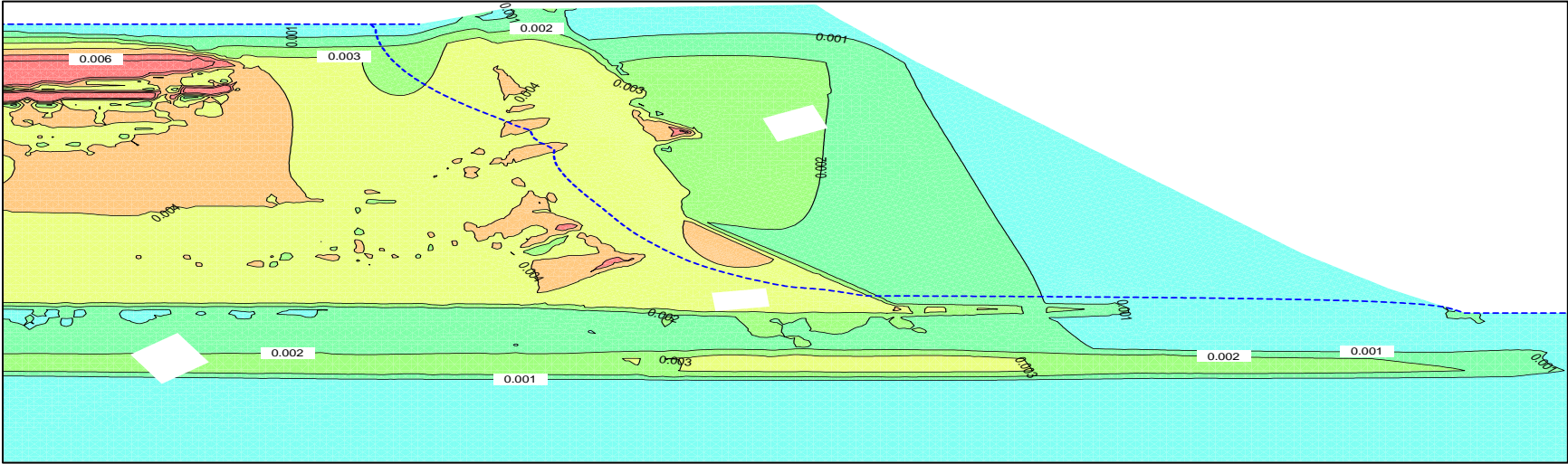


Figure 23: Maximum Shear Strain (ϵ_{max}) at 9th stage (ESA: Case 1)

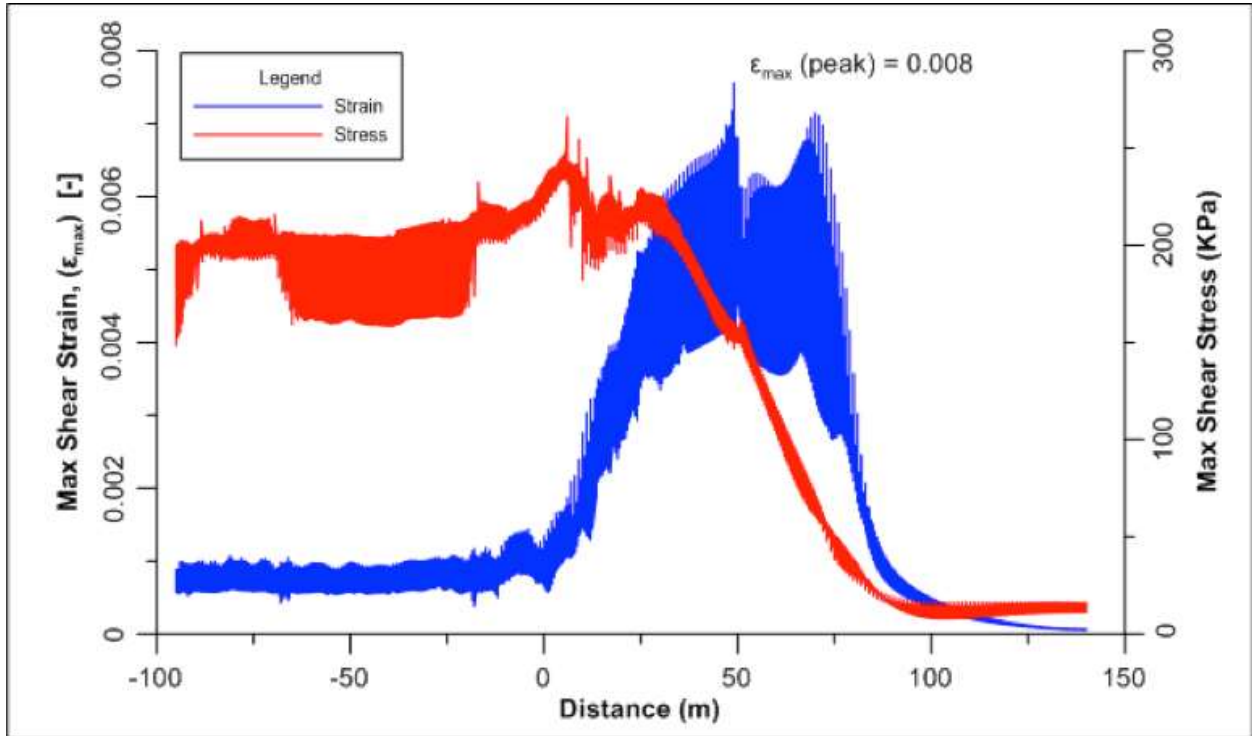


Figure 24: Maximum Shear Strength and Strain plot for GLU in 8th stage (ESA: Case 1)

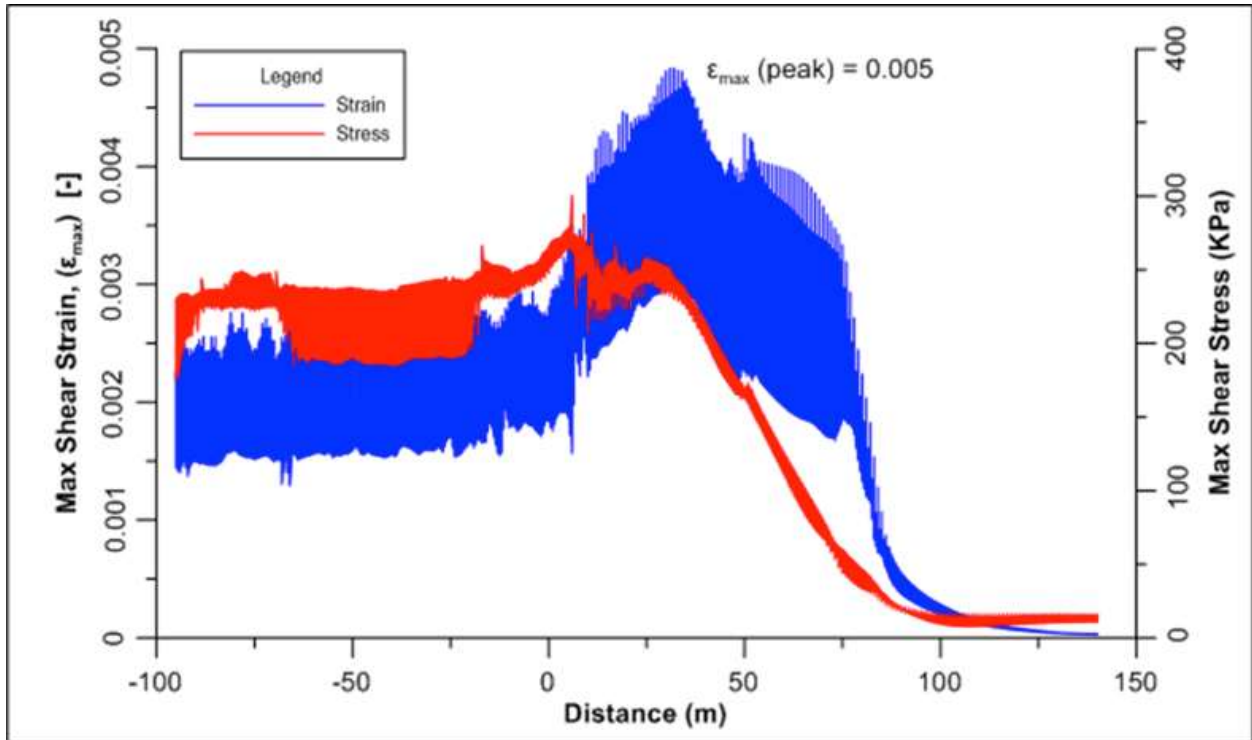


Figure 25: Maximum Shear Strength and Strain plot for GLU in 9th stage (ESA: Case 1)

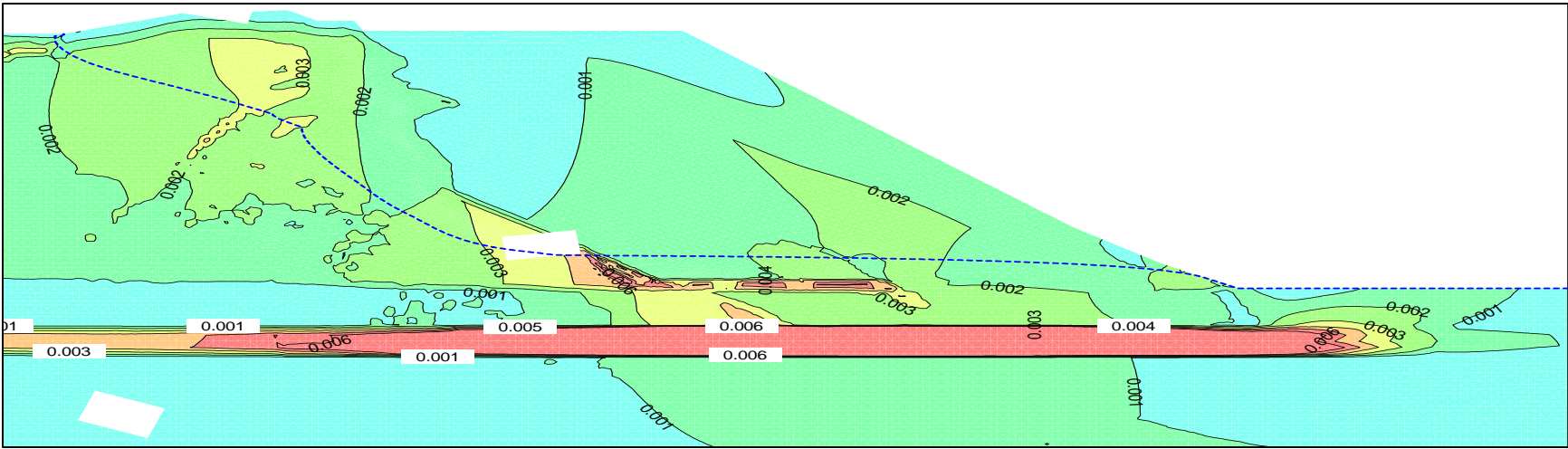


Figure 26: Maximum Shear Strain (ϵ_{max}) at 8th stage (ESA: Case 2)

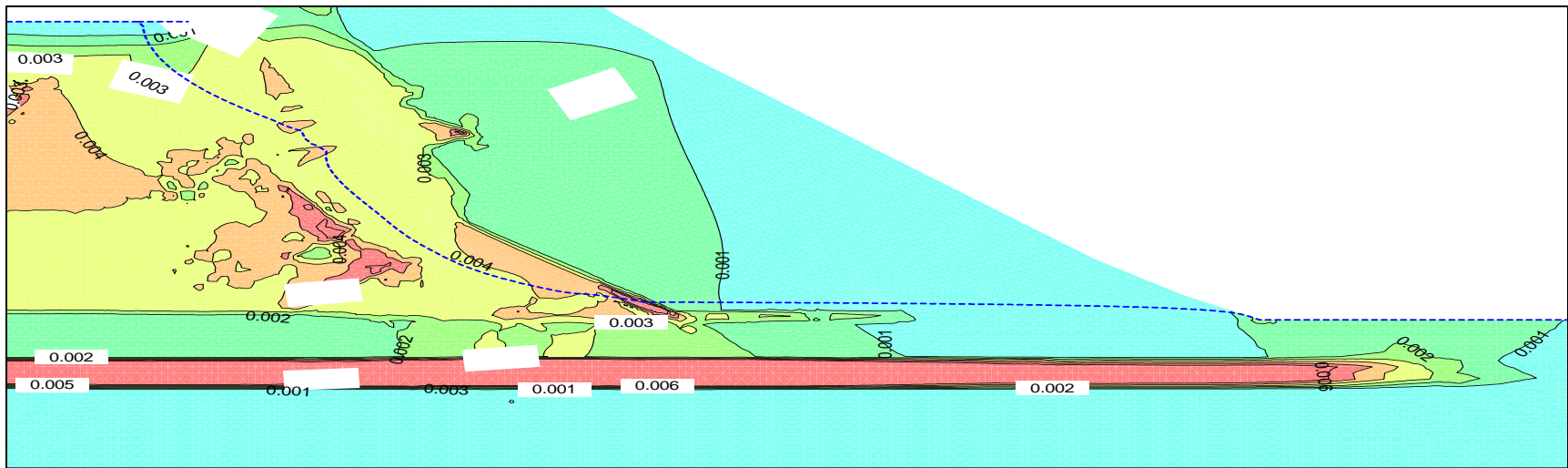


Figure 27: Maximum Shear Strain (ϵ_{max}) at 9th stage (ESA: Case 2)

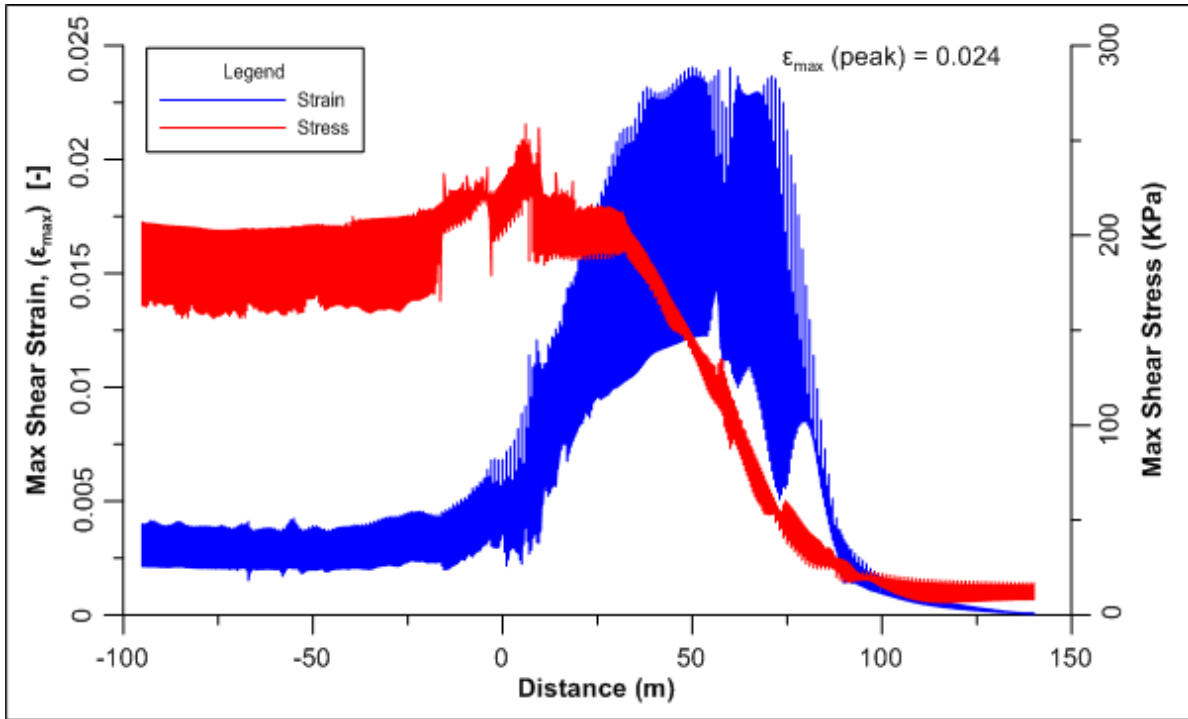


Figure 28: Maximum Shear Strength and Strain plot for GLU in 8th stage (ESA: Case 2)

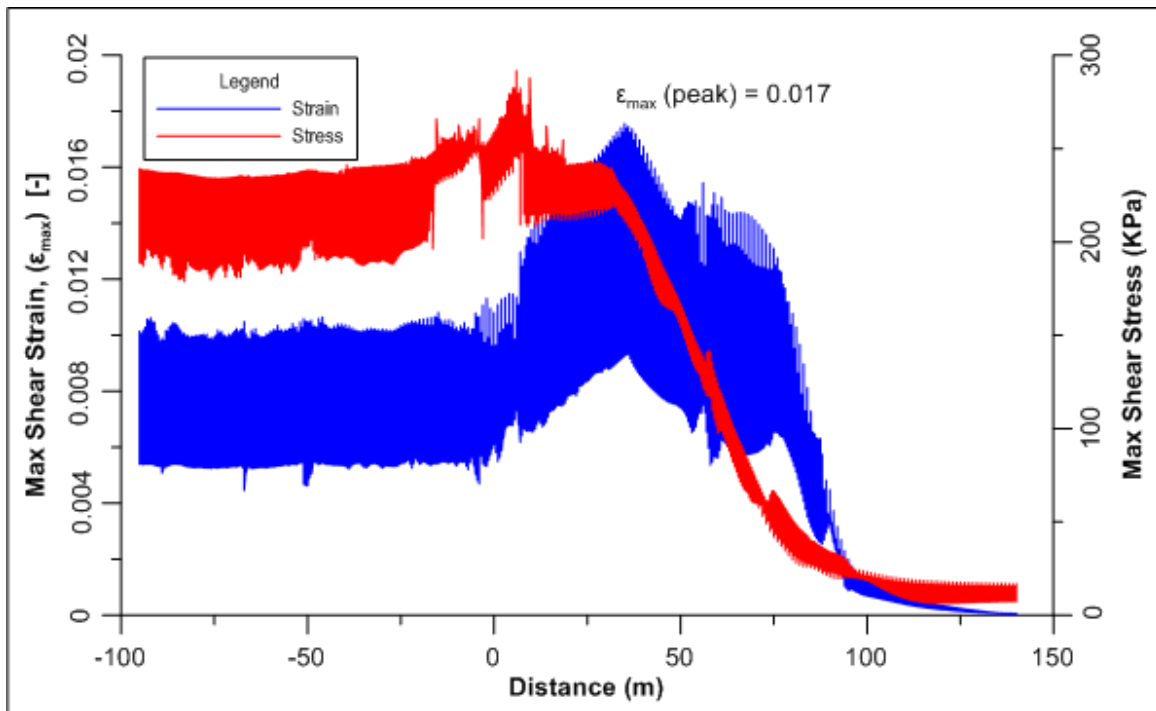


Figure 29: Maximum Shear Strength and Strain plot for GLU in 9th stage (ESA: Case 2)

3.3.4.4 Total Stress Analysis (TSA)

Total Stress Analysis provides undrained responses of the soil domain. This is the quicker response from the soil when a load is applied or removed. For this part of current analysis, all the layers, except the concerned GLU layer, had been assigned in effective stress parameters. GLU had been assigned in total stress parameters as per Table 10. Stiffness parameter were assigned as per Table 13.

Maximum shear strain (ϵ_{\max}) contours for 8th and 9th stages of construction for case 3 and 4 are shown in Figure 30, 31, 34 and 35. The patterns of shear strain changes were similar to that of ESA analyses; however, the values were different. Figure 32, 30, 33 and 34 provide superimposed graphs of maximum shear stress and maximum shear strain (ϵ_{\max}) to understand the shear strength mobilization within GLU layer.

For Case 3, where the relative stiffness of the GLU layer is not very low, the maximum shear strains are 0.6% and 3% respectively for stage 8 and 9 (Figure 32 and Figure 33). These changes in shear strain is relatively high; however, the values of maximum shear strain (ϵ_{\max}) is within the acceptable limit. For case 4 with lower relative stiffness of GLU layer, the maximum shear strain (ϵ_{\max}) increased from 0.8% in 8th stage to 8% in 9th stage at mobilized shear stress around 160 KPa (Figure 36 and Figure 37). This shear strain is high enough to initiate a distortion in the system and might act as the first step in a progressive failure.

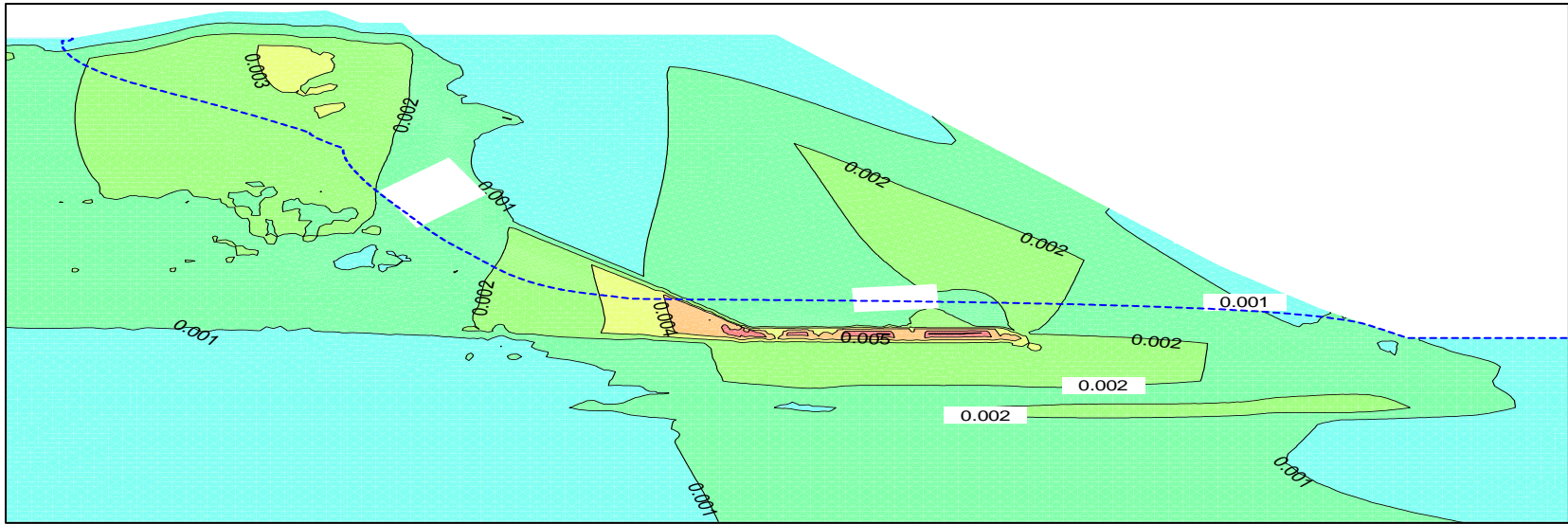


Figure 30: Maximum Shear Strain (ϵ_{max}) at 8th stage (TSA: Case 3)

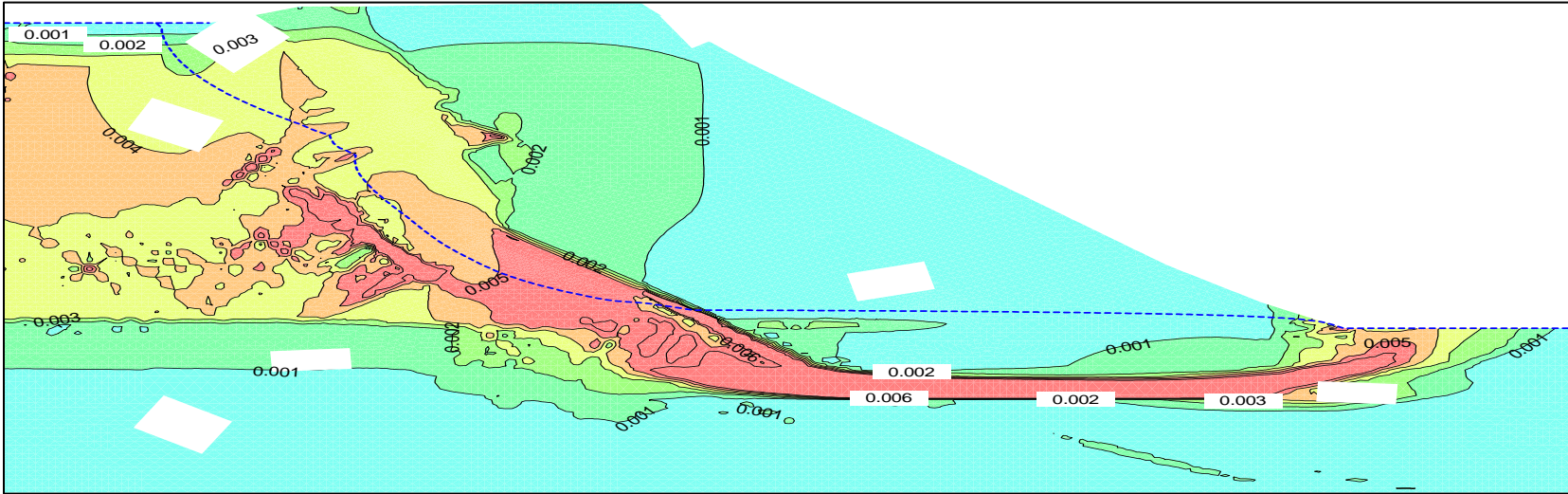


Figure 31: Maximum Shear Strain (ϵ_{max}) at 9th stage (TSA: Case 3)

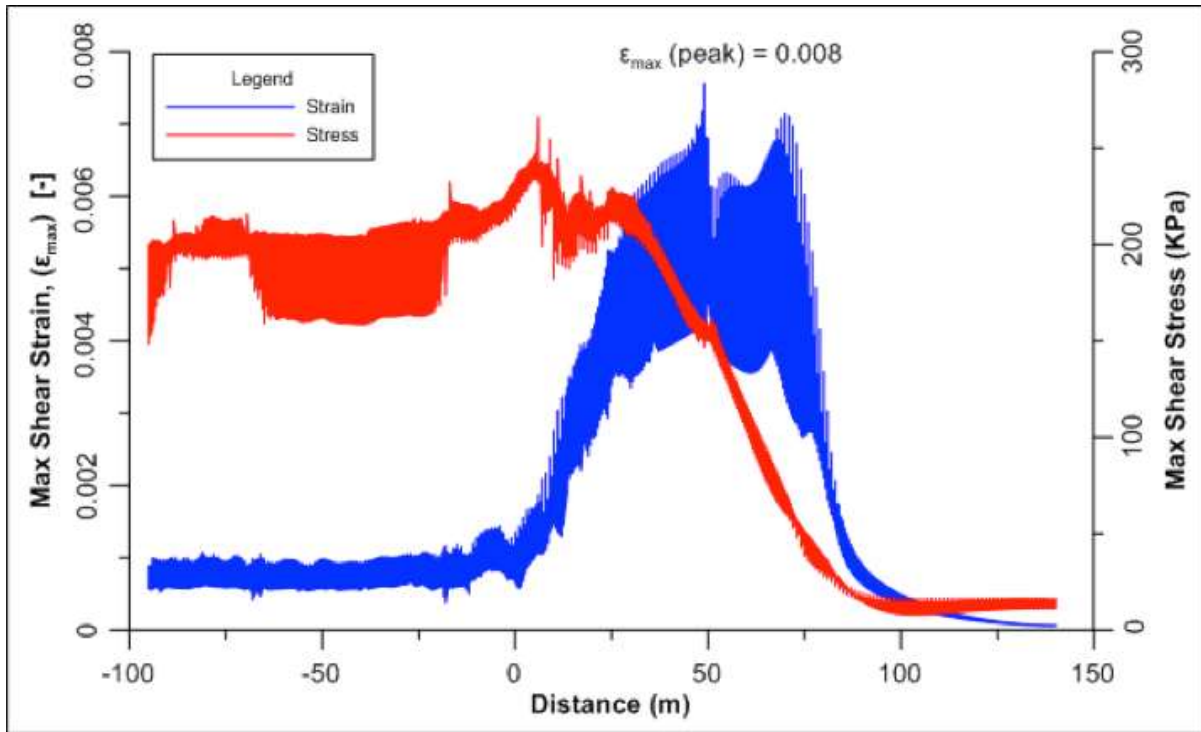


Figure 32: Maximum Shear Strength and Strain plot for GLU in 8th stage (TSA: Case 3)

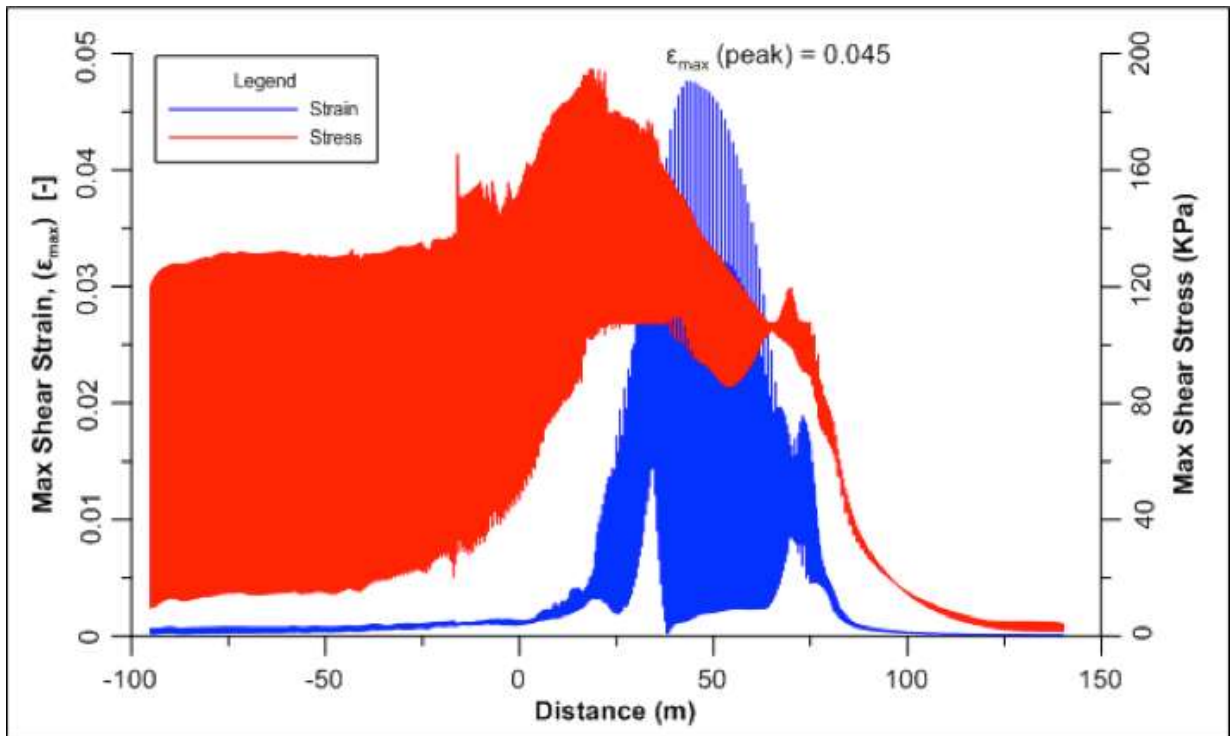


Figure 33: Maximum Shear Strength and Strain plot for GLU in 9th stage (TSA: Case 3)

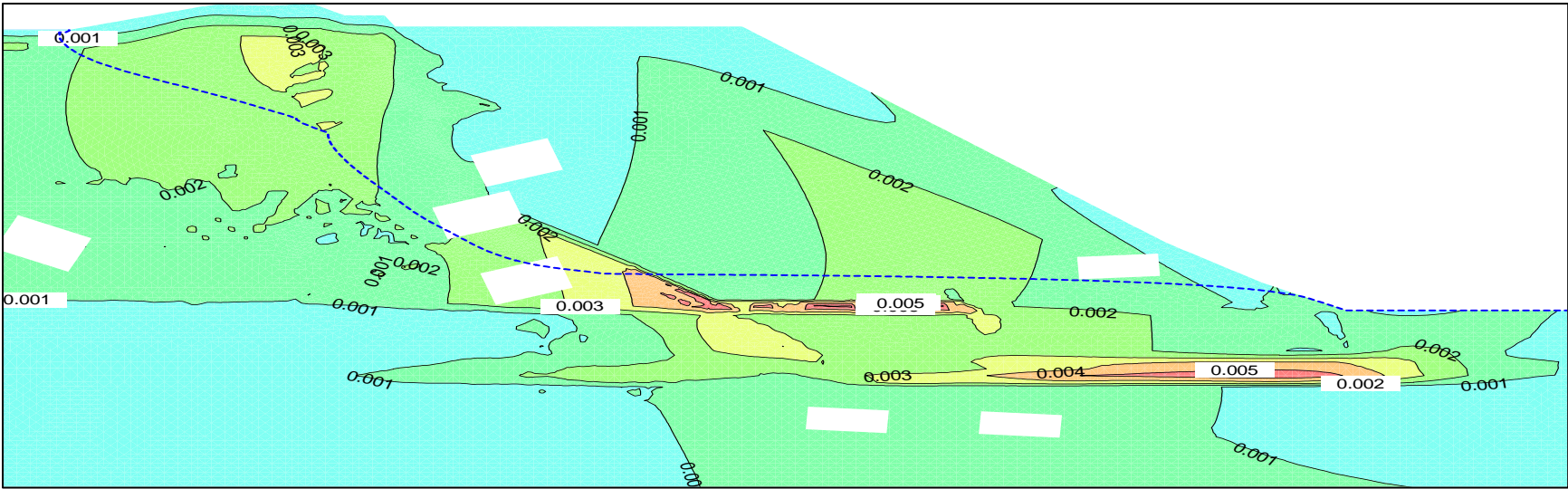


Figure 34 Maximum Shear Strain (ϵ_{max}) at 8th stage (TSA: Case 4)

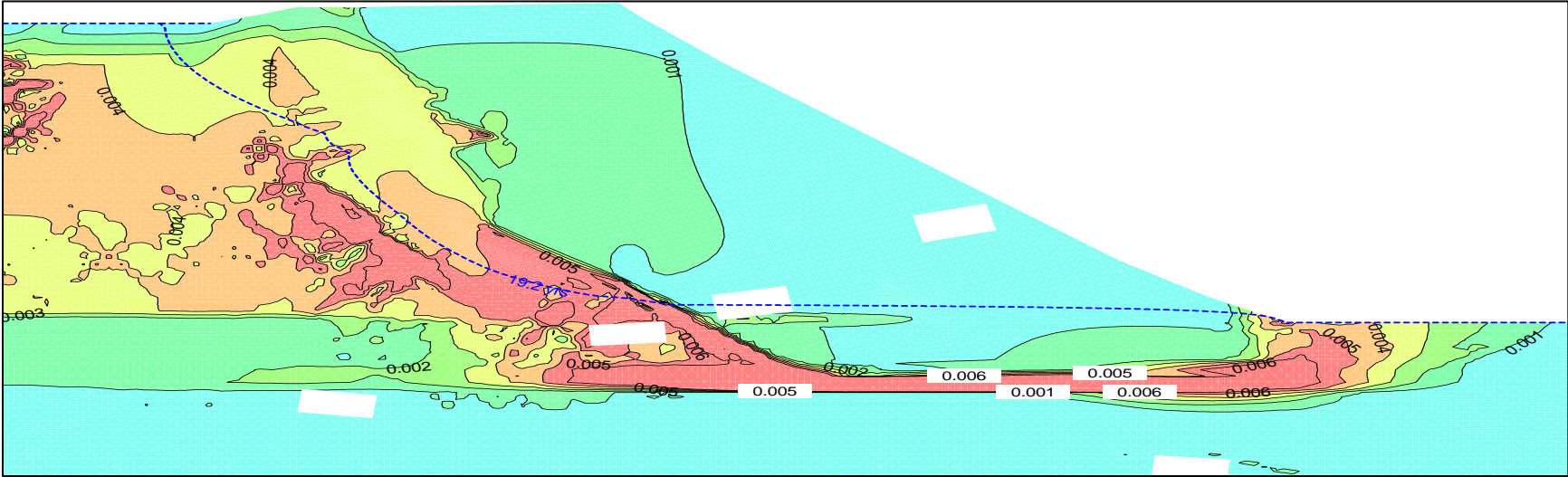


Figure 35 Maximum Shear Strain (ϵ_{max}) at 9th stage (TSA: Case 4)

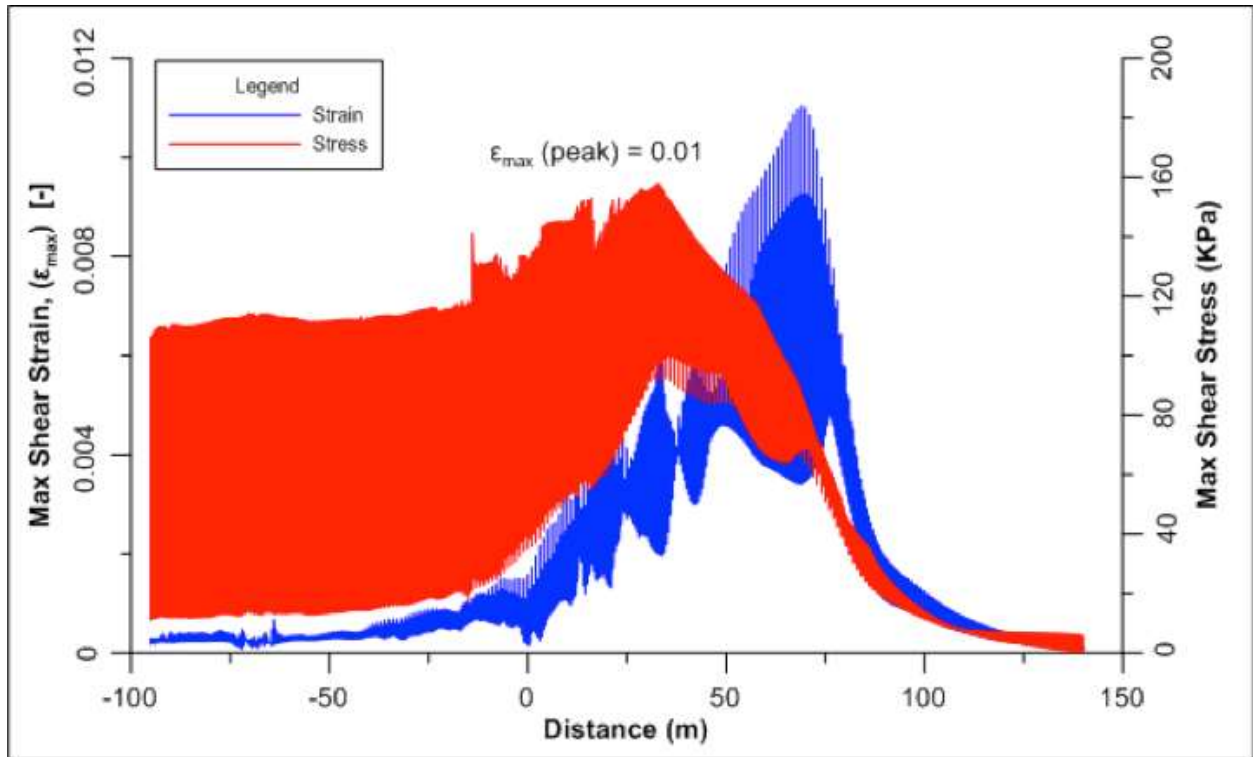


Figure 36: Maximum Shear Strength and Strain plot for GLU in 8th stage (TSA: Case 4)

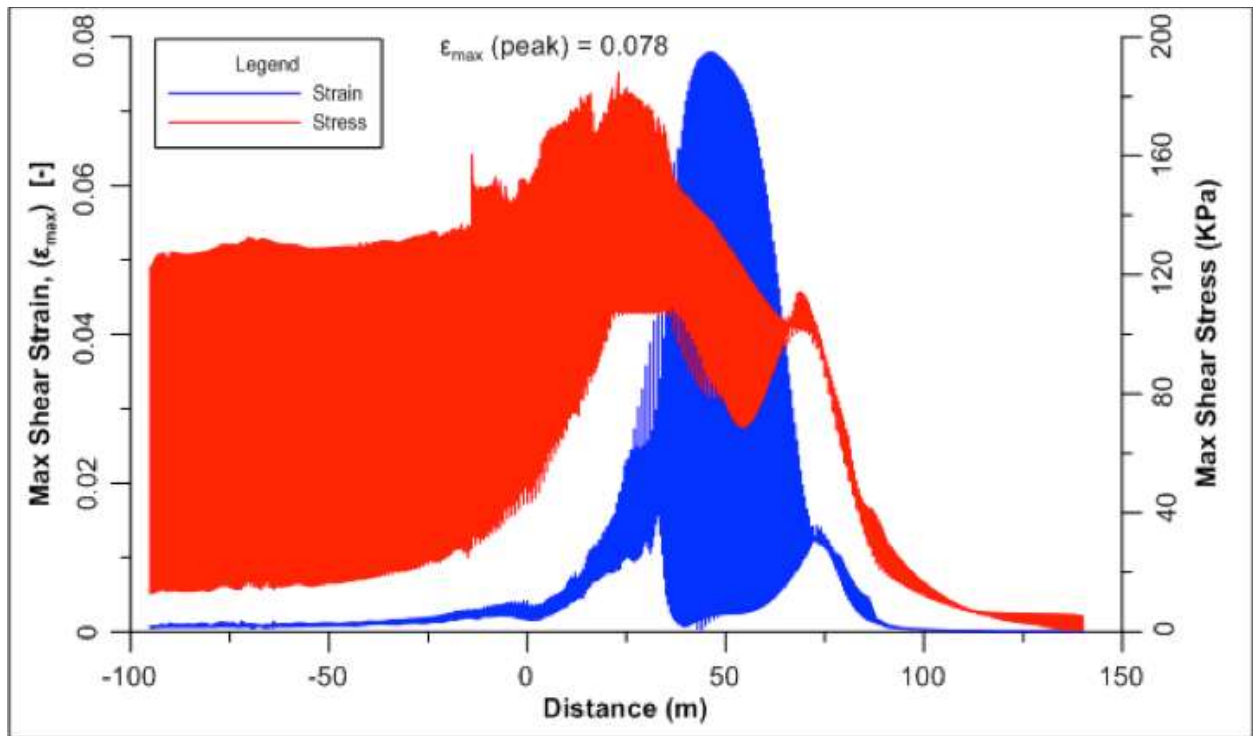


Figure 37: Maximum Shear Strength and Strain plot for GLU in 9th stage (TSA: Case 4)

Table 14: Factors of Safety FEA of each stage for all cases

Stages	Factors of Safety			
	Case 1	Case 2	Case 3	Case 4
One	1.90	1.90	1.92	1.75
Two	1.80	1.82	1.80	1.67
Three	1.75	1.79	1.75	1.65
Four	1.42	1.43	1.62	1.53
Five	1.67	1.65	1.55	1.50
Six	1.50	1.52	1.27	1.26
Seven	1.45	1.46	1.18	1.13
Eight	1.40	1.41	1.10	1.09
Nine	1.35	1.32	1.03	1.01

3.4 Deformation Analysis

Deformation analysis provides overall deformation pattern of the structure. Deformation analysis was performed using SIGMA/W. Both vertical and horizontal deformations for case 4 (as this is the critical case with the lowest relative stiffness) are shown in Figure 38 and Figure 39 respectively. This low values of horizontal deformation indicates that the dam might have not failed due to horizontal translation. Figure 40 and Figure 41 show the comparison of vertical and horizontal deformation in 9th stage for all the cases. The comparison was done along the Embankment Setting Out Line (S.O.L.). S.O.L is an arbitrary reference line, usually the centreline of the dam core, from which horizontal measurements are determined (Vick 1990). In this dam, S.O.L is drawn along '0' (zero) m on X-axis (distance) in Figure 19.

The following four figures show that the maximum values of the deformation were not concentrated near the concerned GLU layer. This was true for all the cases discussed here.

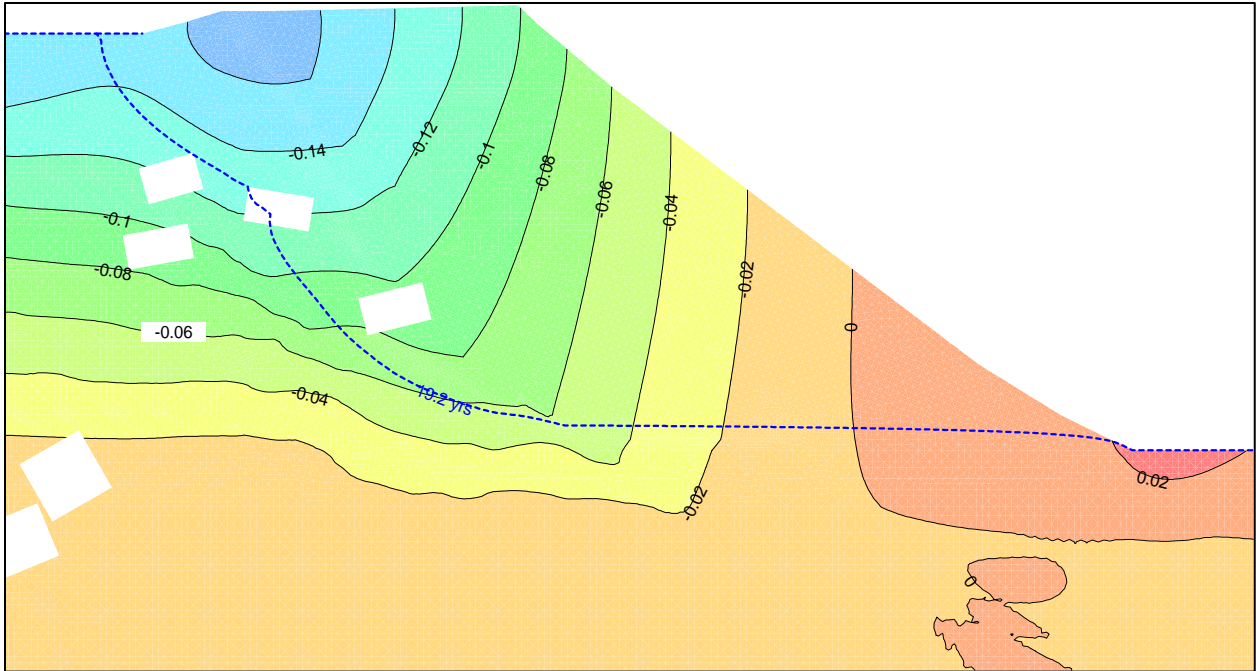


Figure 38: Global vertical deformation in meter after 9th stage (Case 4)

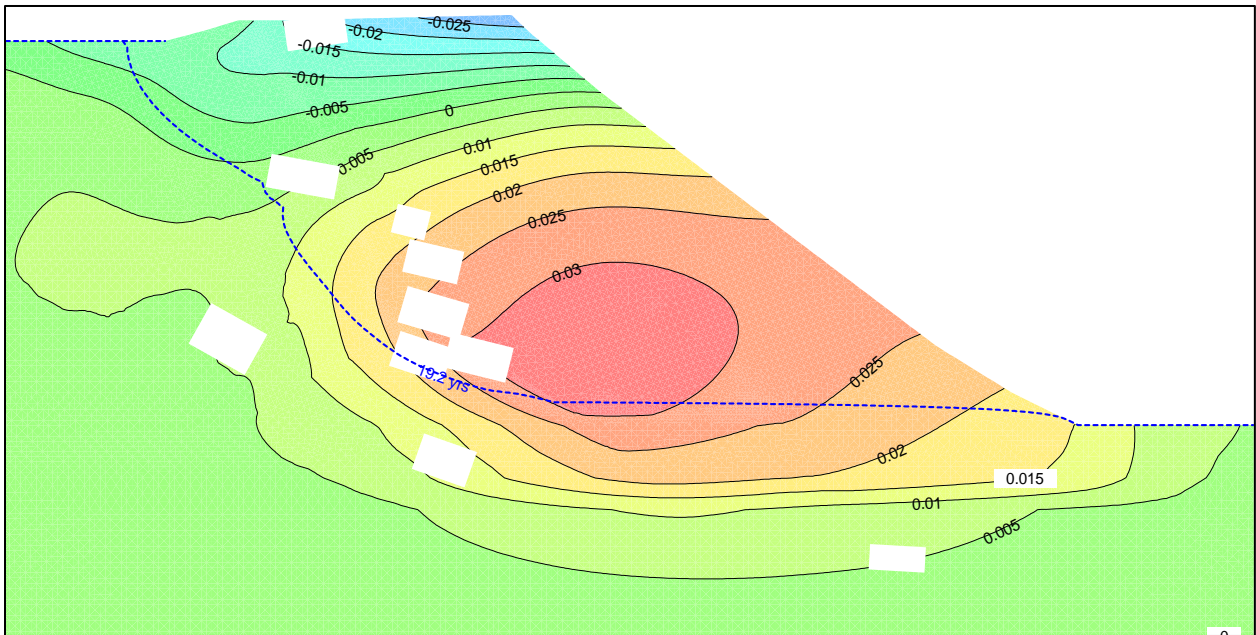


Figure 39: Global horizontal deformation in meter after 9th stage (Case 4)

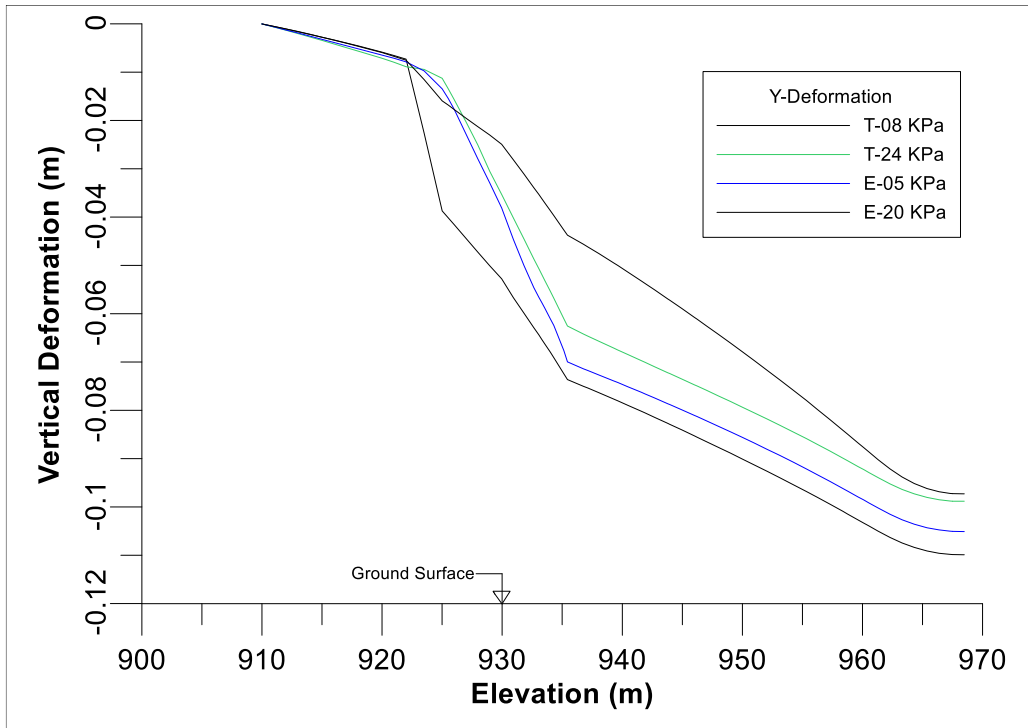


Figure 40: Comparison of global vertical deformation along S.O.L

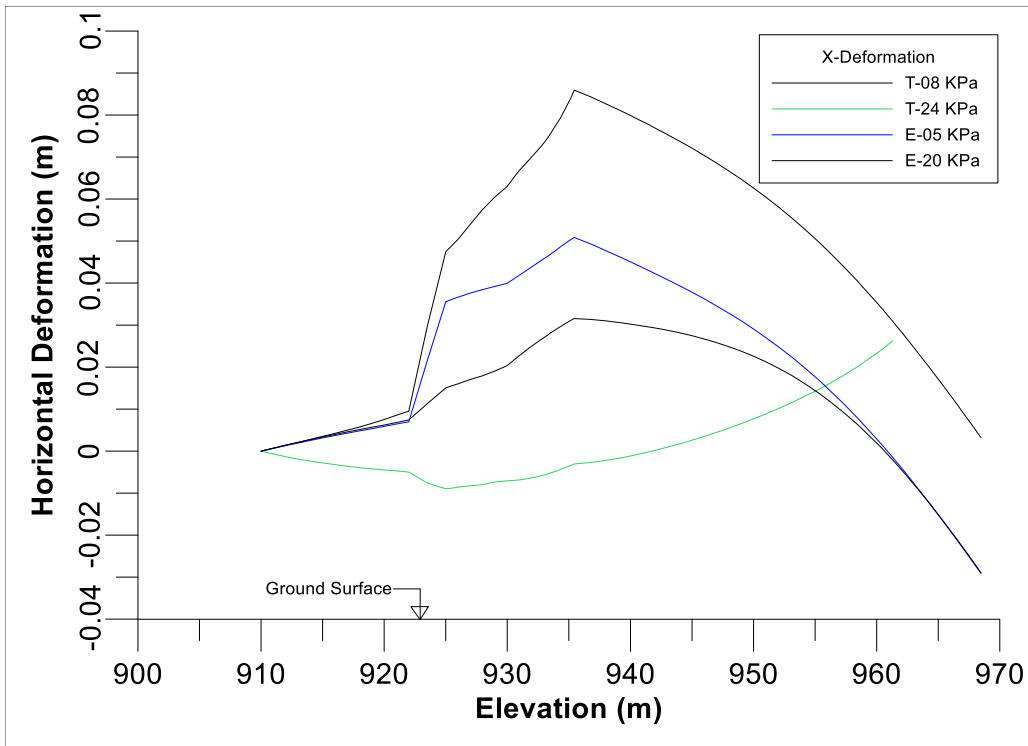


Figure 41: Comparison of global horizontal deformation along S.O.L

3.5 Summary of Results

On-site engineering observations can eliminate some potential failure mechanism that could have happened to the dam. Thus, it saves time and efforts in numerical analysis. It has been reported by Morgenstern *et al.* (2015) that no excessive precipitation or seismic activities were recorded before the failure. Internal erosion through the dam body was insignificant. Surface cracking were also not clearly visible on the slope and core during their visit to the site. It was also noted that the seepage collection ponds in the downstream sides of the dams were working properly until the failure. This rules out the possibility of filter material incompetency. These observations limit the failure mechanism to either the foundation or the geometry of the dam section.

It has been clear from the shown analyses that the design dam sections had changed from time to time; it became more irregular. Significant changes were seen in assigning foundation layers beneath the dam. Nevertheless, the material properties of each layer did not differ much. Factors of safety obtained in preliminary design (Table 7 in Analysis 1) were much higher than the recommended factors of safety by Canadian Dam Association (2012). The design engineers of this phase of design were more concerned about the liquefaction possibility of the tailings material. So, they ran different simulations by changing various undrained shear strength ratios of tailings for different phreatic surfaces. A dam which is constructed using modified centreline method does not rely on tailings much. So, it is not unusual to have similar values of FOS for different simulations where the changes were made only in tailings material properties. However, the engineers did not consider any possibility of undrained responses in the foundation. A previous geological review spotted a highly consolidated and lowly permeable Glaciolucustrine unit which was primarily comprised of silts and some clay (Knight Piesold Consultant 2005). It

would be a more rational approach to check for the undrained response when a low permeable layer was present in the system.

The simplistic shape of the dam body could not be maintained during construction stages. That is why, more complex dam sections based on the site requirements evolved in later design phases. The 9th stage stability analysis by AMEC (2012) was the latest design analysis with the updated dam geometry. This analysis also provided FOS higher than recommended FOS in Analysis 2 although the downstream slope was steepened from 2H:1V to 1.3H:1V. The design engineers continued to put reliance only on tailings materials to check undrained response. That's why, they also ran different simulations by varying the tailings properties. Calculated FOS were not much different between the simulations, because the dam was constructed using the modified centreline method. The foundation layer for this analysis differed significantly from the previous analysis. Rather than having two simple soil layers in the foundation, it had five layers of foundations in two different material properties (Figure 17). The design foundation layers were provided in Mohr-Coulomb parameters for the stability analysis. They did not consider any short-term stability for the dam, however.

Post-failure review analysis (Analysis 3) for 9th stage by Morgenstern *et al.* (2015) stated that a previously undetected weak GLU layer was the major problem in this failure. This weak layer was found in a detailed geomorphological investigation after the failure. The calculated FOS was approximately 1 for different undrained shear strength ratios (0.22 and 0.27). They concluded that the designers, being unaware of this weak layer, did not consider the existence of the non-pervasive weak GLU layer just beneath the failure zone. This layer was susceptible to the undrained failure when it was subjected to the additional load in 9th stage. Additionally, they also suggested that a steep downstream slope (1.3 H: 1V) triggered the failure. The analysis by

Morgenstern *et al.* (2015) was replicated for the purpose of this study. Nevertheless, the analysis was extended beyond the single analysis of 9th stage. The FOS for each stage were shown in Table 12. A consistency in low FOS in most of the stages suggests that the failure might not have happened due to sudden pore water pressure increase as a consequence of the added load in 9th stage.

The current study based on the finite element analysis (Analysis 4) had taken the same geometry and material strength properties for the failed section from Morgenstern *et al.* (2015); however, it also considered the ‘weak’ GLU layer in stress-strain condition. For Case 1 and 2, where the Effective Stress Analysis (ESA) was performed, adding a new layer of embankment in 9th stage did not change the maximum shear strain (ϵ_{\max}) by a significant amount (Figure 24, 22, 25 & 26). The mechanism was similar for case 3 of Total Stress Analysis (TSA), where the GLU layer was assigned with a high stiffness parameter (Figure 32 & 30). Instead, case 4 of TSA had a lower stiffness compared to the adjacent upper and lower ‘Till’ layers. This layer showed a significant increase in maximum shear strain (ϵ_{\max}) from 8th stage to 9th stage in this case (Figure 36 & 34).

FOS calculated by numerical analysis for all the cases in each stage were shown in Table 14. Respective FOS were higher in ESA than in TSA. For both cases of ESA, FOS values were similar to each other and they were higher than the recommended FOS. For both cases of TSA, FOS were also similar to each other and they were lower than the recommended FOS in last three stages. The similarities in FOS for different stiffness parameters in respective stages were also observed, because the concept FOS was developed based on the strength parameters only. That is why, many previous studies (e.g., Alsharedah 2015) stated that stiffness parameters of soil are not as important as the strength parameters in FOS based stability analysis. However, numerical simulations in case: 4 indicated that the stiffness of materials, especially the relative

stiffness, was significant in the stability of the dam. A layer with a very low relative stiffness can generate very high shear strain along the layer when a threshold load is applied in any particular stage of the construction. This happened in the 9th stage construction in MP-TSF. This mechanism is comparable in a way that the weak materials of the GLU layer were channeling through a conduit made of stiff clay soil. Thus, a localized weak zone of soil in the foundation could initiate an excessive deformation. This large deformation decreased the insitu soil strength to the residual strength. This might led to the instability of the dam in a progressive manner. For higher relative stiffness of GLU layer, the shear strain was not very high to initiate an excessive deformation, however.

The assessment of the long-term deformation of an earthen structure is also very important. The allowable vertical and horizontal deformations of the dam body are not readily available in the codes yet, however. This is probably due to the extents of the geometric irregularities in tailings dam. The general practice is to establish an agreed allowable deformation based on the site characteristics among the consulting engineers before the construction starts. In MP-TSF, the maximum vertical and horizontal deformations were numerically found to be -0.12 m and +0.03 m respectively (Figure 38 and Figure 39). The differences in deformations along S.O.L for four cases were not significant (Figure 40 and Figure 41). These low values of deformation indicate that the dam might not have failed due to long-term deformation in the dam body. It also rules out the horizontal thrust provided by tailings materials. The onsite inclinometers which had an overall maximum displacement rate of 4 mm/year (BGC Engineering 2013) supports this numerical deformation study.

Numerical results from this current study agree with the findings by Morgenstern *et al.* (2015) that the failure did happen in undrained condition. However, the mechanism of failure is

different than the findings by Morgenstern *et al.* (2015) as their findings relied only on the strength parameters of soil. They concluded that the sudden increase of the pore water pressure in the 9th stage decreased the effective stress of the soil, causing a static liquefaction in the GLU layer. Instead, this current study shows that an excessive increase in shear strain (causing large deformations) in weak GLU layer during 9th stage construction reduced the soil strength to the residual strength. This residual strength of the soil was not capable to stabilize the dam. Thus, these research findings highlight the importance of the stiffness parameters in the staged construction while analyzing the stability of a tailings dam.

4 PARAMETRIC STUDY FOR PERFORMANCE IMPROVEMENT

This chapter provides a numerical parametric study regarding the failed dam's stability improvement. Finite Element (FE) Method based SIGMA/W software is used for the stability assessment. The effects of modification of dam geometry, material properties, and hydraulic conditions have been studied extensively. Additionally, Limit Equilibrium Method based SLOPE/W software is used to calculate the strength parameter sensitivity. The chapter ends with a summary of parametric results.

4.1 Numerical Parametric Study

The material properties were kept as same as the properties in case # 4 as given in the 'Chapter 3: Analysis' (Table 5 and 8). Case # 4 is the critical condition as GLU stiffness was found as low as 8,000 kPa in the total stress parameter. To simplify the simulation, most of the changes were made in the final stage (9th). The FOS of the failed dam, in insitu condition, was found close to 1 (one). According to Canadian Dam Association (2012), the recommended factors of safety are 1.3 and 1.5 for operational stage and the long term respectively. The aim of this parametric study is to increase the factor of safety up to 1.3 by modifying the dam design parameters, while keeping the economic perspective in mind.

4.2 Study 1: Downstream Slope Flattening

The downstream slope in the original 9th stage of the dam was steep; 1.3 H: 1V (Morgenstern *et al.* 2015). For this simulation, the downstream slope of dam was changed to 2H:1V to see the effects (Figure 42). A flattened slope helps to distribute the stresses over a larger area; and it also

provides resistance against slips. The factor of safety was found to be 1.20. Although, this value is less than the recommended value, it could have prevented the failure as it is considerably greater than the unity of FOS. A long-term factor of safety was calculated as 1.6 which is also greater than the recommended value. The additional calculated volume required in the dam body was approximately 380 m^3 per linear meter along the length of the perimeter dam.

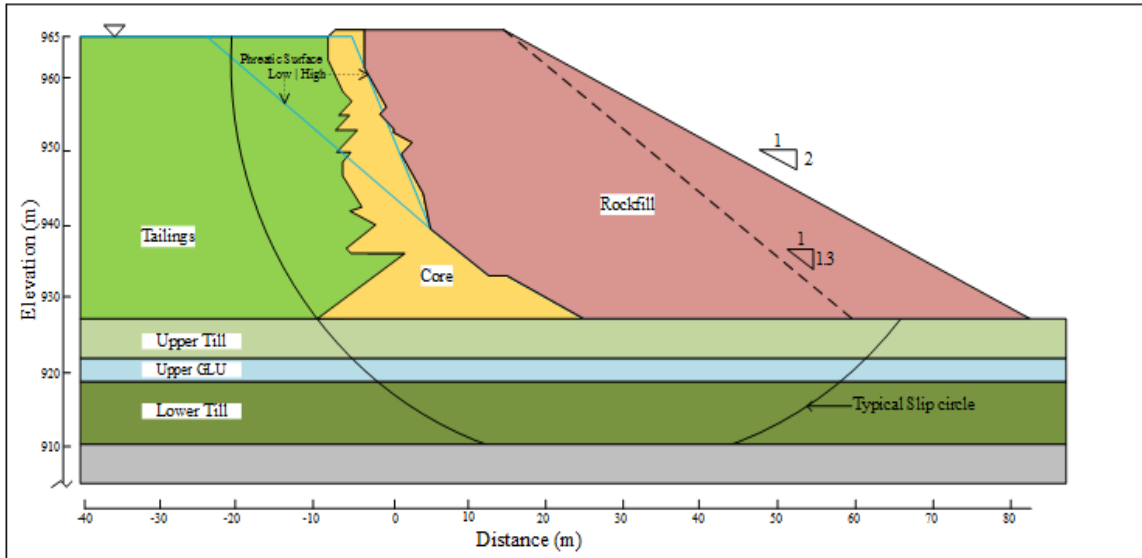


Figure 42: Perimeter dam with downstream slope of 2H:1V

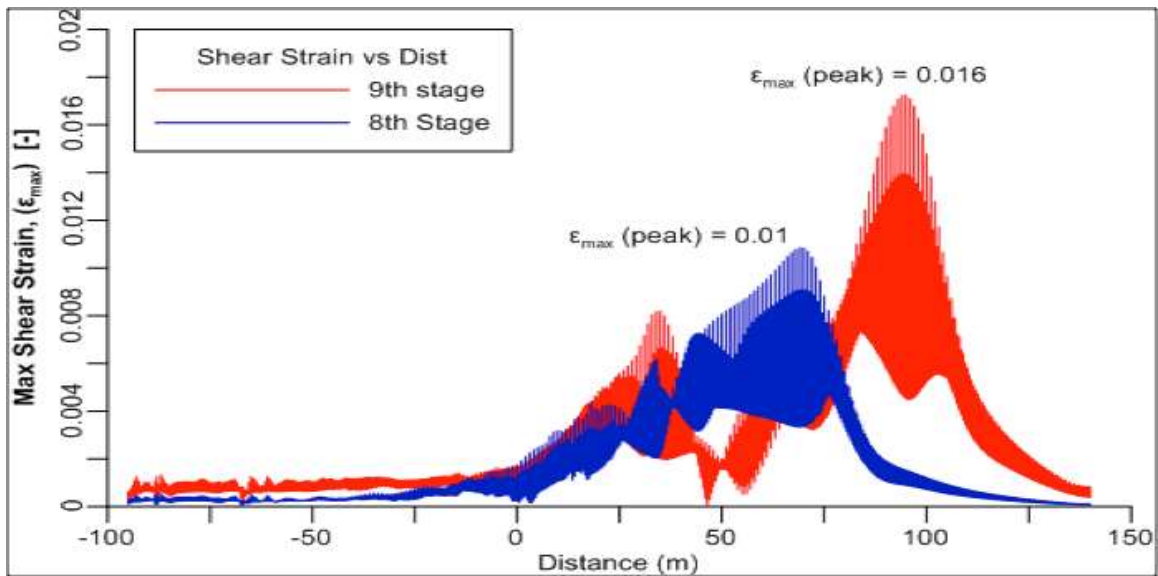


Figure 43: Maximum shear strain (ϵ_{max}) along GLU layer for 8th & 9th stage (With flattened d/s

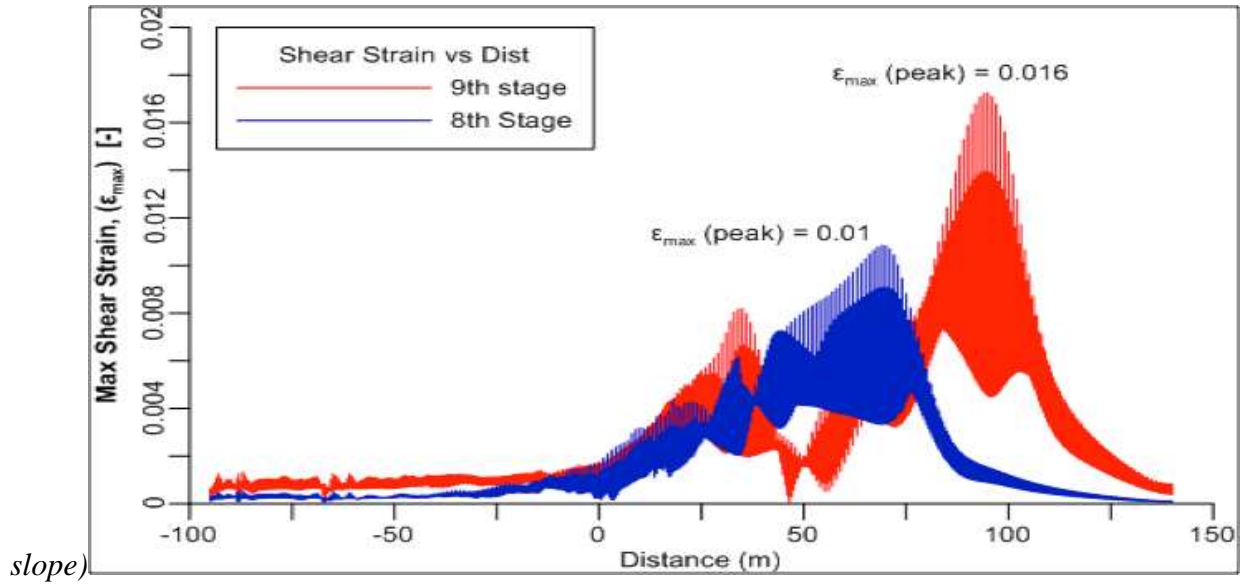


Figure 43 shows that the maximum shear strain (ϵ_{max}) did not jump from 1.2% (8th stage) to 1.6% (9th stage). This negligible increase in shear strain indicates that if the slope were mild, the stability of the dam would improve. Further flattening of downstream slope would earn higher factor of safety.

4.3 Study 2: Addition of Berms to Downstream Slope

Adding a berm to the downstream side of the dam increases the factors of safety. It gives lateral supports to the downstream as well as it helps to distribute the stresses over the foundation (Chowdhury *et al.* 2010). An advantage of the berm installation is that it may be used as the ‘access road’ to the dam. The berm size of 30 m x 14 m (Trapezoidal) provide increases the factor of safety up to 1.2 (Figure 44). The additional volume required in the dam body was approximately 420 m³ per linear meter.

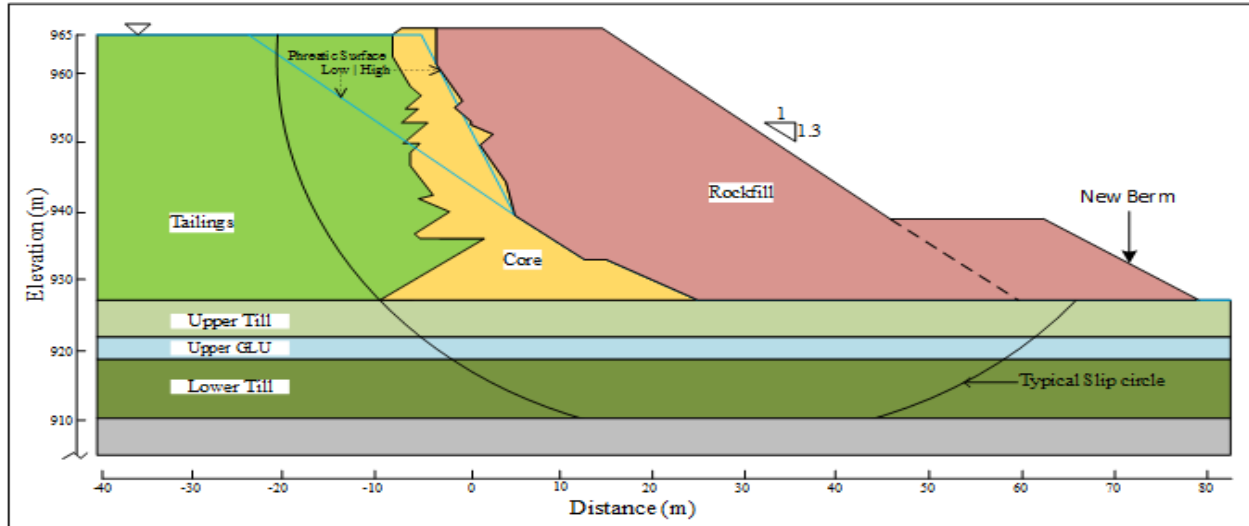


Figure 44: New berm has been added to the downstream slope of perimeter dam

Figure 45 shows the maximum shear strain (ϵ_{max}) in stages 8 and 9 which are 1% and 1.6% respectively. The data shows that the magnitude and change in maximum shear strain (ϵ_{max}) are insignificant to initiate an instability in the dam system.

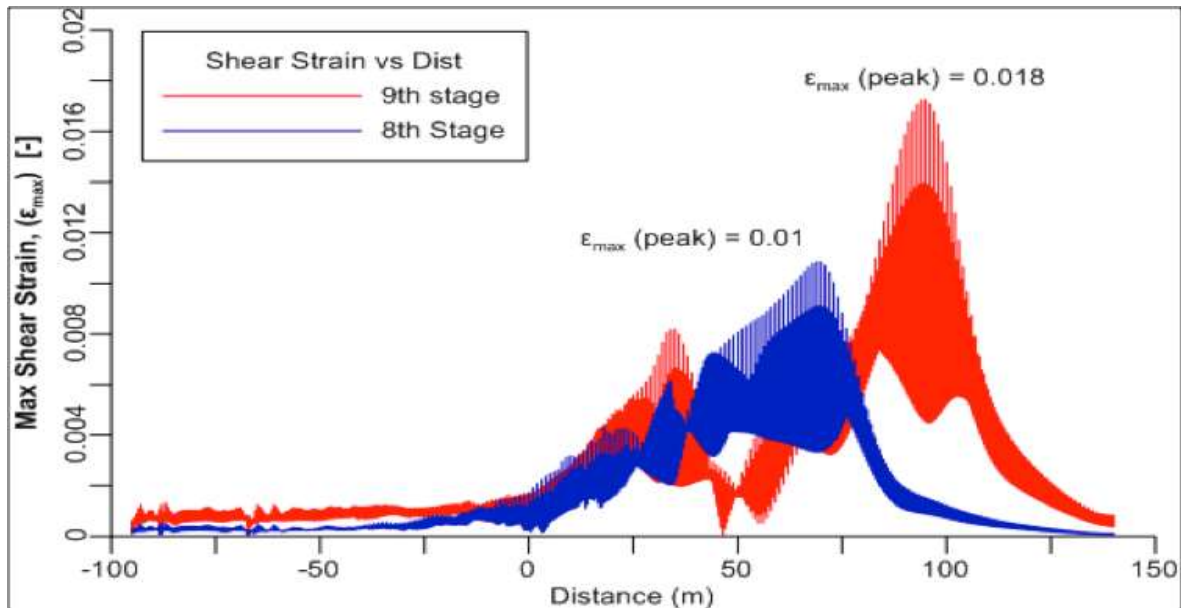


Figure 45: Maximum shear strain (ϵ_{max}) along GLU layer for 8th and 9th stage (with a new d/s berm)

4.4 Study 3: Widening of Core

It was reported by Morgenstern *et al.* (2015) that the ‘core material’ crest width of the perimeter dam was approximately 4 m. That might have affected the overall stability of the dam. An increase in the crest width while keeping the core shape intact may have some effects on the dam stability. Figure 46 shows a modified dam section with a new crest width of 8 m. The FE analysis, however, shows that factors of safety obtained for the modified section did not increase. It remained close to 1 (one).

Figure 47 indicates that maximum shear strain (ϵ_{max}) jumps from 1% in 8th stage to 8% in 9th stage. This excessive shear strain in 9th stage is sufficient to allow distortion and deformation in the foundation system. The failure mechanism in this case is similar to that of the original dam section. Thus, the dam remains unstable even thickness of the core material increases.

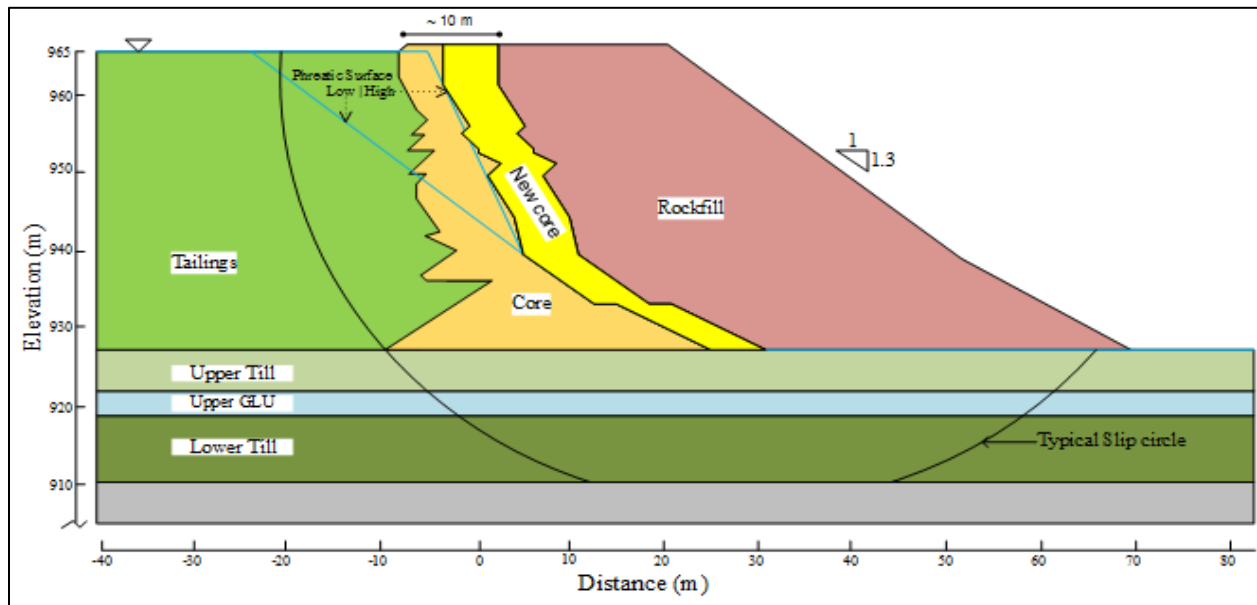


Figure 46: Perimeter dam with widened core of 10 m

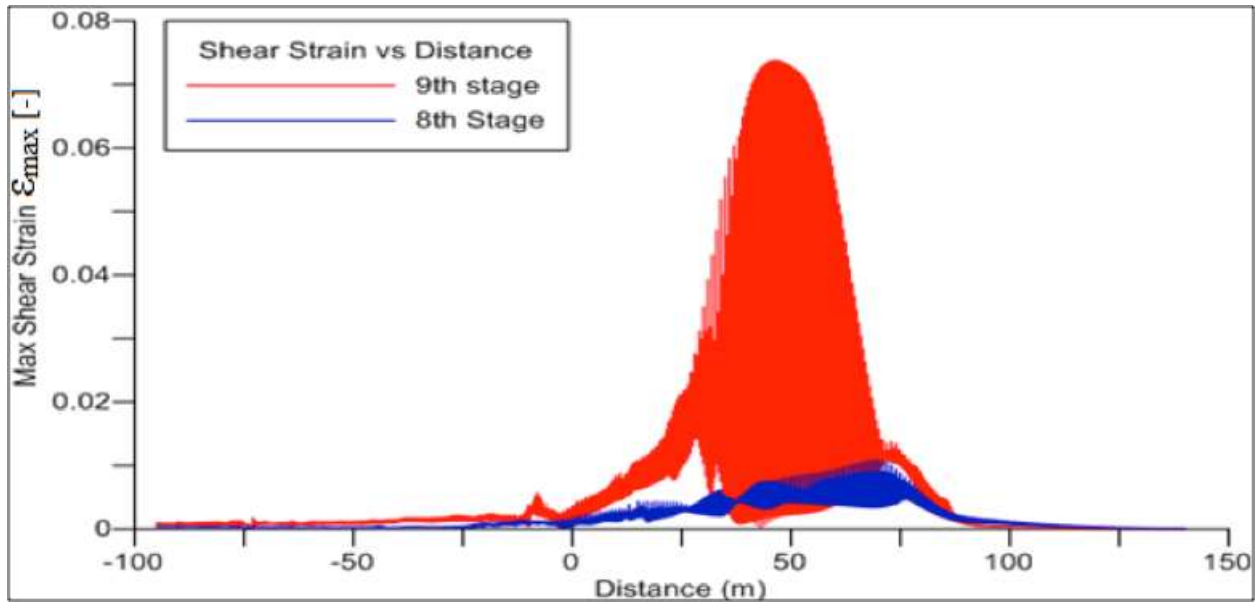


Figure 47: Maximum shear strain (ϵ_{max}) along GLU layer for 8th and 9th stage (With widened core)

4.5 Study 4: Addition of Extra layer of Rockfill

Zardari (2011) described that an additional patch of the rockfill added to the downstream slope can increase the stability of the dam. This additional rockfill supports the dam laterally and it distributes the stress over a large area of the foundation. The following simulation shows an increase of the FOS due to a new rockfill layer (Figure 48). The simulated rhomboidal size of 38m x 22m provides a factor of safety of 1.20. The additional volume required in the dam body was 830 m³ of crushed rock per linear meter.

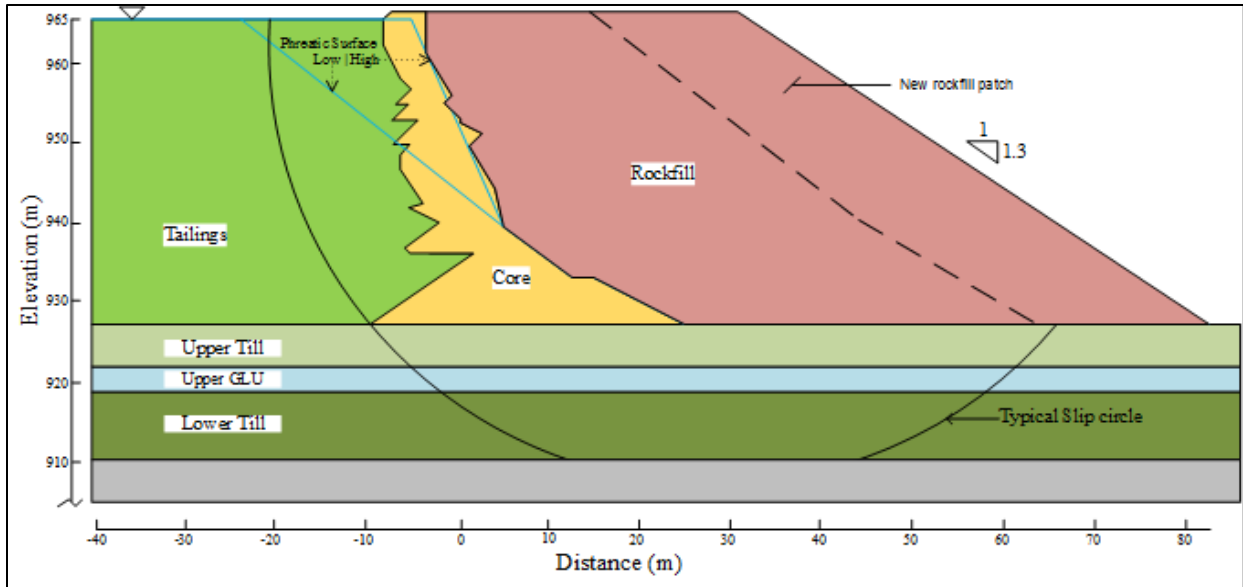


Figure 48: New rockfill patch added to the downstream of the perimeter dam

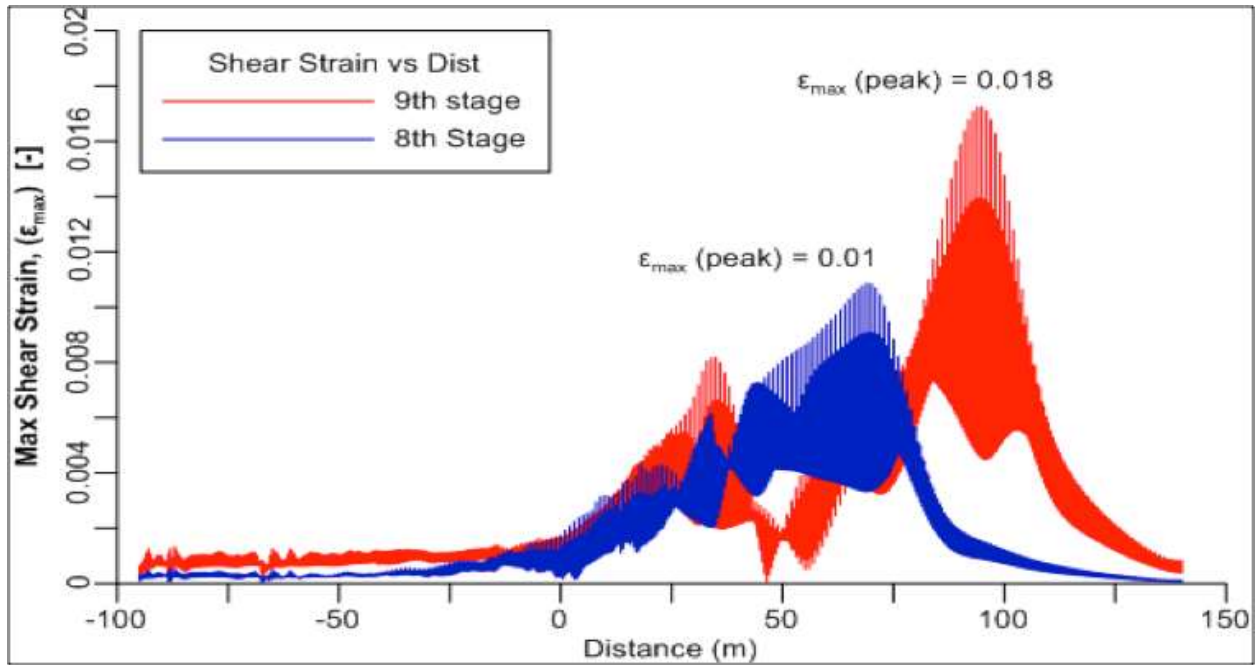


Figure 49: Maximum shear strain (ϵ_{max}) along GLU layer for 8th and 9th stage (new rockfill patch in downstream)

The differences in magnitudes of maximum shear strain (ϵ_{\max}) in 8th and 9th stages are negligible, 1.1% and 1.7% respectively (Figure 49). These shear strains are not sufficient to cause instability in the system.

4.6 Study 5: Thickened Tailings

Thickened tailings by using of mechanical/ hydraulic thickening (e.g. Azam *et al.* 2009) or the soil additives (e.g.; Alsharedah 2015) may provide better bearing in the upstream side of the dam. The following simulation is performed with different tailings properties. The unit weight, angle of internal friction and total stiffness were different among the simulations (*Table 15*). The result shows that changing the tailings properties did not increase the stability of the dam. Because, in the dams built with modified centreline method, the dam body does not rely on the tailings.

Table 15: Factor of safety for different tailings properties

Case #	Unit weight, KN/m ³	Angle of internal friction, Φ	Stiffness, KPa	Factor of safety
Base case	18	30	15,000	~1.00
Case A	18	30	25,000	~1.00
Case B	18	35	15,000	~1.00
Case C	18	35	25,000	~1.00

4.7 Sensitivity Study

A sensitivity analysis was conducted in SLOPE/W to assess the influence of the each parameter on the slope stability. This analysis represents an approximate gradient in factor of safety for each parameter. By this way, the most influential parameter can be established. In MP-TSF, a sensitivity analysis was done by varying Unit Weights (UW) and shear strengths of the material.

The result is shown in Figure 50. From the graph, it is understandable that some parameters, like the angle of internal friction (Φ) of ‘core material’, UW of the Till (upper Till) and undrained shear strength (SSR) are more sensitive to changes than other parameters.

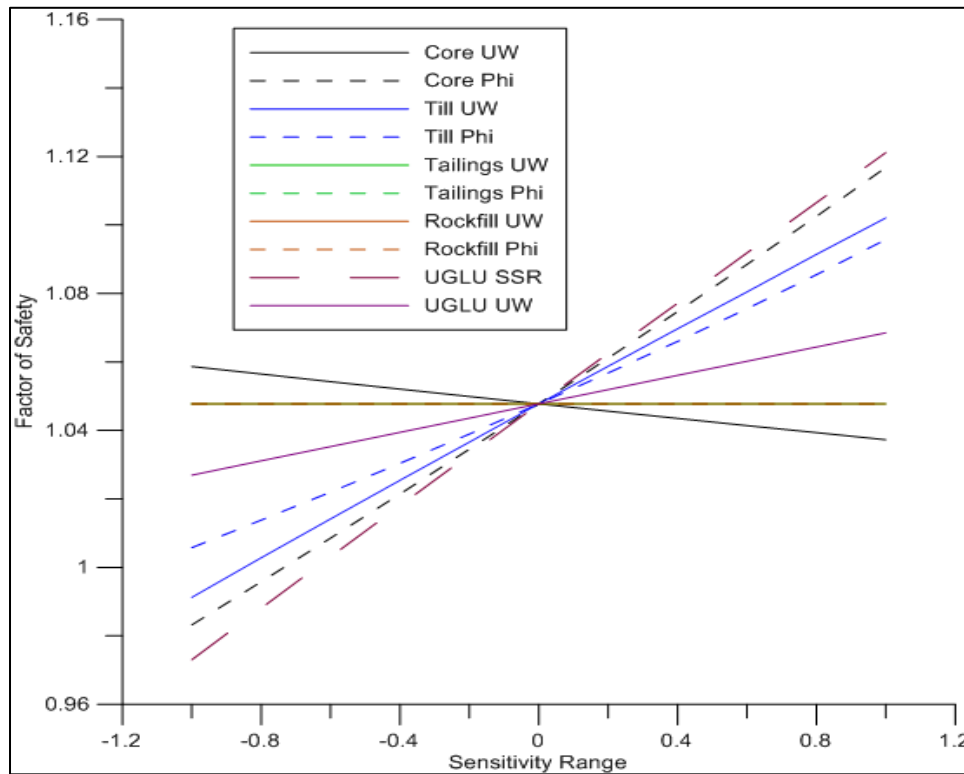


Figure 50: Sensitivity of the perimeter dam analysis (UW refers to Unit Weight)

4.8 Summary of Results

The parametric study was done by changing the geometry of the dams as well as material properties of the tailings material. The parametric study shows that more than one approach could be used to achieve higher factor of safety. ‘Flattening the downstream slope’, ‘Addition of Extra layer of Rockfill’ and ‘Addition of Berms to Downstream Slope’ individually could improve the stability of the dam. However, based on the economy in material requirements and

the convenience in construction, the “Flattening the downstream slope” would be the best option to stabilize the perimeter dam of MP-TSF.

5 CONCLUSION

In this research, the failure of Mount Polley Tailings Dam Facility (MP-TSF) was studied with the help of Finite Element Analysis within GeoStudio 2012. The perimeter dam of MP-TSF suddenly failed, without any prior indication, on August 4, 2014. After the failure, the Provincial Government of British Columbia established an Independent Review Panel (IRP) to investigate the incident. The review report was published on January 30, 2015. The IRP stated that a weak Glaciolustrine layer in the foundation failed in an undrained manner when a new stage of construction ended. They extended in their review that a steep downstream slope may have triggered the failure (Morgenstern *et al.* 2015).

This study verified the findings by IRP. A numerical parametric study was also conducted to determine the ways in which the failure could have been prevented. The summary of results and recommendations are summarized below.

5.1 Summary of Results

The current simulation agrees to findings of IRP that the dam failed in the weak Glaciolustrine (GLU) layer of the foundation. IRP stated that the dam failed due to a sudden increase of pore water pressure in the GLU layer as a result of new construction load in the 9th stage. The current numerical study conducted within GeoStudio 2012 suite, however, finds that the dam failed due to an excessive increase in shear strain in the concerned GLU layer. The shear strain in undrained condition rose up to approximately 8% in the 9th stage of construction. This was a significant jump in shear strain compared to just 2% in the 8th stage. The distorted soils in the

GLU layer acted like a flow of soil channeling through the weak layer. Thus, it created instability in the overall dam system, and led the dam to fail suddenly.

This study highlights an often-neglected aspect of stability analysis: stiffness, especially the relative stiffness of a layer. Analysis of slope stability often encompasses the strength parameters only, neglecting the stiffness parameters (Alsharedah 2015). The absence of Stiffness in the stability analysis may lead to erroneous result. A soil with low stiffness can compress and distort due to applied external loading. This can create instability in two ways: by distorting the soil domain itself or by increasing the pore water pressure within it if the hydraulic conductivity is low. Thus, it is recommendable to check both strength and stiffness parameters of soil for stability analysis, especially for the structures are constructed in multi-stages and have complex geometry of different soil layers.

5.2 Recommendations That Could Have Prevented the Failure

Modifications in the dam system were made to check the ways in which the failure could have been prevented. The Factor of Safety of the dam could be improved by either flattening the downstream slope, adding a berm or adding a rockfill patch to the downstream side. As the dam was constructed using modified construction method, any modification in the upstream side, like strengthening of tailings by adding soil additive or by mechanically/ hydraulically thickening, may not improve the overall stability of the dam.

Based on the achieved stability and economy in material sourcing, flattening the downstream slope to 2H:1V or more would provide the best option of stability of the dam.

5.3 Future Research Possibilities

The results herein can be extended as follows:

1. A comprehensive 3D Finite Element Analysis by considering stress-strain and hydraulic anisotropy would provide better insight into the stability of the dam.
2. How the shape, size and position of a localized soil zone with low stiffness in the dam system would influence the overall stability of the dam.
3. A similar approach for stability checking described in this study could be extended to other two dams of the Mount Polley Tailings Storage Facility: main and south dam. It is also recommended for other tailings dam operators to conduct extensive soil investigation to check for potential weak soil layers in the foundation.

REFERENCES

- Alonso, E. E., and Gens, A. (2006). "Aznaicóllar dam failure. Part 1: Field observations and material properties." *Geotechnique*, 56(3), 165–183.
- Alsharedah, Y. A. (2015). "Slope Stability Enhancement of an Upstream Tailings Dam: Laboratory Testing and Numerical Modelling." Geotechnical, University of Western Ontario, London, Canada.
- AMEC Consultant. (2013a). "As-Built and Annual Review Report.pdf."
- AMEC Consultant. (2013b). *Stage 9 Tailings Storage Facility Construction Drawings and Stability Analyses for Embankment Raise to El. 970 m*. Design Report, Likely, British Columbia.
- Azam, S., Jeeravipoolvarn, S., and Scott, J. D. (2009). "Numerical modeling of tailings thickening for improved mine waste management." *Journal of Environmental Informatics*, 13(2), 111–118.
- Azam, S., and Li, Q. (2010). "Tailings dam failures: a review of the last one hundred years." *Geotechnical News*, 28(4), 50–54.
- Basham, P. W., Weichert, D. H., Anglin, F. M., and Berry, M. J. (1982). **New Probabilistic Strong Seismic Ground Motion Maps of Canada: A Compilation of Earthquake Source Zones, Methods and Results*. La Direction.
- Berghe, J.-F. V., Ballard, J. C., Pirson, M., and Reh, U. (2011). "Risks of Tailings Dams Failure."
- BGC Engineering. (2013). *Mount Polley Mine: Tailings Storage Facility 2012 Annual Review*. Annual Report, British Columbia, Canada.
- Bjelkevik, A., and Knutsson, S. (2005). "Swedish tailings—Comparison of mechanical properties between tailings and natural geological materials." *Proceedings securing the future, International Conference on Mining and the Environment Metals and Energy Recovery*, 117–129.
- Blight, G. E., and Amponsah-da Costa, F. (1999). "Improving the erosional stability of tailings dam slopes." *Tailings and Mine Waste '99*.
- Breitenbach, A. J. (2009). "Improvement in the stability of upstream method phosphate tailings dams with rock fill shells."
- Cambridge, M. (2014). "Liquefaction failure in a Derbyshire fluorspar tailings dam."
- Canadian Dam Association. (2012). "Dam Safety Review Guidelines." Canadian Dam Association.
- Carelsen, S. (2013). "Influence of capillary bridges on weathered tailings material." *Applied Earth Science*, University of Twente, Netherlands.
- Cassidy, J. F., Rogers, G. C., Lamontagne, M., Halchuk, S., and Adams, J. (2010). "Canada's earthquakes: 'The good, the bad, and the ugly.'" *Geoscience Canada*, 37(1).
- Chandler, R. J., Tosatti, G., and others. (1995). "The Stava tailings dams failure, Italy, July 1985." *Proceedings Of The Institution Of Civil Engineers. Geotechnical Engineering*, 113, 67–79.
- Cheng, Y. M., and Lau, C. K. (2008). *Slope stability analysis and stabilization: new methods and insight*. Routledge, London ; New York.
- Chowdhury, R., Flentje, P., and Bhattacharya, G. (2010). *Geotechnical slope analysis*. CRC Press, Boca Raton.

- ConeTec Investigations Ltd. (2014). *Presentation of Site Investigation Results: Mount Polley Mine, Likely, BC, Canada*. Soil Investigation, Richmond, BC.
- Das, M. B. (2010). *Principles of Geotechnical Engineering*. Cengage Learning Inc.
- Davies, M., and Martin, T. (2002). “Static liquefaction of tailings—fundamentals and case histories.”
- Davies, M. P. (2002). “Tailings impoundment failures: are geotechnical engineers listening.” *Geotechnical News, September, 2002*, 31–36.
- Degago, S. A., Grimstad, G., Jostad, H. P., Nordal, S., and Olsson, M. (2011). “Use and misuse of the isotache concept with respect to creep hypotheses A and B.” *Géotechnique*, 61(10), 897–908.
- Duncan, J. M. (1996). “State of the art: limit equilibrium and finite-element analysis of slopes.” *Journal of Geotechnical engineering*, 122(7), 577–596.
- Federal Emergency Management Agency. (2008). *Geotextiles in Embankment Dams*.
- Fell, R., MacGregor, P., Stapledon, D., and Bell, G. (2014). “Chapter 19: Mine and industrial tailings dams.” *Geotechnical engineering of dams*, CRC Press.
- Foster, M., Fell, R., and Spannagle, M. (2000). “A method for assessing the relative likelihood of failure of embankment dams by piping.” *Canadian Geotechnical Journal*, 37(5), 1025–1061.
- Fourie, A. B., Blight, G. E., and Papageorgiou, G. (2001). “Static liquefaction as a possible explanation for the Merriespruit tailings dam failure.” *Canadian Geotechnical Journal*, 38(4), 707–719.
- Gao, Y., Song, W., Zhang, F., and Qin, H. (2015). “Limit analysis of slopes with cracks: Comparisons of results.” *Engineering Geology*, 188, 97–100.
- Griffiths, D. V. (2001). “Stability analysis of highly variable soils by elasto-plastic finite elements.” *Advanced Numerical Applications and Plasticity in Geomechanics*, Springer, 159–229.
- Haile, J. P., and Brouwer, K. J. (1994). “Modified Centreline Construction of Tailings Embankments.” Perth, Australia.
- Hu, S., Chen, Y., Liu, W., Zhou, S., and Hu, R. (2015). “Effect of seepage control on stability of a tailings dam during its staged construction with a stepwise-coupled hydro-mechanical model.” *International Journal of Mining, Reclamation and Environment*, 29(2), 125–140.
- Imperial Metals. (2015). “Mount Polley Mine.” *Mount Polley Mine*, Mining Company Website, <<http://www.imperialmetals.com/s/MountPolleyMine.asp?ReportID=584863>> (Feb. 24, 2015).
- Ishihara, K., Ueno, K., Yamada, S., Yasuda, S., and Yoneoka, T. (2015). “Breach of a tailings dam in the 2011 earthquake in Japan.” *Soil Dynamics and Earthquake Engineering*, 68, 3–22.
- Javadi, N., and Mahdi, T.-F. (2014). “Experimental investigation into rockfill dam failure initiation by overtopping.” *Natural Hazards*, 74(2), 623–637.
- Knight Piésold Consultant. (1997). “Mount Polley TSF Updated Design Report.”
- Knight Piesold Consultant. (2005). *Design of the tailings storage facility to ultimate elevation*. Design Repor, BC, Canada.
- Knight Piésold Consulting. (2005). *Preliminary Design of the Tailings Storage Facility to its Ultimate Elevation*. Design Report, BC, Canada.
- Kondalamahanthy, A. K. (2013). “2D and 3D back analysis of Forest City (South Dakota) landslide.” Citeseer.

- Konrad, J.-M., and Watts, B. D. (1995). "Undrained shear strength for liquefaction flow failure analysis." *Canadian Geotechnical Journal*, 32(5), 783–794.
- Kossoff, D., Dubbin, W. E., Alfredsson, M., Edwards, S. J., Macklin, M. G., and Hudson-Edwards, K. A. (2014). "Mine tailings dams: Characteristics, failure, environmental impacts, and remediation." *Applied Geochemistry*, 51, 229–245.
- Krahn, J. (2004a). "Stress and deformation modeling with SIGMA/W, an engineering methodology." *GEO-SLOPE International Ltd., Calgary, Alberta*.
- Krahn, J. (2004b). "Stability modeling with SLOPE/W: An engineering methodology." *The 1th Edt. Canada*.
- Krahn, J. (2004c). "Seepage modeling with SEEP/W: An engineering methodology." *GEO-SLOPE International Ltd. Calgary, Alberta, Canada*.
- Kujawa, C. (2011). "Cycloning of tailing for the production of sand as TSF construction material."
- Kwon, Y. (2015). "Geotechnical Hybrid Simulation to Investigate the Effects of the Hydraulic Conductivity on One-Dimensional Consolidation Settlement." *Marine Georesources & Geotechnology*, 1–15.
- Lambe, T. W., and Whitman, R. V. (1969). "Soil mechanics, series in soil engineering." *Jhon Wiley & Sons*.
- Leps, T. M. (1970). "Review of shearing strength of rockfill." *Journal of Soil Mechanics & Foundations Div*.
- List, F. (1999). "Increasing the safety of tailing dams using geotextiles and geogrids." *Mine Water and Environment, 1999 IMWA Congress, Sevilla, Spain*.
- Lucchi, G., and Tosatti, G. (2009). "Lessons Learnt From the Sgorigrad and Stava Disasters." *Sgorigrad Vratza-Blugaria - Stava Tesero-Italia: identiche sciagure = Zgorigrad Vraca-B'lgarija - Stava Tezero-Italija : identini bedstviija = identical disasters*, Arca, Lavis (TN).
- Martin, T. E. (1999). "Characterization of pore pressure conditions in upstream tailings dams." *Tailings and Mine Waste*, 303–313.
- Martin, T. E., and McRoberts, E. C. (1999). "Some considerations in the stability analysis of upstream tailings dams." *Proceedings of the Sixth International Conference on Tailings and Mine Waste*, 287–302.
- McCrae, M. A. (2015). "Several casualties feared after tailings dam bursts in Brazil." *www.mining.com*, Professional Information, <<http://www.mining.com/several-casualties-after-tailings-dam-bursts-in-brazil/>> (Jan. 24, 2016).
- McLeod, H., and Murray, L. (2003). "Tailings dam versus a water dam, what is the design difference?" *ICOLD Symposium on Major Challenges in Tailings Dams, Montréal, Quebec, Canada*.
- Mittal, H. K., and Morgenstern, N. R. (1975). "Parameters for the design of tailings dams." *Canadian Geotechnical Journal*, 12(2), 235–261.
- Morgenstern, N. R., Vick, S. G., and Van Zyl, D. (2015). *Independent expert engineering investigation and review panel report on Mount Polley tailings storage facility breach*. Review Report, British Columbia, Canada.
- Ormann, L., Zardari, M. A., Mattsson, H., Bjelkevik, A., and Knutsson, S. (2013). "Numerical analysis of strengthening by rockfill embankments on an upstream tailings dam." *Canadian Geotechnical Journal*, 50(4), 391–399.

- Pastor, M., QUECEDO, M., MERODO, J. A. F. N., and HERRORES, M. I. . (2002). “Modelling tailings dams and mine waste dumps failures.”
- Penman, A. D. M. (2001). “Tailing dams—risk of dangerous occurrences.” *Int. Comm. Large Dams—Bull*, 121, 145.
- Poulos, H. G., and Bunce, G. (2008). “Foundation design for the Burj Dubai—the world’s tallest building.” *Proceedings of the 6th international conference case histories in geotechnical engineering, Arlington, Virginia, Paper*.
- Priscu, C. (1999). “Behavior of mine tailings dams under high tailings deposition rates.” McGill University.
- Psarropoulos, P. N., and Tsompanakis, Y. (2008). “Stability of tailings dams under static and seismic loading.” *Canadian Geotechnical Journal*, 45(5), 663–675.
- Qiu, Y. (Jason), and Sego, D. C. (2001). “Laboratory properties of mine tailings.” *Canadian Geotechnical Journal*, 38(1), 183–190.
- Reddi, L. N., Ming, X., Hajra, M. G., and Lee, I. M. (2000). “Permeability reduction of soil filters due to physical clogging.” *Journal of geotechnical and geoenvironmental engineering*, 126(3), 236–246.
- Rico, M., Benito, G., Salgueiro, A. R., Díez-Herrero, A., and Pereira, H. G. (2008). “Reported tailings dam failures.” *Journal of Hazardous Materials*, 152(2), 846–852.
- Robinson, P. (2008). “Karamken Dam Break Information.” *Southwest Research and Information Center (SRIC), Research*, <http://www.sric.org/enr/docs/2009-09-07_KaramkenDamBreak.pdf> (Jan. 26, 2016).
- Rodriguez, J. M., Edeskär, T., and Knutsson, S. (2014). “Mechanical weathering effect on tailings.”
- Santos, R. N. C. dos, Caldeira, L. M. M. S., and Serra, J. P. B. (2012). “FMEA of a tailings dam.” *Georisk: Assessment and Management of Risk for Engineered Systems and Geohazards*, 6(2), 89–104.
- Sarsby, R. W. (2013). “Chapter 15: Tailings Dams.” *Environmental geotechnics*, Ice Publishing, London, 365–391.
- Stark, T. D., and Mesri, G. (1992). “Undrained shear strength of liquefied sands for stability analysis.” *Journal of Geotechnical Engineering*, 118(11), 1727–1747.
- Strydom, J. H., and Williams, A. A. B. (1999). “A review of important and interesting technical findings regarding the tailings dam failure at Merriespruit: technical paper.” *Journal of the South African Institution of Civil Engineering= Joernaal van die Suid-Afrikaanse Instituut van Siviele Ingenieurswese*, 41(4), p–1.
- Sun, E., Zhang, X., Li, Z., and Wang, Y. (2012). “Tailings Dam Flood Overtopping Failure Evolution Pattern.” *Procedia Engineering*, 28, 356–362.
- Thomson, B. M., Longmire, P. A., and Brookins, D. G. (1986). “Geochemical constraints on underground disposal of uranium mill tailings.” *Applied geochemistry*, 1(3), 335–343.
- Thorntwaite, C. W. (1948). “An approach toward a rational classification of climate.” *Geographical review*, 55–94.
- US EPA. (1994). “Design and evaluation of tailings dams.” U.S. Environmental Protection Agency.
- Van Niekerk, H. J., and Viljoen, M. J. (2005). “Causes and consequences of the Merriespruit and other tailings-dam failures.” *Land Degradation & Development*, 16(2), 201–212.
- Vick, S. G. (1990). *Planning, design, and analysis of tailings dams*. BiTech, Vancouver.

- Villavicencio, G., Espinace, R., Palma, J., Fourie, A., and Valenzuela, P. (2014). "Failures of sand tailings dams in a highly seismic country." *Canadian Geotechnical Journal*, 51(4), 449–464.
- WISE Uranium Project. (2016). "Chronology of major tailings dam failures." *Tailings Dam Safety, Chronology*, <<http://www.wise-uranium.org/mdaf.html>> (Jan. 14, 2016).
- Yi-Shu, Z., Zhou Xiao, and JING Xiao-fei. (2015). "Experimental Study on Overtopping Failure Mode of Reinforced Tailings Dam." Atlantis Press, Zhuhai, China.
- Zandarín, M. T., Oldecop, L. A., Rodríguez, R., and Zabala, F. (2009). "The role of capillary water in the stability of tailing dams." *Engineering Geology*, 105(1–2), 108–118.
- Zardari, M. A. (2011). "Stability of tailings dams: focus on numerical modelling." Numerical Modeling, Luleå University of Technology, Luleå, Sweden.

APPENDIX

This appendix provides the download link for GeoStudio files.

Download link [Expiry: 2019]: <http://bit.ly/2jS4wSS>

The owner of these GeoStudio files can be contacted directly via alarafat@yorku.ca